Stock Assessment of Uku (*Aprion virescens*) in Hawaii, 2020

Marc O. Nadon, Michelle Sculley, and Felipe Carvalho

Stock Assessment of Uku (*Aprion Virescens*) in Hawaii, 2020

Marc O. Nadon[1,2], Michelle Sculley[2], and Felipe Carvalho[2]

[1]Joint Institute for Marine and Atmospheric Research
    University of Hawaii
    1000 Pope Road
    Honolulu, Hawaii 96822

[2]Pacific Islands Fisheries Science Center
    National Marine Fisheries Service
    1845 Wasp Boulevard
    Honolulu, HI 96818

U.S. Department of Commerce
Wilbur L. Ross, Jr., Secretary

National Oceanic and Atmospheric Administration
Neil A. Jacobs, Ph.D., Acting NOAA Administrator

National Marine Fisheries Service
Chris Oliver, Assistant Administrator for Fisheries

Table of Contents

iv

List of Tables

List of Figures

Executive Summary

The uku snapper (*Aprion virescens*, family Lutjanidae) inhabits the coastal waters of the main Hawaiian Islands (MHI) at depths ranging from 20 to 200 meters. The MHI uku population was first assessed with other snappers using a catch-only method applied at the family level (Sabater & Kleiber 2013). That assessment determined that snappers were not overfished. In 2017, uku was assessed at the species-level using a length-based mortality model and a relatively simple numerical population model to obtain fishing mortality rates and spawning potential ratio (SPR). Using this approach, it was determined that the stock was not experiencing overfishing (Nadon 2017). The current assessment builds off these previous efforts and uses catch, catch-per-unit-effort (CPUE), diver surveys, and size composition time-series in the Stock Synthesis modeling framework (Methot & Wetzel 2013). Stock Synthesis 3.30 is an integrated statistical catch-at-age model that fits a population model to relative abundance and size composition data in a likelihood-based statistical framework to generate maximum likelihood estimates of population parameters, derived outputs, and their associated variability. These outputs are then used to determine stock status and to develop stock projections under different management scenarios.

All available fishery data from recreational and commercial fisheries in the MHI were used for this stock assessment. Total recreational catch for the 2003–2018 period was obtained from the Hawaii Marine Recreational Fishing Survey (HMRFS) and reconstructed for the 1948–2003 period by relating historical catch to human population trends in the MHI. Total commercial catch was obtained from the Division of Aquatic Resources (DAR) fisher reporting system (FRS). Commercial catches for uku were dominated by the deep-sea handline fishing gear although trolling and inshore-handline catches have increased in recent decades. CPUE data were obtained from all three main fishing gears in the FRS while size composition data were obtained for the deep-sea handline gear only, due to limited data availability. Deep-sea handline data were the only CPUE time-series available for 1948–2002, as trolling and inshore handline data were sparse for this period. Additionally, information from NOAA diver surveys was incorporated as a fishery-independent abundance index between 2005 and 2016.
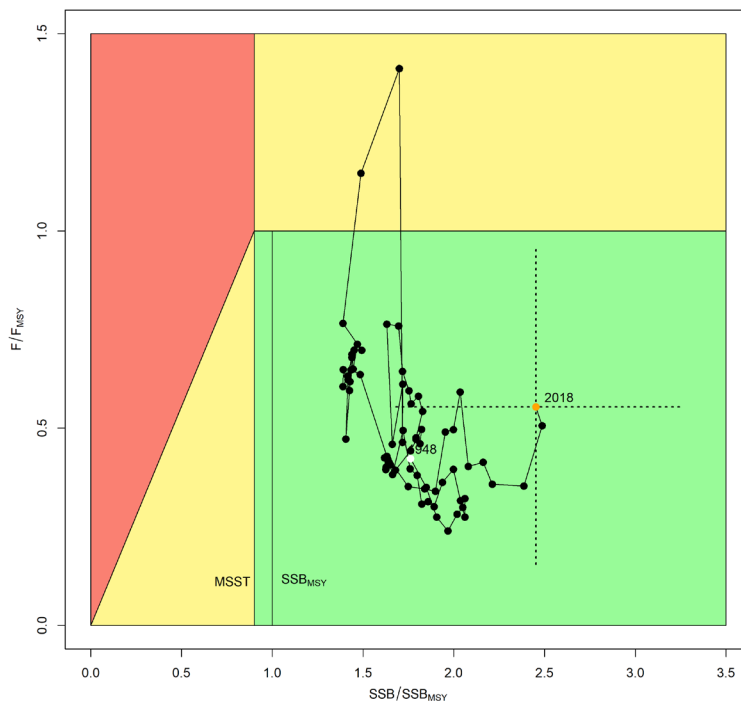
Figure S1. Kobe plot of the trends in estimates of relative fishing mortality (average of age 5–30) and spawning stock biomass of uku from 1948 to 2018.

Uku catches increased from 1948 to the late 1980s and have been declining slowly since then. Model estimates of population biomass show a gradual decline from 1948 to the late 1980s,

followed by a brief period of stability and a substantial increase in biomass starting in the early 2000s. Fishing mortality on the stock (average F on ages 5–30) is currently 0.08 with an F/F_{MSY} value of 0.57 (Figure S1). Fishing mortality has only been above F_{MSY} (0.14) twice, in 1988 and 1989 when F reached 0.19 and 0.16, respectively. The 2018 spawning stock biomass (SSB) of 819 mt is 272% above the SSB_{MSST} (301 mt). Therefore, relative to the reference points defined by the Fisheries Ecosystem Plan, overfishing is not occurring and the MHI uku stock is not overfished (Figure S1).

Stock projections for uku were conducted using the age-structured projection model software AGEPRO (Brodziak et al. 1998). Stochastic projections were conducted using results from the base-case model to evaluate the probable impacts of constant catch quotas on future spawning stock biomass and yield for uku in the MHI. Results show the projected female spawning stock biomasses and fishing mortality rates under each of the constant-catch scenarios. For example, a constant catch limit of 135 mt each year from 2020 to 2026 would result in a 50% chance of overfishing occurring in 2026.

1 Introduction

1.1 Background

This report presents the stock assessment of the ukupalu snapper, commonly known as "uku", in the main Hawaiian Islands (MHI) covering the period from 1948 to 2018. Uku is a wide-ranging reef-associated snapper (family Lutjanidae) that is found between 35° N and 31° S from East Africa to Hawaii. The scientific name for this species is *Aprion virescens* and it goes by several common English names in other regions, typically "green jobfish" or "gray snapper."

The Hawaii uku population was first assessed with other snappers using a catch-only method applied at the family level (Sabater & Kleiber 2013). That assessment determined that snappers were not overfished in the MHI. In 2017, uku were assessed at the species-level using a length-based mortality model and a relatively simple numerical population model to obtain fishing mortality rates and spawning potential ratios (SPR). Using this approach, it was determined that this stock was not experiencing overfishing (Nadon 2017), with a spawning potential ratio of 0.33, which was above the 0.3 limit defining overfishing.

The current assessment builds upon the previous effort by including time series of catch, catch-per-unit-effort (CPUE), diver surveys, and size composition. To do this, we used the Stock Synthesis 3.30 modeling framework (Methot & Wetzel 2013) to integrate these various data types into a unified model. This report presents the first integrated stock assessment of a domestic stock in the U.S. Pacific Islands region.

1.2 Distribution and biology

Uku are found throughout the Hawaiian Archipelago, which extends 2,600 km along a SE–NW axis from 19°N, 155°W to 28°N, 178°W (Figure 1). The archipelago is composed of 18 islands and atolls that are typically divided into two broad regions: the inhabited main Hawaiian Islands (MHI; current population approximately 1.4 million individuals; dbedt.hawaii.gov/census) and the mostly uninhabited Northwestern Hawaiian Islands (NWHI). The MHI consists of eight geologically young, high (4,205 m maximum elevation) volcanic islands while the NWHI have low elevation (275 m max elevation). The level of connectivity of the uku sub-populations around the MHI and the significance of larval exchanges or adult movements between the different Hawaiian Islands are still not entirely clear. In this report, the uku stock was analyzed at the MHI scale (Figure 1 and Figure 3) due to data limitations and current management stock definitions. Further population connectivity studies may suggest that future stock assessments be conducted at different spatial scales for this species. As shown in Figure 1, the longest distance between islands in the MHI is 116 km (Oahu to Kauai), with other islands separated by much shorter distances. While inter-island movements have not been detected for tagged uku (Meyer et al. 2007), significant larval dispersal cannot be ruled out. Recent genetic parentage analyses of groupers in Australia have found parent-offspring pairs at distances up to 250 km, with a median dispersal distance of 110 km (Williamson et al. 2016). Another parentage study conducted on Hawaii Island found yellow tang surgeonfish parent-offspring pairs separated by up to 184 km, although they did not attempt to find cross-channel pairs (Christie et al. 2010). Furthermore, a recent study of passive pelagic particle connectivity in the MHI, based on a pelagic larval duration of 45 days, found a median distance for successful settlements around 100 km (Wren et al. 2016)

and that cross-channel dispersal can be common. Uku population connectivity within the MHI will require further investigation; however, based on current research, it appears that our MHI-scale analyses are appropriate. It is generally well-accepted that the MHI and NWHI reef fishes form different stocks, and that minimal larval or adult exchange exists between these two regions given the dominant current direction and the large distances involved (Toonen et al. 2011; Wren et al. 2016).

Uku is a coastal semi-pelagic species found in the water column above both hard and soft bottom habitats at depths ranging from around 20m to 200m (Pyle et al. 2016; Asher et al. 2017; Figure 2). They typically grow to about 75 cm fork length (FL; about 6 kg) although larger specimens up to 101 cm (14 kg) have been reported in Hawaii (Sundberg & Underkoffler 2011). They reach maturity around 45 cm (approximately 3 years) and spawn primarily during the summer months (Everson & Williams 1989). They can live up to 32 years in Hawaii (Table 1; O'Malley, pers. comm.).

1.3 Fisheries

Coastal fish, including uku, have been exploited since around AD 1250, when the MHI were settled (Kittinger et al. 2011). The NWHI were never permanently inhabited; however, they were a focus of commercial fishing, especially in the 19th century (Kittinger et al. 2011). They are now part of the Papahānaumokuākea Marine National Monument and fishing has been prohibited in that entire region since 2006.

The uku fishery around the MHI involves near-shore recreational/subsistence fishing combined with a commercial fishing sector. Almost a third of Hawaii households are involved in recreational-subsistence fishing (Hamnett et al. 2006); this sector represents 52% of total uku caught, significantly more by boat (78% of recreational catch; Ma & Ogawa 2016) than shore-based fishing (22%). The commercial sector is an almost exclusively boat-based fishery that targets uku using deep-sea handlines (63% of total commercial catch), inshore handlines (15%), and trolling (10%; Figure 4). In most years, the majority of the commercial catch for uku comes from the Maui Nui sub-region (54%; Figure 1 and Figure 5) with Penguin Bank, off the western tip of Molokai, representing about 36% of the total commercial catch alone (Figure 2 and Figure 5). In recent years, the recreational sector has been catching about 55 metric tons of uku annually, while the commercial sector has been catching about 50 metric tons annually (Figure 6). Historically, the commercial sector captured around 30 metric tons of uku annually in the 1950s. Commercial landings increased until they reached a sharp peak in 1988 (156 mt) before declining to about 35 mt in the 1990s (Figure 6). Commercial landings have been increasing since then, reaching around 50 mt in recent years. Dealer-reported data collected by PIFSC indicate that the price per pound for uku has been steadily increasing from 2003 to 2018, going from 3.92 $/lb to 5.31 $/lb (adjusted for inflation). Uku are caught year-round, but their catch peaks during the summer months coinciding with their spawning season. The State of Hawaii has regulations enforcing a minimum size of 1 pound for uku targeted by spear or for sale.

Of note, the 1988−1989 peak in catch is remembered by fishermen and scientists as a notable appearance of a large number of ukus in the MHI that could have been associated with a strong recruitment event or even migration from the NWHI correlated with unusually cold temperatures

in that region (D. Kobayashi, J. Polovina, R. Morioka, and L. Yamada, pers. comm.). The sharp drop in catch for commercial deep-sea handline between 2017 and 2018, from 39 mt to 15 mt, may be related to a strong increase in shark depredation in 2018, especially on Penguin Bank (R. Morioka, pers. comm.).

2 Methods

2.1 Stock assessment model

Stock Synthesis (SS) is an integrated statistical catch-at-age model that is widely used for stock assessments in the United States and throughout the world (Methot & Wetzel 2013). SS takes relatively unprocessed input data in the form of observed catch, size/age composition, and relative abundance indices such as catch-per-unit-effort (CPUE), and incorporates the main population processes (e.g., mortality, selectivity, growth) to recreate population biomass trajectory and derived indicators of stock status. Because many of these inputs are correlated, the theory behind SS is that these should be modeled together, which helps to ensure that uncertainty in the input data is propagated through the assessment. SS is comprised of three subcomponents: (1) a population subcomponent that recreates the numbers- and biomass-at-age using estimates of natural mortality, growth, fecundity, etc.; (2) an observational sub-component that consists of observed (measured) quantities such as CPUE or proportion at length, weight, and/or age; and (3) a statistical subcomponent that uses likelihoods to quantify the fit of the observations to the re-created population. Basic equations and technical specifications underlying Stock Synthesis can be found in Methot (2000). We used SS version 3.30.14 with AD Model Builder (ADMB version 12.0, released 07/19/2019).

In the current assessment, our SS model was informed by four types of data: historical commercial and recreational catches, catch-per-unit-effort time series, body size (weight) frequencies time series, and fishery-independent diver surveys. The sections below describe how each data source was processed to generate the inputs necessary for the SS model while also going into greater detail on the functioning of Stock Synthesis itself. Table 2 presents the main assumptions built into our Stock Synthesis model and includes links to the relevant sections in this report.

2.2 Model inputs

We used the following datasets in the current assessment:

- **Fisher Reporting System (FRS)** from the State of Hawaii Division of Aquatic Resources (DAR; Pacific Islands Fisheries Science Center 2020). This dataset is composed of self-reported catch in numbers and weights per record at the species level, with records corresponding roughly to individual trips (see CPUE standardization section 2.2.2 for details). Of note, only commercial fishers are required to report to this system and this dataset does not capture the catch from fishers who do not have a commercial license. Data collection in this system started on January 1, 1948 and continues to this day. This dataset was used to obtain **CPUE indices**, **size frequencies**, and annual **commercial catch** from 1948 to 2018, which are the years included in the current assessment.

- **Hawaii Marine Recreational Fishing Survey (HMRFS)** is conducted by the Hawaii Division of Aquatic Resources (DAR) and NOAA Fisheries Marine Recreational Information Program (MRIP; Ma & Ogawa 2016). This dataset provides annual **recreational catch** by combining phone interviews estimating total fishing effort with onsite fisher interviews for CPUE for boat-based and shore-based activities. Data collection in this system started in 2003 and is ongoing (note: phone interviews were replaced with mail surveys in 2018). Total recreational catch per year was used in the current assessment from 2003 to 2018 (NMFS Office of Science and Technology 2020).
- **Pacific Reef Assessment and Monitoring Program (RAMP)** are SCUBA diver survey cruises conducted by the Pacific Islands Fisheries Science Center and provided a fishery-independent **abundance index** every 2 to 3 years starting in 2005, with the latest cruise completed in 2016 (Ayotte et al. 2015; Pacific Islands Fisheries Science Center 2020b, 2020c).

The data used in our model are summarized in Figure 7 while the sources of key input parameters are presented in Table 1.

2.2.1 Catch reconstruction

The total harvested biomass of uku (referred to in the rest of the report as "catch") is the sum of commercial and recreational landings by weight in a given year from 1948 to 2018 (Table 2).

Commercial catch from 1948 to 2018 was obtained from 101,804 catch records in the FRS dataset that reported landing uku (DAR species code "20"). We first assigned the uku records to the main Hawaiian Islands (MHI) and Northwestern Hawaiian Islands (NWHI) zones based on the reported DAR fishing areas (Figure 1 and Figure 3). We assigned 97,048 records to the MHI, 4,587 records to the NWHI, and only 169 records had invalid reported areas. The catch from these 169 records was assigned to the MHI zone according to the ratio of MHI/NWHI catch in the corresponding year. Total commercial catch by year was obtained by simply summing the total weight of all uku MHI records. We assumed that the commercial catch was known with relatively low uncertainty and assigned a low coefficient of variation (CV) of 0.05 to the deep-sea handline fleet and a CV of 0.1 to the remaining commercial fleets' data.

Recreational catch from 2003 to 2018 was obtained from the HMRFS program by querying the MRIP website (https://www.fisheries.noaa.gov/topic/recreational-fishing-data) for the "green jobfish" (i.e., uku) annual catch time series. This dataset provided the number of uku caught by fishing mode (shore or private/rental boat) by year. We did not use the MRIP estimate of catch in weight given that the mean weight of uku used in that calculation is typically derived from only a few individual fish measurements in each reporting "wave" (there are 6 waves in a year) and the mean weight estimates are sometimes not available in a given wave. Instead, we obtained catch in weight by multiplying the number of uku caught in a year by the overall mean weight of uku in the HMRFS dataset between 2003 and 2018 (mean of 3.26 kg from 151 individuals). Due to a recognized error in the household count for Maui County, the 2003−2010 estimates of catch had to be divided by 1.22 (Ma 2013). Since the HMRFS program also captures some commercial fishing effort from non-fulltime fishers, it was necessary to remove the HMRFS uku catch that was claimed to be sold to avoid this catch being accounted for in both the commercial and recreational

tallies. To do so, we obtained the proportion of uku catch sold by year from HMRFS fisher interviews and multiplied the total HMRFS uku catch by one minus the year-specific proportion (Hongguang Ma, pers. comm.). To reconstruct recreational catch before 2003, we first calculated the mean recreational catch between 2003 and 2007, as well as the mean Hawaii human population size for those years. We multiplied the mean 2003−2007 recreational catch by the ratio of the mean 2003−2007 human population size to the human population size in any given year from 1948 to 2002:

$$Rec.catch_{year} = Rec.catch_{2003-2007} \cdot \frac{Population_{year}}{Population_{2003-2007}} \qquad \text{Eq. 1}$$

We used the 2003−2007 mean recreational catch instead of simply using the 2003 catch to avoid giving too much weight to that single year, given the high uncertainty associated with the HMRFS recreational catch estimates. The assumption behind this approach is that pre-2003 recreational catch is proportional to the Hawaii population size and participation in the recreational fishery would be expected to increase as the overall population in Hawaii increases. An alternative approach would have been to apply the ratio of recreational to commercial catch in the 2003−2018 datasets to the 1948−2002 commercial catch to re-create the recreational catch (this scenario seems less plausible but was tested as a sensitivity run). As previously mentioned, the recreational catch estimates are highly uncertain and a mean CV of 0.4 was used in our model for all years. This CV was obtained directly from the queried HMRFS dataset.

As noted previously, in 2018 the HMRFS program switched from a phone to a mail survey to estimate recreational fishing effort. Starting in 2017, the program conducted both surveys to calibrate the estimates and found that effort estimates derived from mail surveys were 2.89 and 2.33 times the same estimates from phone surveys for shore- and boat-based activities, respectively (data from the NMFS Office of Science and Technology). The differences may be related to a progressive reduction in the number of households with phone landlines and it is not clear how these correction factors would evolve from 2003 to 2016 (this is currently under research by MRIP). Given this, we only applied the correction factors (2.89 and 2.33) to the 2017 recreational catch. The sensitivity of the model to this assumption was explored post hoc.

2.2.2 CPUE abundance indices
Overview: We used the FRS dataset to produce fishery-dependent indices of uku abundance based upon methods used in the Deep-7 bottomfish assessment (Langseth et al. 2018). Starting in January 2003, the FRS data reporting system was improved by requiring fishers to report the number of hours fished per record, thus allowing fishing effort to be standardized to an hourly rate. Before this, fishing effort was provided as individual fishing days. This difference in fishing effort reporting resulted in different CPUE scales, leading us to split the CPUE time series into two time periods, 1948−2002 and 2003−2018, each with an estimated catchability coefficient (q). Furthermore, we selected the three dominant fishing gears used to catch uku in the MHI to generate CPUE indices: deep-sea handline (DAR gear code "3"), inshore handline (gear code "4"), and trolling (gear codes "6","61","62","63", and "70"). Before the early 2000s, inshore handline and trolling fishing gears were used only sporadically to catch uku (Figure 4). We therefore only

generated CPUE indices for the recent 2003−2018 period for those gears due to small sample sizes. In total, our assessment model included four CPUE indices:

- Deep-sea handline 1948−2002
- Deep-sea handline 2003−2018
- Inshore handline 2003−2018
- Trolling 2003−2018

The data processing and filtering steps used to clean the data for CPUE standardization were built on the many improvements brought forward from various bottomfish data workshops (Yau 2018) and the latest Deep 7 assessment (Langseth et al. 2018). These include the ability to track individual fishers through the entire time series with names assigned to practically all records between 1977 and 2018, and most records for the rest of the time series. Notable exceptions were the 1954−1958 period where less than 50% of records had unique fisher names and 1976 where no fisher name information could be located (Langseth et al. 2018). Furthermore, the Deep 7 assessment and its associated data workshops spent significant time improving the following steps: (1) selecting targeted records, (2) accounting for multi-day trips in the 1948−2002 period, (3) selecting records representative of the fishery, and (4) identifying factors affecting CPUE trends. These steps are described below.

Selecting uku-targeted records: Depending on the species targeted, the three gears selected for CPUE indices (deep-sea handline, inshore handline, and trolling) can be deployed in different configurations and different habitats. Therefore, targeting may have a non-negligible impact on CPUE. Unfortunately, the FRS dataset does not include species targeting information. We controlled for species targeting in two separate steps: (1) we applied certain basic filters to fishing records (see below) and (2) we used a principal component analysis (PCA) on species composition in the catch to generate principal components that were then used in the CPUE standardization model (Winker et al. 2014; see CPUE standardization section 2.2.2 below).

We filtered for non-uku fishing events mainly for records before 2003, when the FRS reporting form was less detailed and individual trips were defined at a much broader daily time scale (note: these steps only apply to the deep-sea handline data given that this was the only CPUE index for the 1948−2002 period). The first step was to filter records with inappropriate or missing data fields: (1) a filter removed records missing a Commercial Marine License (CML) number since this would prevent us from defining individual trips, (2) another filter removed records with no fisher name, which would prevent us from using this important variable in the standardization model. These two steps removed 44,864 records out of the original 771,233 deep-sea handline records.

It is unlikely that fishers targeting uku failed to catch any while successfully capturing certain pelagic or Deep-7 species. Therefore, trip records were removed if no uku was caught in an entire day of fishing but at least one pelagic management unit species (PMUS; WPRFMC 2009), Deep-7 species, or unknown species (species code "0") were reported. This step reduced the number of records from 726,369 to 343,234. Furthermore, for management grids off the southern tip of Hawaii Island (grid 100−102, 108, 120−122, and 128 in Figure 3), in years before 1985, catch records with less than 50 pounds of uku containing PMUS were considered non-uku targeting and filtered out (removing another 7,603 records). The steep bathymetry in this area can lead

fishers targeting PMUS to catch uku and other semi-pelagic species. Furthermore, before 1981, gear types targeting tunas did not have unique codes. Some of these fishing events were recorded as deep-sea handline.

Two final data filtering steps related to targeting were implemented based on feedback from fishers during various workshop: (1) we removed all records from fishers that never reported catching uku, and (2) we removed records from fishery-independent scientific fishing surveys. These steps removed 5,763 out of 335,631 records. It is highly unlikely that certain fishers targeted uku under an active commercial license but failed to catch a single one throughout their period of commercial activity.

Accounting for multi-day trips: As previously identified, the pre-2003 fishing records do not provide a clear estimate of fishing effort. The only way to re-create effort for the CPUE calculation was to combine all reported catch in individual fishing days by combining CML numbers and dates to generate a unique trip identification. However, this raised the issue that catch reported under a single CML–date combination could be aggregated over multiple fishing days (Yau 2018). To deal with this issue, we used the approach presented in Yau (2018) and Langseth et al. (2018), which consisted of identifying potential multi-day trips by calculating the distance traveled between fishing areas and different ports. To reduce the number of distances needing manual measurements, a series of centrally located "common" ports were used (J. Ault and S. Smith, U. of Miami, pers. comm.). Some records could not be assigned distances due to missing port information and were filtered out (2,549 out of 180,599 pre-2003 records). Only 56 out of 71,069 trips had multiple ports and these were filtered out as well. For the 772 trips that reported more than one fishing area, we used the furthest to assign distance traveled. Once distances were available for all trips, we analyzed the frequency distribution of distances in 10-year time blocks and compared our results to those from the Deep 7 assessment (Yau 2018). We found similar patterns and decided to use the 30 nm cutoff to define a single day of fishing (i.e., distances between 0 and 30 nm were assigned a single fishing day, distances between 30.1 and 60 nm were assigned two days of fishing, and so forth). Overall, 34,387 out of 177,750 pre-2003 records were assigned effort values greater than one fishing day; the majority (24,115) were for two fishing days. Another concern was that certain fishers before 2003 were reporting the entirety of their monthly catch at either the first or the last day of the month (Yau 2018). To control for this issue, we removed all 1,033 records from fisher-year combinations that only reported on those two days. After reassembling the pre-2003 data with the 2003–2018 data, the remaining number of catch records was 327,019.

Explanatory variables for CPUE standardization: In addition to *year*, *area*, *fisher name*, and *month*, we added the following variables to the CPUE dataset: (1) *fisher experience*, measured as the cumulative number of fishing events associated with an individual fisher, (2) *wind speed*, and (3) up to 2 principal components (*PC1* and *PC2*) related to species catch composition (see details below). The original *area* variable taken directly from the DAR reporting grid had 279 distinct values in the MHI (shown in Figure 3). We simplified this variable slightly by combining the corresponding offshore/inshore areas together (e.g., areas 300 and 320). This reduced the total number of areas to 230. These offshore/inshore paired areas are not drastically different given that they are typically split at the 2 nm line extending from land. At this distance from shore,

some areas of the ocean are already very deep, while other areas are still relatively shallow, exhibiting no clear pattern, thus making this distinction unhelpful for CPUE standardization purposes.

Wind data starting in July 1987 were available at a spatial scale similar to the reported DAR fishing area, with some gap in coverage. Average wind speed and direction values at a 0.25-degree scale were downloaded from https://www.ncdc.noaa.gov/data-access/marineocean-data/blended-global/blended-sea-winds (accessed 5/23/2019). These data were spatially merged with the CPUE dataset based on fishing date and the GPS coordinates of the center points of each DAR fishing area. Given the restricted availability, we could only use this variable for the 2003−2018 CPUE models.

As previously mentioned, we also explored a new approach to infer the degree of targeting of uku in individual fishing events. The Direct Principal Component (DPC) approach consists of including principal components scores (PCs) derived from the species composition in the catch as predictors in the CPUE model (Winker et al. 2014). This procedure builds on the common assumption that the species composition of the catch is directly related to the extent of targeted effort (Pelletier & Ferraris 2000). For example, a deep-sea handline fishing record containing semi-pelagic species (e.g., kahala, ulua) and few Deep 7 species would likely indicate greater targeting of the semi-pelagic uku, as reflected by the relationship between the different PCs and uku CPUE. If there were a temporal trend in uku targeting for deep-sea handlines, this would be directly reflected in changes in the catch composition and their associated PC values. The first step in this procedure was to select the top species caught by each of the three gears used for CPUE indices. Following Winker et al. (2014), we kept species representing a minimum of 1% of the total catch by gear, which resulted in keeping 12 species for deep-sea handline, and 7 for inshore handline and trolling. The second step was to calculate the proportion of each of the species for each fishing record and doing a fourth-root transformation on these values to reduce the influence of the more abundant species on the PCA (Winker et al. 2014). The third step was to run the PCA analyses using the "prcomp" base R function and extracting the PC scores for each fishing record (labeled as "PC1", "PC2", etc.). A final step was to select the principal components to keep for the CPUE standardization model. Following Winker et al. (2014), we used the "nFactors" R package to obtain the Optimal Coordinate solution for Cattel's scree test (Raîche et al. 2013) while also selecting PCs which had eigenvalues higher than 1 (Kaiser-Guttman rule). Using the AIC and BIC values from the CPUE standardization model to select PCs was not recommended by Winker et al. (2014) as it tends to select for unnecessarily complex models with a high number of PCs. Following these rules, we selected PC1 and PC2 for deep-sea handline, inshore handline, and trolling. Figure 8 shows the full PCA catch composition results for all three gear types. This figure showed some non-linear patterns in catch composition between uku and other groups. For example, the trolling PCA showed that uku were more likely to be targeted when PC1 and PC2 are closed to zero, which suggested that a u-shaped quadratic relationship might be appropriate for these variables in the CPUE standardization model. For this reason, we also added second-degree polynomial terms to the standardization models (i.e., $PC1^2$ and $PC2^2$).

Final processing of CPUE data: Following the DPC analysis, we discarded the non-uku catch data, which were no longer necessary, and summed the uku catch by the remaining variables

(*trip ID, year*, *month, area*, *effort* (i.e., # of days or hours, depending on dataset), *fisher name*, *fisher experience*, *wind speed, PC1*, *PC1²*, *PC2*, and *PC2²*.

The original unique trip identifier (*trip ID*) was created by combining CML number and fishing date since this was the only way to define an individual fishing activity for the 1948−2002 time series. However, the recent 2003−2018 time series contains information on fished hours that can differ within a single day for any given CML (i.e., a fisher is reporting different activities conducted over different numbers of hours). These likely represent separate fishing activities. Fishing records from a given CML containing differing information on hours fished were therefore separated into individual fishing activities by creating new trip IDs.

A relatively small number of fishing events contained multiple areas. There was no information to allow us to partition effort by area within those specific events; therefore, we assigned the area with the greatest catch of uku to the rest of the records within these fishing events. If the uku catch was the same between areas, we simply defaulted to the lowest area number (this was the case for only a few fishing events).

The final step was to calculate CPUE for each fishing event, which was calculated as the total weight (kg) of uku caught per day (1948−2002 time series) or per hour (2003−2018 time series). This provided us with the following number of fishing events for each CPUE indices:

- 70,854 deep-sea handline events for 1948−2002
- 58,802 deep-sea handline events for 2003−2018
- 61,457 inshore handline events for 2003−2018
- 489,447 trolling events for 2003−2018

CPUE standardization models: All four CPUE indices were standardized using generalized linear models (GLM) and generalized mixed-effects models (GLMM). A considerable proportion of trips in each CPUE dataset was represented by zero catches: deep-sea handline 39% (1948−2002) and 79% (2003−2018); inshore handline 93% (2003−2018); and trolling 99% (2003−2018). Given the large proportion of zero catches, a delta-lognormal approach was used to standardize the CPUE indices. In this type of approach, the probability of catching an uku in a unit of fishing effort and the weight of the catch in a unit of effort (when uku are caught) are modeled separately. A binomial distribution was used to model the probability of catching an uku in a given trip (1 = caught, 0 = not caught) with the explanatory variables described previously and listed below using a logit link function. Positive-only CPUE data were modeled with the following explanatory variables using a lognormal response variable implemented by taking the natural logarithm of positive CPUE observations.

The *year* categorical variable was included in all models, given that our goal is to produce annual estimates of uku relative abundance. The following variables were also tested for inclusion in all models:

- Categorical fixed-effect: *month, area, area*month,* and *area*year* interactions
- Categorical random-effect: *fisher name*

- Continuous: *wind speed*, *fishing experience*, catch-composition *PC1, PC1^2, PC2*, and *PC2^2*

These variables were selected using Akaike's Information Criterion: AIC = 2 × number of parameters − 2 × log(likelihood) (Burnham 2004). We used a forward-selection process using a 0.1% AIC improvement threshold for variable inclusion (i.e., the model with the extra variable needs to have an AIC value 0.1% lower than the previous, simpler model). We chose this approach given that a large number of data points in CPUE datasets generally leads to large likelihood values and overly complicated models with little improvement to variance explanation (Maunder & Punt 2004). Maximum likelihood parameter estimation was conducted using the GLM function in R version 3.4 for models excluding the *fisher name* random effect and using the *lmer* function in R package lme4 to run mixed-effect models using this variable.

Overall, models with the *area*year* interaction and the *fisher name* random-effect for the logistic regression models did not converge, similar to the Deep 7 analyses (Langseth et al. 2018). The *area, month, wind speed, PC1*, *PC1^2, PC2^2,* and *PC^2* variables were selected in almost all models, while fisher experience was kept in two models and the *area*month* interaction was only kept for the deep-sea handline 1948−2002 model (Table 4; see Table 5 Table 6, Table 7 for a list of models tested for all four CPUE indices).

Model diagnostics and index calculation: Pearson residual plots (lognormal regression) and quantile residuals plots (logistic regression; Dunn & Smythe 1996) were used to assess model fit. Quantile-quantile plots were also used to assess normality for the lognormal models. The diagnostic residual plots for all 8 CPUE standardization models (both logistic and lognormal regression models) showed no major deviation from normality and heteroscedasticity assumptions (Figure 9 to Figure 16). Some patterning could be seen on the second-degree polynomial variables for *PC1* and *PC2* in some models, but these were not considered indicative of serious model assumption violations. Furthermore, residual plots for individual explanatory variables showed no obvious patterns.

After selecting the best regression models, we generated indices of relative abundance for the 4 CPUE datasets by (1) exponentiating the *year* effect of the lognormal models and (2) multiplying this value by the back-transformed expected logit value for each year for the logistic regression models (Maunder & Punt 2004). For the lognormal models, we added half the square of the standard deviation of the *year* effect before exponentiating as a bias-correction factor. For the logistic models, we selected typical factor levels for the categorical variables and the median level for continuous variables to obtain expected logit values for each year (i.e., June for the *month* effect and area 331 for the *area* effect; Maunder & Punt 2004). The variance of the indices was calculated using a Monte Carlo simulation by drawing random values for the *year* effects (lognormal models) and expected logit value per year (logistic models) derived from the standard deviation of the *year* effect in both models, and fitting a lognormal distribution to the resulting dataset. Figure 17 and Figure 18 present the resulting standardized CPUE indices of abundance vs. their corresponding nominal values. The final indices used in our stock synthesis model are presented in Table 8.

As a check on the effect of calculating CPUE in hourly versus daily effort units, we also calculated CPUE indices for the 2003−2018 period in daily units and compared these to the original hourly values. We did not find significant changes in the CPUE trends for the daily versus hourly units (Figure 19).

2.2.3 Size frequency data

Size composition data were obtained from the FRS dataset where commercial fishers are required to enter total number and weight of fish caught during individual fishing events. Individual fish measurements were generally not available since most records contained multiple ukus. However, it was possible to select fishing records where only a single uku was reported to build annual size frequencies for the dominant fishing gear (deep-sea handline). Other fishing gears, such as inshore handline and trolling, did not have sufficient single-fish reports to generate consistent size frequencies on an annual basis. The reported individual fish weights in pounds were converted to kilograms for consistency within the SS model. The effective sample size in each year was calculated by multiplying the number of weight measurements in each of the four regions of the MHI (Figure 1) by their respective regional weights. Regional weights were calculated as the proportion of total uku habitat (depth <200 m) available in each region (Hawaii: 0.23, Maui Nui: 0.58, Oahu: 0.11, and Kauai-Niihau: 0.08). This down-weighted the effective sample size in years where weight measurements came disproportionality from smaller sub-regions.

It was also possible to convert these individual weight measurements from the FRS dataset to their corresponding lengths by using the following relationship:

$$L = \left(\frac{W}{\alpha}\right)^{\left(\frac{1}{\beta}\right)}$$

Eq. 2

where α is the scaling and β is the volumetric parameters of the typical length-weight relationship ($W = \alpha L^{\beta}$) (see Table 1 for parameter values). These length data were not used in the SS model, which used the weight data, but were used to estimate selectivity for the remaining gear types (see *Selectivity* in section 2.2.6).

2.2.4 Fishery-independent diver survey

Starting in 2005, trained divers from the NOAA Pacific Islands Fisheries Science Center (PIFSC) have been conducting visual surveys around the MHI. The diver surveys were used to obtain a fishery-independent index of abundance in addition to the CPUE indices described above. An in-depth description of this survey program is available in Ayotte et al. (2015). Below is a brief description of the survey protocol.

Diver survey sites were randomly selected within strata defined by depth bins (shallow, 0–6 m; mid, 6–18 m; and deep, 18–30 m). All coastlines from all islands in the MHI were surveyed, except for the small, restricted island of Kahoʻolawe. For practical and safety reasons, surveys were limited to depths above 30 m. During a typical survey day, a NOAA ship deployed 3 to 4 small dive boats that sampled pre-assigned random sites along 10 to 12 miles of coastline. The daily

starting location of the ship along different coastlines of the MHI was set systematically to cover as much of the shoreline as possible. At each site, stationary point counts were implemented by two paired divers inside contiguous 15-m diameter cylinders that extended from the bottom to the surface. Divers first listed all observed fish species during an initial 5-minute period. The divers then went through this list, one species at the time, recording the number of individuals and estimating the sizes of all fish seen within the cylinder. Fish sizes were recorded as total lengths to the nearest cm. Fishes from species not listed during the initial 5-minute period but observed later in the survey were also recorded but classified in a different data category (i.e., non-instantaneous count). Divers were continuously trained between cruises in size estimation using fish cutouts of various sizes. Diver performance during research cruises was evaluated by comparing size and count estimates between paired divers.

Total numerical density estimates (individuals per 100 m^2) were obtained by dividing fish counts in each survey by the survey area (353 m^2 from two 15-m diameter survey cylinders) and multiplying by 100. An individual survey consisted of the combined fish counts from the two divers deployed at a single site. To obtain fishery-targeted numerical density, we multiplied total numerical density at a given size by uku-specific selectivity coefficients derived from the L_{S50} and L_{S95} parameters obtained from the Length-Based Spawning Potential Ratio (LBSPR) model for the trolling fishing gear. The overall fishery-targeted numerical density was obtained by (1) averaging site-level density estimates within a MHI sub-region (Figure 1) and (2) averaging all sub-region-level density estimates together using sub-region weights (the same ones used for the size-frequency effective sample size). Standard deviations were obtained by bootstrapping the diver survey data set by re-sampling survey sites within each sub-region. Fishery-targeted biomass density (kg per 100m^2) was calculated directly from fishery-targeted numerical density by converting fish lengths to weight using the length-weight relationship ($W = \alpha L^{\beta}$, see Table 1 for parameter values). The distribution of survey sites in each year is presented in Figure 20.

It is important to note that the 2005 and 2007 surveys were conducted using a different diver observation method (belt transects). These were calibrated to the Stationary Point Count method using a comparison dataset collected during 2007−2009 cruises during which both methods were implemented at all sites. The results of these analyses for uku showed that the positive-only belt transect density needed to be divided by 0.94 and that the logit-transformed observation probability needed to be subtracted by −0.8 to convert these data to SPC equivalent, which was done for the 2005 and 2007 surveys before being used in our SS model.

2.2.5 Population dynamics
This section describes the source of the various biological parameters used in our Stock Synthesis model, as well as some key assumptions related to population demographic structure (Table 2).

Spatial and temporal span: As discussed in the introduction, the uku stock was analyzed at the scale of the MHI as a single, well-mixed, population (Figure 1 and Figure 3). This assessment covers the 1948 to 2018 period with the first year matching the start of the FRS data collection program, which represents the oldest data available. The end year of 2018 was selected since the 2019 data were incomplete at the time of our analyses.

Sex structure: There was no evidence of consistent sex-specific patterns related to growth (O'Malley, pers. comm.) or a sex ratio different from 1:1. Therefore, recruitment was split evenly between both sexes. Growth was treated similarly between males and females (see below). The only sex-specific parameter was maturity (see below), which was defined solely for females, given the spawning stock biomass and its relationship to recruitment was strictly related to mature female biomass (Methot & Wetzel 2013).

Reproduction and recruitment: Maturity was defined as a function of length using a logistic relationship. Everson and Williams (1989) estimated that female uku reach 50% maturity at 44.8 cm and 95% maturity at 45.7 cm (Table 1; Figure 21). The length at 50% maturity corresponds roughly to age 3 and the first mature female can appear as early as age 2. Fecundity (number of eggs per female) was set to be proportional to female body weight. Total reproductive output for the uku population was therefore set to be directly proportional to total mature female biomass.

Because catch and CPUE data were available annually, a single season per year was used in the base-case model. Therefore, the uku population was assumed to have one spawning and recruitment period at the beginning of each time step, which corresponds to the first month of each year. A standard Beverton-Holt stock-recruitment relationship was used in this assessment. The expected annual recruitment (R) was a function of spawning biomass (SSB) in a given year using the steepness (h) and virgin recruitment (R_0) parameters. Steepness is defined as the fraction of recruitment from a virgin population (R_0) when the spawning stock biomass is at 20% of its unfished level (SSB_0). Deviations around expected recruitment values were assumed to follow a lognormal distribution with standard deviation (σ_R) (Methot 2000; Methot & Wetzel 2013). These annual recruitment deviations were estimated based on the information available in the data and the central tendency that penalizes the log (recruitment) deviations in excess of σ_R. The σ_R parameter was fixed to approximate the expected variability of 0.39 based on an independent estimate of σ_R from the FishLife 2.0 R package (Thorson 2019), derived from other snappers. The log of R_0 (virgin recruitment), annual recruitment deviations, and the offset for the initial recruitment relative to virgin recruitment, R_1, were estimated in the base-case model for the 1948−2017 period. Early recruitment deviations, beginning 10 years before the main recruitment in 1948, were also included in the model. The estimation of early recruitment deviations allows for recruitment in early periods and the model to develop a non-equilibrium age structure without biasing recruitment estimates in the main period. Recruitment deviations are estimated on the log scale in Stock Synthesis. Consequently, the expected recruitments require a bias adjustment so that the resulting recruitment level on the standard scale is mean unbiased. The years chosen for bias adjustment and the maximum bias adjustment parameter value were obtained from the Stock Synthesis output with the program r4ss (Methot & Taylor 2011). Recently, Lee et al. (2012) concluded that steepness is estimable for relatively low productivity stocks with good contrast in spawning stock biomass, given a correctly specified model. However, estimating steepness h within the assessment model for uku is likely to be imprecise and biased because the contrast in the spawning biomass over the assessment period is relatively poor. Given this, we followed the same approach as for σ_R and used an independent estimate of steepness from the FishLife 2.0 R package (Thorson 2019) derived from other snappers (h = 0.81; Table 1). Nevertheless, we note here that this steepness estimate is subject to considerable uncertainty and further work is

needed to evaluate steepness for uku. Sensitivity runs on steepness were used to evaluate the model's sensitivity to this parameter.

Age and growth: The maximum age in the model was 32 years based on the maximum observed age for uku in the Hawaiian Islands (O'Malley, pers. comm.). This value was obtained from a large length and age dataset (n = 419) collected in both the MHI and NWHI and is the oldest recorded value for this species. Note that the 32-year age bin also served as the accumulator for all potential older ages in the SS model.

We modeled the relationship between fork length (FL) and age with a von Bertalanffy growth function using the Schnute (1981) parameterization:

$$L_2 = L_{Amax} + (L_1 - L_{Amax})e^{-K(A_2 - A_1)}$$
Eq. 3

where L_1 and L_2 are the sizes associated with ages, A_1 and A_2, respectively, L_{Amax} is the length at the maximum age A, and K is the growth coefficient. In this assessment, L_1 and A_1 were fixed at 51.6 cm at age 3. The L_{Amax} and K parameters were fixed at 76.5 cm for the maximum age of 32 and 0.136 yr^{-1} (Table 1; Figure 22). The coefficients of variation (CV) parameters that describe the variability of individual fish length at specific ages were fixed at 0.12 for both younger (ages ≤3) and older (ages >3 years) fish. These parameters were obtained directly from the von Bertalanffy model fitted to the raw age-length data. Stock Synthesis assumes linear growth between ages 0 and A_1.

Natural mortality: We obtained an estimate of natural mortality (M) equal to 0.10 using the procedure of Alagaraja (1984), similar to Hewitt and Hoenig (2005), and recently updated by Then et al. (2015), assuming that 4% of a cohort survives to the observed maximum age (a_λ) by which we defined longevity:

$$M = \frac{-\log(0.04)}{a_\lambda}$$
Eq. 4

We used the 4% cohort survivorship value based on the analyses of Nadon et al. (2015) which showed that this is an appropriate survivorship value for coastal fishes in Hawaii. We did not have independent estimates of *M per se* and had to rely on this longevity-based approach. Although there are other data-poor methods for estimating natural mortality, involving other parameters (e.g., K, L_{inf}, L_{mat}, water temperature), two recent scientific papers on the subject clearly suggest that longevity-only methods are better performing (Kenchington 2014; Then et al. 2015). It is important to consider the potential difficulty in obtaining a representative longevity value in heavily exploited stocks. However, our estimate comes from a combined dataset that included individuals from the remote NWHI. We also verified the validity of our M estimate by estimating total mortality (Z) in the NWHI, which can be assumed to be close to M given the exceptionally low fishing mortality in this region. For this analysis, we obtained size data from the FRS dataset that were available for the NWHI (before it was closed to fishing) and compared the observed mean length with the expected mean length when Z is set to 0.1. We observed a NWHI mean length of 70.1

cm and the model predicted a value of 70.8 cm for an *M* = 0.1, which therefore supports our *M* estimate.

Weight-at-length: We used a non-sex-specific weight-length relationship to convert between catch-at-weight and weight-at-length data ($W = \alpha L^{\beta}$) within the SS framework. The α scaling parameter was 0.0118 and the β volumetric parameter was 3.043, obtained from the MHI uku samples collected in Sundberg and Underkoffler (2011) (Table 1).

Initial conditions: It was necessary to make some assumptions about the structure of the stock before the start of the main population dynamics period (pre-1948). Typically, two approaches are used to achieve this assumption. The first approach starts the model as far back as necessary to satisfy the notion that the period before the estimation of population dynamics was in an unfished or nearly unfished state. In this assessment, the second approach was used in which initial conditions were estimated assuming equilibrium catch. The equilibrium catch is the catch taken from a fish stock when it is in equilibrium with fishery removals and natural mortality balanced by stable recruitment and growth. The initial fishing mortality rates in the assessment model that remove these equilibrium catches were estimated to allow the model to start at an appropriate depletion level.

2.2.6 Fishery dynamics

Selectivity: Stock synthesis needs gear-specific selectivity parameters to relate catch, size frequency, and CPUE observations to population dynamics. Size structure patterns in the uku FRS dataset suggested that selectivity was related to body length and followed a simple logistic pattern that was time-invariant. For example, Figure 23 shows no significant changes in selectivity in different decades for deep-sea handline, using size data from the FRS dataset. Given this, selectivity curves were gear-specific and assumed to be only a function of size for the four commercial gear types (deep-sea handline, inshore handline, trolling, and "other") and the recreational sector. The following logistic equation relating selectivity (*S*) to length was used in the SS model:

$$S_L = \frac{1}{1 + e^{\left[-\ln(19)\frac{L - L_{S50}}{L_{S95} - L_{S50}}\right]}}$$

Eq. 5

where L_{S50} and L_{S95} are the sizes at 50% and 95% selectivity, respectively.

By providing Stock Synthesis with size frequencies from the deep-sea handline fleet, the model was able to estimate size selectivity parameters for this fishing gear. However, SS still required selectivity parameters for the other commercial fishing gears (inshore handline, trolling, and "others") as well as for the recreational sector. To provide these parameters, we selected one-fish records from the FRS dataset for the inshore handline, trolling, and "other" fishing gears and fitted a Length-based Spawning Potential Ratio (LBSPR) model to these data sets. The LBSPR model is a relatively simple modeling approach that fits abundance-at-length data by estimating two selectivity parameters (L_{S50} and L_{S95}) and fishing mortality (Hordyk et al. 2016). We also had to group length data by decade, instead of by year, due to the limited sample size available for these gear types. We did not observe significant differences in length structure between decades,

16

and therefore selected the most recent data (2008−2018) to fit the LBSPR model and obtain the required selectivity parameters. Lastly, for the recreational sector, we obtained length observations from the HMRFS interviews for 2003−2018 (n = 151) and used the LBSPR model to obtain selectivity parameters. All L_{S50} and L_{S95} parameters for these gear types were entered directly in SS as fixed values. The LBSPR model fits are presented in Figure 24 and the associated parameters are in Table 1. The selectivity curves for all fishing gears and sectors are presented in Figure 25.

In the SS model, selectivity curves for CPUE indices were set to mirror their corresponding catch fleets.

Catchability: Catchability (q), the proportion of the stock captured per unit of effort, was estimated (solved analytically) for each CPUE index assuming these were proportional to vulnerable biomass with a scaling factor of q. It was assumed that q was constant over time for each index.

Fishing mortality: Fishing mortality was estimated as a full parameter providing a continuous annual estimate of F for each fleet.

Data Observation Models: The current assessment model fitted three data components: (1) total catch, (2) CPUE and diver relative abundance indices, and (3) size composition data. Stock Synthesis estimates population and fishing parameters by minimizing the negative log-likelihood of an objective function from the provided input data components or assumptions.

The reported FRS commercial total catches were assumed unbiased and relatively precise and were fitted assuming a lognormal error distribution with standard error (SE) of 0.05 for deep-sea handline and 0.10 for the other three gears (inshore handline, trolling, and "other"). As discussed in section 2.2.1, the recreational fishery catches were uncertain with a CV of 0.4. The high CV on recreational catch and the estimation of fishing mortality as individual annual parameters (i.e., F method = 2) gave Stock Synthesis a fair amount of freedom to adjust the recreational catch data within the model (see Results for final catch estimation).

The relative abundance indices were assumed to have lognormally distributed errors with SE in log space, which is approximately equivalent to CV (SE/estimate) in natural space where the log(SE) = $\sqrt{\log_e (1 + CV^2)}$. The estimated CVs of each index in this assessment are shown in Table 8. However, the reported CVs for the abundance indices only capture observation errors within the standardization model and do not reflect process errors that are inherent in the link between the unobserved vulnerable population and observed abundance indices, and are related to the number of data points in the analysis, with larger datasets having smaller CVs. Total observation errors for abundance indices are typically assumed to range from 0.1 to 0.4 (Francis et al. 2003; Francis 2011), while Francis et al. (2003) suggested that the portion of the observation variance that accounts for the inter-annual variation in catchability can typically range from 0.15 to 0.2. For the uku assessment, all indices had mean CVs below 0.2 and we therefore added 0.10 to the CVs of all indices, including the diver survey (in order to maintain its relative weight in the model) to increase all CVs to over 0.2.

The size composition data were assumed to have a multinomial error distribution with the error variance determined by the effective sample size (see section 2.2.3). In this stock assessment, size measurements of fish were assumed random samples of fish from the entire population. Size compositions for the deep-sea handline were included (see Section 2.2.3) with the variance determined by the observed sample size and frequencies.

2.3 Model Diagnostics

Model diagnostics were used to assess issues associated with convergence, model structure, parameter misspecification, and data conflicts in the base-case model. The following diagnostic tools were employed in this assessment: (1) model convergence tests, (2) R_0 likelihood profiles, (3) residual analyses, and (4) a retrospective analysis.

2.3.1 Model convergence

Model convergence was assessed using several criteria. The first diagnostic was whether the Hessian (i.e., the matrix of second derivatives of the likelihood with respect to the parameters) inverts. The second measure is the maximum gradient component, which, ideally, should be low (<0.0001 is a standard value). The third diagnostic involved altering or jittering the starting values of the parameters to evaluate whether the model converges to a global solution rather than a local minimum (typically by a maximum of 10%).

2.3.2 Residual analysis

Model fit to the CPUE and diver survey abundance indices were assessed by looking at the residuals of the observed versus predicted CPUE indices by gear. We looked for any signs of conflicting information between different time series and autocorrelated patterns in a given period. We also looked at the overall root mean square error (RMSE) for each index, with values below 0.3 suggesting a good model fit to the abundance index data (Winker et al. 2018).

2.3.3 Likelihood profile on virgin recruitment (R_0)

This diagnostic was implemented by sequentially fixing the equilibrium recruitment parameter, R_0, on the natural log scale, $\log(R_0)$, to a range of values (x to y, step size of 0.1). The maximum likelihood estimates of all other model parameters were obtained from the Stock Synthesis output.

The relative change in negative log-likelihood units over the range of fixed values for $\log(R_0)$ (the R_0 profile) was compared among the Stock Synthesis model likelihood components for CPUE, size composition, and recruitment deviations using two diagnostic tests. First, a relatively large change in negative log-likelihood units along the R_0 profile was an indication of a relatively informative data source for that particular model. Second, a difference in the location of the minimum negative log-likelihood along the R_0 profile among data sources was an indication of either conflicts in the data or model misspecification (or both; Carvalho et al. 2017). Ideally, catch and abundance indices should be the primary sources of information on the population scale in a model (Lee et al. 2014).

2.3.4 Retrospective Analysis

A retrospective analysis is a way to detect bias and model misspecification (Hurtado-Ferro et al. 2015). A retrospective analysis as described in Carvalho et al. (2017) was applied to the base-

case model. The diagnostic was implemented here by sequentially eliminating the five most recent years of data from the full stock assessment model (a 5-year "peel") and then re-estimating all stock assessment model parameters from each peel and from the base-case model. Although measuring retrospective pattern has proved challenging, the most commonly used metric is the rho ("ρ") statistic proposed by Mohn (1999), which measures the relative difference between an estimated quantity from an assessment with a shorter time series and the same quantity estimated from the full time-series. Interpreting the Mohn's rho statistic is subjective. However, a rule of thumb was proposed by Hurtado-Ferro et al. (2015), which states that values of Mohn's rho falling outside the range of −0.15 to 0.20 indicate the presence of a noticeable retrospective pattern for long-lived species.

2.3.5 Assessment strategy

During the model development phase, we first focused on improving the fits to the observed data (CPUE and size-frequency) and obtaining a stable likelihood profile with an informative minimum. A key part of the early exploration involved assessing which parameters could be estimated from the input data and which needed to be fixed. The base-case was chosen as the version of the model with the best fit to the data while also making reasonable assumptions about model parameterization. From this base-case, a set of one-off sensitivities was chosen to test the impact on model results of choices made regarding key fishery and biological parameter assumptions. These sensitives are as follows:

Life history parameters: We tested alternative specifications for L_{Amax}, L_{mat50}, and M. Our estimates of L_{Amax} and L_{mat50} came from robust local studies and while there is a high degree of confidence in these parameters, these parameters are known to disproportionality impact model outcome. Natural mortality is a parameter that is hard to estimate and is influential in most assessments. We tested values representing plus and minus 10% adjustments for each of these parameters (L_{Amax}: 68.9 cm and 84.2 cm; L_{mat50}: 40.3 cm and 49.3 cm; M: 0.09 and 0.11). We also tested the use of age-specific M values under the Lorenzen natural mortality option in Stock Synthesis.

Recruitment: Steepness is a challenging parameter to estimate from observations or within a stock assessment model, but it tends to be very influential on assessment predictions given that it mediates the relationship between spawners and recruits. We examined the impact of the different values of steepness of 0.73 and 0.89 in comparison to the 0.81 used in the base-case. We also tested values representing positive and negative 10% adjustments for the recruitment deviation parameter σ_R (0.35 and 0.43). Finally, we tested an alternative model where σ_R was estimated within Stock Synthesis.

Catch scenarios: Current and historical recreational catch estimates are, in general, highly uncertain and this is particularly true for coastal stocks in Hawaii. While our base-case model did consider the uncertainty in recreational catch (CV = 0.40), we also wanted to test our model's sensitivity to a few alternative catch histories. In the first alternative scenario, we estimated recreational catch as a fixed ratio of commercial catch, which is known with greater certainty. This ratio was calculated by dividing the yearly HMRFS recreational catch estimates by their corresponding commercial catch between 2003 and 2018 (the years for which recreational catch

is available) and averaging these yearly ratios to obtain an overall ratio. For the second and third alternative scenarios, we adjusted the pre-2003 recreational catch by a positive and negative factor of 30%.

CPUE standard error: The standard errors estimated from the CPUE standardization model were small especially for deep-sea handline (mean CV 0.065). This forces the assessment model to be more constrained by the CPUE index. We allowed the model to obtain a more relaxed fit to the CPUE in the base-case by adding a constant of 0.10 to all CPUE indices CVs (see section 2.2.6). However, we also tested the sensitivity of predictions using the standard error estimated from the CPUE standardization model directly. Finally, we tested our model outcome when the CPUE information was limited to deep-sea handline for the 1948−2002 period combined with either deep-sea handline, inshore handline, or trolling CPUE indices individually for the recent 2003−2018 period.

Size frequency data: Size frequency data provide a highly informative source of information on trends in fishing mortality that can often overshadow the CPUE indices. We tested the robustness of our model results to a lower importance of this source of data by lowering its weight in the likelihood calculation to 10% (i.e., lambda = 0.1).

Alternate CPUE timelines: Given the paucity of inshore handline data before 2003, we decided not to include a 1948−2003 CPUE time series for this fishing gear. However, we tested extending the inshore handline CPUE data to 1992 (the oldest year with sufficient data) in two scenarios: (1) including a 1992−2018 time series using daily effort units and (2) including a 1992−2002 time series using both daily (pre-2003) and hourly (post-2003) effort units. Similarly, we tested including the deep-sea handline CPUE data as a single 1948−2018 time series using daily effort units. Finally, we tested the sensitivity of our results to an alternate model specification that included both the 1992−2018 and 1948−2018 time series for inshore and deep-sea handline gears, as well as using the Lorenzen M estimate.

Alternate model start year: The starting year of a model can sometimes have a significant impact on underlying population dynamics. This is especially true if the early years contain data of lesser quality that may skew certain population parameter estimates (e.g., R_0, recruitment deviations). We tested the impact of starting our Stock Synthesis model in 1970 as opposed to 1948 to ensure that it was not sensitive to the first few decades of data.

Alternate model specifications: We tested a few alternate specifications to our Stock Synthesis model to ensure that these did not have drastic impacts on our results. We ran alternative models with (1) time-varying catchability (q) as opposed to constant catchability, (2) effective sample size for the size-frequency data as suggested by Stock Synthesis, and (3) no diver survey data.

2.4 Reference points

The Fishery Ecosystem Plan for Hawaii (WPRFMC 2009), following guidelines from Restrepo et al. (1998), uses a Maximum Fishing Mortality Threshold (MFMT) defining overfishing as the fishing rate that leads to an equilibrium biomass that is below the Minimum Stock Size Threshold (MSST) of (1-M) × SSB_{msy}. In our model, SSB_{msy} is defined as the equilibrium spawner biomass at F_{msy}, where F_{msy} is the F that produces maximum equilibrium catch (i.e., MSY), which is found

through an iterative search algorithm in SS (Methot & Wetzel 2013). Note that when *SSB* falls below the MSST, management of the fishery would shift to using a rebuilding control rule, as represented in Figure 26.

2.5 Catch projections for 2020–2026

Stock projections for uku were conducted using the age-structured projection model software AGEPRO (Brodziak et al. 1998). Stochastic projections were conducted using results from the base-case model to evaluate the probable impacts of constant catch quotas on future spawning stock biomass and yield. For the projections, a series of constant catch quotas were run from 0 to 200 mt in one mt increments to provide the probability of overfishing in each year.

Initial conditions for the stochastic projections were based on the estimated initial population size-at-age in the year 2018 from the base case model. A total of 100 bootstrap replicates of the 2018 uku population size-at-age were calculated in SS to characterize the uncertainty in the initial population size. In each projection, 1000 total simulations were run for each bootstrap replicate to characterize the effects of process errors in future recruitment, life history, and fishery parameters. This gave 100,000 total simulated trajectories to evaluate the central tendency and variability of population and fishery quantities of interest (*SSB* and probability $F > F_{msy}$) in each projection.

Recruitment for the stochastic projections was based on three hypotheses about future recruitment processes. The first hypothesis was that future recruitment would be similar to recent short-term recruitment. This hypothesis was based on the observation that recruitment estimates have remained relatively high since 2000 and the expectation that this trend may continue in the near future (Thorson et al. 2014). In particular, the short-term recruitment scenario was based on resampling the empirical recruitment distribution of recruitment observed during 2000−2017. The AGEPRO recruitment sub-model 3 resampled the estimated recruitment from those 18 years with equal probability. Under the short-term recruitment scenario, the average recruitment was 91,444 age-1 fish with a CV of 27%. For each projection, 20% of the simulations were run using the short-term recruitment scenario. The second hypothesis was that future recruitment would be similar to the long-term recruitment pattern. The long-term recruitment scenario was based on resampling the empirical recruitment distribution of recruitment observed during 1949−2017. The AGEPRO recruitment sub-model 3 resampled the estimated recruitment from those 69 years with equal probability. Under the long-term recruitment scenario, the average recruitment was 72,220 age-1 fish with a CV of 30%. For each projection, 20% of the simulations were run using the long-term recruitment scenario. The third hypothesis was that recruitment would follow a Beverton-Holt stock-recruitment curve with lognormal deviations, which is the same assumption made in our SS model. AGEPRO parameterizes the Beverton-Holt stock-recruitment relationship as:

$$R = \frac{\alpha \cdot SSB}{\beta + SSB} \cdot e^w$$

Eq. 6

where,

$$\alpha = \frac{4hR_0}{5h-1} \quad \text{and} \quad \beta = \frac{B_0(1-h)}{5h-1}$$

<div align="right">Eq. 7 and 8</div>

as defined in Brodziak et al. (1998). Our alpha (α = 81.1) and beta (β = 78.6) parameters were derived from the steepness of h = 0.81, virgin recruitment of R_0 = 76.3 thousand recruits, and virgin SSB (i.e., SSB_0) of 1261.87 mt, all derived from our SS model. Since AGEPRO is a pooled-sex model while SS uses female-only SSB, we multiplied our β parameter by 2 to convert our female-only S-R curve to a male+female equivalent curve in AGEPRO (β_{AGEPRO} = 157.2). We also doubled our SSB_{msst} threshold in AGEPRO from 300.6 mt to 601.2 mt to control for this mismatch in model structure. The recruitment and SSB scaling parameters in AGEPRO were both set to 1000 given that our S-R relationship is in units of 1000s of fish and metric tons, while AGEPRO operates in units of individual fish and kilograms. The variability around the stock-recruitment curve was set to be equal to σ_R = 0.39 (inputted as a variance of 0.152) also from the SS base model. For each projection, 60% of the simulations used the stock-recruitment relationship to estimate future recruitment. We also ran an alternative projection scenario with a more pessimistic recruitment assumption, where recruitment was empirically resampled with replacement from the bottom 25th percentile of estimated recruitments between 1948 and 2018.

Fishery selectivity for the stochastic projections was based on the estimated selectivity in the base case model. All of the gear-specific fishery selectivities by size were logistic in the base case model; of these, only the commercial deep-sea handline fleet was estimated in the base case model. The catch data in AGEPRO were entered by individual fishing gear with their respective selectivity-at-age values provided from Stock Synthesis. For stochastic projections, fishery selectivity-at-age was sampled with a multiplicative lognormal process error with a mean of unity and a CV of 10% to represent uncertainty about future selectivity.

Life history parameters for the projections were based on the same values as were used in the base case model. This included age-invariant natural mortality, maturity at age, and mean spawning weights at age. Mean fishery catch weights-at-age were based upon the catch from each fleet as for selectivity-at-age inputs. For stochastic projections, life history parameters at age were sampled with a multiplicative lognormal process error with a mean of unity and a CV of 10% to represent uncertainty about future values, except natural mortality and maturity at age, which were sampled with a CV of 1%.

Catch-based projections ran from 2019 to 2026; total catch in 2019 was set to be the status quo catch (average in 2016−2018, 108 mt) based upon the assumption that 2019 catches would likely be similar to recent catch amounts. Annual catches during 2020−2026 were set to the projected catch. The maximum catch was set to give a 50% probability of overfishing in the final year of the projections.

3 Results

3.1 Base-case model

Results for the base-case model provided estimates of biological reference points for uku and annual estimates of total stock biomass, spawning stock biomass, recruitment, and fishing mortality, along with a Kobe plot indicating stock status over time. In this section, we first discuss model fit and diagnostics before presenting the results of the base-case model and projections.

3.1.1 Model diagnostics

Model convergence: All estimated parameters in the base case model were within the set bounds, the final gradient of the model was less than 0.0001, and the Hessian matrix for the parameter estimates was positive definite, which indicated that the model had converged to a local or global minimum. Results from 200 model runs with different random initial starting values for estimated parameters using the internal "jitter" routine in SS supported the result that a global minimum was obtained (i.e., there was no evidence of a lack of convergence to a global minimum, Figure 27). Seven of the 200 jitter model runs did not converge and were filtered out of Figure 27.

Likelihood profiling: Figure 28 presents the likelihood profile of the logarithm of the unfished recruitment parameter ($\log[R_0]$) for each data component. Detailed information on changes in negative log-likelihoods among the various fishery data sources is shown in Table 9, Table 10, and Figure 29.

Changes in the likelihood of each data component indicate how informative that component is to the overall estimated model fit. Our results showed that the estimation of the catch was the most informative likelihood components followed by the estimated recruitment deviations, fit to the size-frequency data, and fit to the abundance indices, respectively. There were also slight differences in the minimum negative log-likelihood along the R_0 axis among data likelihood components with abundance indices converging on R_0 = 4.2 and the catch and size-frequency components converging on R_0 = 4.3.

The change in negative log-likelihood of abundance indices was relatively small, particularly in the lower limit of the population scale. The deep-sea handline 1948−2002 index showed the largest changes in negative log-likelihood values across values of R_0 among abundance indices (max Δ 6.6), followed by the inshore handline index (max Δ 3.4), and the trolling index (max Δ 1.2). The 2003−2018 deep-sea handline index and diver surveys had lower likelihood changes (max Δ 1.1 and max Δ 0.2, respectively; Table 10, Figure 29).

Goodness-of-fit of abundance indices: Goodness-of-fit diagnostics are presented in Table 11 and plots of predicted and observed CPUE by gear type for the base case model are shown in Figure 30. Results showed that both deep-sea handline indices had an RMSE less than 0.3, which indicated that the model fit this CPUE index well. The inshore handline and trolling indices had an RSME approximately equal to 0.3 and the diver survey had an RSME greater than 0.3, which suggests that fits to these data were poorer.

Residuals analysis of size composition data: Comparisons between observed and expected mean values of size composition data (Francis 2011). Figure 31 showed that the expected mean weight values passed within 95% confidence intervals for all years.

There appeared to be little pattern in the residuals of the size composition data (Figure 32), although there were more small fish than expected in the 1970s to early 1980s, and there were higher positive residuals for the larger size classes. Assuming the standardized residuals were normally distributed, 95% of the measurements would fall within two standard deviations of the mean. Some Pearson residuals did not meet this criterion (Figure 32); in particular, very small fish in 1984−1986 and fish over 10 kg. Overall, the model fitted the weight modes in size composition data fairly well using the imputed effective sample sizes (Figure 33).

3.1.2 Stock assessment results

Given the uncertainty associated with the recreational catch (CV = 0.4), Stock Synthesis had substantial freedom in adjusting the observed values of catch in the fitting process. This resulted in some differences between the observed versus expected recreational catch. As shown in Figure 34, Stock Synthesis greatly reduced the high peaks in recreational catch seen in 2005 and 2012, which were likely sampling outliers. Interestingly, SS did not dramatically adjust the pre-2003 recreational catch estimates, with only a short period between 1972 and 1985 showing some positive adjustment in the catch estimates (Figure 34). Figures 35 and 36 present catch and fishing mortality broken down by fishing gear, respectively.

Estimates of population biomass (i.e., age 1 and older fish at the beginning of the year) increased from 1,243 mt in 1948 to a high of 1,420 mt in 1954, and then varied while generally declining to a low of 976 mt in 1996. The population biomass then increased to its largest value at around 1,700 metric tons in the final 3 years of the 2019 stock assessment time horizon (2016−2018; Table 12 and Figure 37). Over time, population biomass has generally varied between 1,000 mt and 1,500 mt (Figure 37).

Female spawning stock biomass (*SSB*) oscillated between 500 and 70 metric tons until the 1990s. *SSB* reached its lowest level of 464 metric tons in 1996 then increased to a high of 831 metric tons in 2017 (Table 12 and Figure 38). The time-series of *SSB* during the past decade averaged 714 metric tons or 57% of unfished *SSB* (1262 mt). Overall, *SSB* has been relatively stable until the 2000s when it began increasing to its current high level.

The estimated recruitment and stock-recruitment relationship were generally consistent with the biology of the stock and assumptions in the base case model. The recruitment deviations from the expected spawner-recruit curve appeared to be relatively well estimated and consistent with the expected distribution of recruitment deviations (Figure 39). Expected recruitment from the stock-recruitment relationship showed little evidence of a relationship between *SSB* and recruits (Figure 40). The change in recruitment bias was consistent with expectations and accounted for in the base case model (Figure 41). Recruitment (age-0 fish) estimates indicated a long-term fluctuation around a mean of approximately 72,000 with periodic strong recruitments (over 140,000 age-0 fish; Table 12 and Figure 42). The model estimated high recruitments in 1970−1971, 1982, 1988, 2002−2003, 2010−2011, and 2013−2014. Additionally, recruitment has

been above average and increasing since 2002. While the overall pattern of recruitment from 1975 to 2017 was variable, there was an apparent increasing trend in recruitment strength over time (Table 12 and Figure 42).

Over the assessment period, estimated fishing mortality (arithmetic average of F for ages 5−30) varied around 0.05 per year until the 1970s when it increased to a high of 0.19 per year in 1988 and then declined to 0.05 in the late 2000s. It has since varied between 0.05 and 0.08 per year (Table 12 and Figure 43).

Biological reference points: Biological reference points were computed from the Stock Synthesis base-case model. Based upon the Fishery Ecosystem Plan for Hawaii (WPRFMC 2009), F_{MSY} and B_{MSST} were used to assess relative stock status (Table 13). The point estimate of the maximum sustainable yield (*MSY*) was 93 metric tons. The point estimate of the female spawning stock biomass to produce *MSY* (SSB_{MSY}) was 334 metric tons and *SSB* at the Minimum Stock Size Threshold (SSB_{MSST}) was 301 metric tons. The point estimate of F_{MSY}, the fishing mortality rate to produce *MSY* on age-5 to age-30 fish, was 0.14 and the corresponding equilibrium value of spawning potential ratio at *MSY* (SPR_{MSY}) was 31%.

Stock status: Compared to the established FEP reference points, the current spawning biomass (2016−2018 average) was 272% of SSB_{MSST} and the current fishing mortality (average for ages 5−30 in 2016−2018) was 57% of F_{MSY}. The Kobe plot indicated that the main Hawaiian Islands uku stock is not currently overfished and is not subject to overfishing relative to the FEP reference points (Table 13, Figure 44).

Retrospective analysis: A retrospective analysis of the base case uku stock assessment model was conducted for the last 5 years of the assessment time horizon to evaluate whether there were any strong changes in parameter estimates through time. The results of the retrospective analysis are shown in Figure 45. The trajectories of estimated spawning stock biomass (as SSB/SSB_{MSST}) and fishing mortality (as F/F_{MSY}) showed there was a tendency for the base case model to overestimate spawning biomass in recent years. Additionally, the model appeared to have difficulty predicting the sharp increase in recruitment in the last 5 years, underestimating the final year in each of the retrospective runs compared to the base-case model (Figure 46). The estimated Mohn's rho for *SSB* was −0.04, which was between −0.15 and 0.20 and consequently indicated that the retrospective pattern was relatively small (Hurtado-Ferro et al. 2014; Carvalho et al. 2017). The Mohn's rho for recruitment and fishing mortality were −0.15 and 0.11, respectively.

3.2 Sensitivity scenarios

We ran 30 alternative model scenarios grouped in 11 categories: natural mortality (Figure 47), growth (Figure 48), maturity (Figure 49), recruitment variability (Figure 50), stock-recruitment steepness (Figure 51), recreational catch re-construction (Figure 52), CPUE index combinations (Figure 53), size-frequency data likelihood weight (Figure 54), CPUE time series alternatives (Figure 55), later model start time (Figure **56**), and alternative model specifications (Figure 57). These figures present comparisons of time series of spawning biomass, recruitment, and fishing mortality, as well as Kobe plots comparing stock status metrics in the terminal year. Overall,

modifying input parameters by +/- 10% did not significantly change our model results or stock status, except for the +10% L_{Amax} scenario (Figure 48), which resulted in significantly higher F values, low population biomass, and the incidence of overfishing in the terminal year. Using the Lorenzen M estimator drastically changed the number of recruits, but none of the other model results.

All scenarios related to recreational catch re-construction, CPUE index combinations, CPUE index time-series lengths, size-frequency data weighting, and model specifications did not significantly affect our model conclusions and current stock status (Figures 52 to 57). Key results for all sensitivity runs are presented in Table 14.

3.3 Projections

The six-year constant catch projection scenarios showed the distribution of outcomes in the probability of overfishing, spawning stock biomass, fishing mortality rates, and the probability of $SSB < SSB_{msst}$ that would occur under various catch scenarios in the MHI during 2020−2026 (Table 14 and Figure 58). Projections indicate that practically none of the catch scenarios explored would result in a probability of being overfished ($SSB/SSB_{MSST} < 1$; Figure 59). Our alternative catch projection that featured low recruitment levels (i.e., the "worst case" scenario) resulted in slightly lower sustainable catch levels (Table 17).

4 Discussion

This report presents the first integrated assessment of a coastal stock in the U.S. Pacific Islands region. Using the Stock Synthesis 3.30 software, we incorporated all available data sources related to the main Hawaiian Islands uku population into a single analytical framework. These data sources included both recreational and commercial catch data, catch-per-unit-effort indices from three main fishing gears, size-frequency data, abundance data from diver surveys, and local life-history parameters. The main conclusions from this integrated assessment are as follows:

- the uku stock is not currently overfished (SSB/SSB_{MSST} = 2.7)
- overfishing is not currently occurring (F/F_{MSY} = 0.57)

Furthermore, our analyses suggest that the uku stock was never in an overfished state during the period covered in this assessment (1948−2018), but that overfishing may have occurred for two years, in 1988 and 1989.

Our model appeared robust to uncertainty in the data and input parameters. One of the main sources of uncertainty was the lack of recreational catch data before 2003. In the base-case model, we re-created the pre-2003 recreational catch series by tying it to human population size trends in Hawaii (see section 2.2.1). However, we also tested four alternate recreational catch scenarios: (1) base recreational catch plus 30%, (2) base recreational catch minus 30%, (3) recent commercial catch (2003−2016) corrected for a bias associated with a decline in landline phone usage, and (4) recreational catch tied to the commercial catch using the ratio of commercial to recreational catch from 2003 to 2018. The last scenario was similar to how unreported catch was estimated in the Hawaii Deep 7 assessment (Langseth et al. 2018) and Kona crab assessment (Kapur et al. 2019). As shown in Figure 52, these different ways of re-creating the recreational catch did not significantly influence trends in population biomass, fishing mortality, and recruitment, and did not change our conclusions regarding stock status. Our model results also appeared robust to changes in CPUE time-series implementations (e.g., removing diver surveys, extending inshore handline to 1992, using a single catchability for deep-sea handline from 1948 to 2018), as shown in Figures 55 to 57. Furthermore, adding or removing 10% from natural mortality, length at maturity, recruitment variability, and stock-recruitment steepness did not significantly influence our model (see section 3.2). However, adding 10% to the L_{Amax} parameter (i.e., from 76.5 cm to 84.2 cm) did significantly change fishing mortality and stock status (Figure 48). This is not entirely surprising, as it is well known that fishing mortality rates inferred from size composition are very sensitive to L_{inf} (or L_{Amax}) (Hordyk et al. 2015). However, the L_{Amax} parameter used in the current assessment comes from an extensive age-length dataset (n = 419) collected in both the main Hawaiian Islands and the pristine Northwestern Hawaiian Islands. Figure 22 shows that the oldest measured uku (age 23−32 years) were all centered on the current L_{Amax} value of 76.5 cm, which suggests that this value is likely not biased by missing larger/older individuals. Of note, using the Lorenzen natural mortality estimator, which significantly increases natural mortality for age-0 fish, doubles the number of recruits in our model without changing other outcomes (Figure 47). In this particular scenario, the high early year M (~0.6) is simply balanced by increased recruitments in order to keep the model-estimated numbers-at-age in agreement with our various observational data types. Finally, we also ran an alternative catch projection scenario where future recruitment was resampled from the bottom 25th percentile of model-

estimated yearly recruitment between 1948 and 2018. This alternative projection scenario resulted in slightly lower catch limits, which suggests that our near-term catch projections are robust to lower recruitment forecasts.

The general trend of population abundance for uku in Hawaii has been of a steady decline from 1948 to the mid-1990s, followed by a 10-year period of stability, and an important increase in biomass from 2005 to the present (Figures 37 and 38). The decrease in catch and fishing mortality (Figures 6 and 43) from 1988 on likely explains some of this population increase, but most of it is modeled in stock synthesis as a period of strong positive recruitment starting in the early 2000s (Figures 39 and 42). Of note, another spike in recruitment in the early 1980s led to a notable peak in catch and CPUE in 1988, which is still remembered by fishers and scientists (D. Kobayashi and others, pers. comm.). It is not clear what could be driving this recent trend in strong recruitment. Besides global climate change, which has led to slowly increasing sea surface temperatures around Hawaii (http://hahana.soest.hawaii.edu/hot/), this recent trend in recruitment did not correlate with the Pacific Decadal Oscillation (PDO) index, the Southern Oscillation Index (SOI), or the Oceanic Niño Index (ONI). An alternative explanation for the positive biomass trend could be that the increase in CPUE that drives this pattern in our model was not due to an increase in uku abundance but to an increase in uku targeting by fishers and/or an increase in catchability by fishers in the deep-sea handline fleet due to improvements in fishing technology. For example, fishers can deploy deep-sea handlines in a configuration that targets Deep-7 bottomfish versus uku, even though both gear configurations would be reported as "deep-sea handline" in the reporting system. An increased interest in uku could thus lead to fishers deploying the uku gear configuration more often and thus lead to an increase in CPUE that is not related to an increase in abundance. However, we did control for species targeting in our CPUE standardization using the DPC approach (Winker et al. 2013). Furthermore, the same increasing CPUE pattern is seen in all three main fishing gears used to catch uku (Figure 17 and Figure 18), and the diver survey index does not contradict this pattern (Figure 30). These observations suggest that the increase in population biomass between 2004 and 2018 may be real and not an artifact related to targeting or other confounding variables.

4.1.1 Previous assessment

The 2017 assessment used a data-limited approach based on a mean-length total mortality model coupled with a relatively simple population model to determine current spawning potential ratio and Monte Carlo simulations to estimate parameter uncertainty (Nadon 2017). This assessment covered 27 species of reef fish in the main Hawaiian Islands, including uku. The 2016 WPSAR panel consensus report (Franklin 2016) made a series of general short- and long-term recommendations for future assessment, some of which are relevant to the current assessment. The two main recommendations relevant to the current approach were to use a 0.04 survivorship at maximum age (S) when estimating M and continue to improve the collection of local life history parameters, both of which were implemented.

The current results differ slightly from the 2017 assessment that used a data-limited approach based on mean length data only. The current assessment estimated a lower recent fishing mortality rate of around 0.08 vs. 0.15 for the 2017 assessment, although the 2017 mortality estimate was highly uncertain given the data-limited approach (CV = 0.5). Both assessments

reached a similar conclusion that overfishing was not currently occurring. The current overfishing limit (under the 2026 constant catch option) is higher than the 2017 overfishing limit based on catch-derived biomass (135 mt vs. 104 mt). Interestingly, the *SPR*-based F_{msy} proxy used in the 2017 assessment (F_{30} = 0.16) is reasonably close to the F_{msy} value estimated in the current integrated assessment (0.14).

4.1.2 Future directions

The Stock Assessment Program at the Pacific Islands Fisheries Science Center (PIFSC) will continue exploring and improving the use of Stock Synthesis for domestic stocks, including integrating potential new sources of data. For example, PIFSC has been conducting an annual Bottomfish Fishery-Independent Survey in Hawaii (BFISH program) since 2016. These surveys consist of a combination of research fishing and underwater stereo video cameras and cover the entirety of the main Hawaiian Islands. These surveys have been used to generate estimates of total biomass for the 2018 Deep 7 assessment, but they are unlikely to generate robust total biomass values for uku given that BFISH primarily targets bottom-dwelling, more sessile species. However, uku are frequently observed (or caught) on these surveys and could provide a new fishery-independent abundance index as well as an extra source of size composition data. This fishery-independent index would complement the ongoing PIFSC diver surveys, which only take place every three years and cover only a fraction of the uku habitat (depths <30 m).

4.1.3 GitHub repository

The data filtering, CPUE standardization, and Stock Synthesis base-case model input files are available on GitHub at the following address: https://github.com/PIFSCstockassessments/MHI-Uku-2020-Final

Acknowledgments

5 References

Alagaraja K. 1984. Simple methods for estimation of parameters for assessing exploited fish stocks. Indian Journal of Fisheries **31**:177–208.

Asher J, Williams ID, Harvey ES. 2017. An assessment of mobile predator populations along shallow and mesophotic depth gradients in the Hawaiian Archipelago. Scientific Reports:10.1038/s41598-017-03568–1.

Ayotte P, McCoy K, Heenan A, Williams I, Zamzow J. 2015. Coral Reef Ecosystem Program standard operating procedures: data collection for rapid ecological assessment fish surveys. Pacific Islands Fisheries Science Center. Administrative Report H-15-07.

Brodziak J, Rago P, Conser R. 1998. A general approach for making short-term stochastic projections from an age-structured fisheries assessment model. Pages 933–954 in F. Funk, T. Quinn II, J. Heifetz, J. Ianelli, J. Powers, J. Schweigert, P. Sullivan, and C. Zhang, editors. Fishery Stock Assessment Models. Alaska Sea Grant, University of Alaska Fairbanks.

Burnham KP. 2004. Multimodel inference: understanding AIC and BIC in model selection. Sociological Methods & Research **33**:261–304.

Carvalho F, Punt AE, Chang Y-J, Maunder MN, Piner KR. 2017. Can diagnostic tests help identify model misspecification in integrated stock assessments? Fisheries Research **192**:28–40.

Christie MR, Tissot BN, Albins MA, Beets JP, Jia Y, Ortiz DM, Thompson SE, Hixon MA. 2010. Larval Connectivity in an Effective Network of Marine Protected Areas. PLoS ONE **5**:e15715.

Dunn P, Smythe G. 1996. Randomized quantile residuals. Journal of Computational and graphical statistics **5**:236–244.

Everson AR, Williams A. 1989. Maturation and reproduction in two Hawaiian eteline snappers, uku, *Aprion virescens*, and onaga, *Etelis coruscans*. Fishery Bulletin **87**:877–888.

Francis CR, Hurst RJ, Renwick JA. 2003. Quantifying annual variation in catchability for commercial and research fishing. Fishery Bulletin **101**:293–304.

Francis RICC. 2011. Data weighting in statistical fisheries stock assessment models. Canadian Journal of Fisheries and Aquatic Sciences **68**:1124–1138.

Franklin EC. 2016. Benchmark review of the 2016 stock assessment of the Main Hawaiian Islands reef-associated fish: consensus panel report. Western Pacific Stock Assessment Review.

Hamnett M, Lui M, Johnson D. 2006. Fishing, ocean recreation, and threats to Hawaii's coral reefs. Hawaii Coral Reef Initiative, Honolulu.

Hewitt DA, Hoenig JM. 2005. Comparison of two approaches for estimating natural mortality based on longevity. Fishery Bulletin **103**:433–437.

Hordyk A, Ono K, Valencia S, Loneragan N, Prince J. 2015. A novel length-based empirical estimation method of spawning potential ratio (SPR), and tests of its performance, for small-scale, data-poor fisheries. ICES Journal of Marine Science **72**:217–231.

Hordyk AR, Ono K, Prince JD, Walters CJ. 2016. A simple length-structured model based on life history ratios and incorporating size-dependent selectivity: application to spawning potential ratios for data-poor stocks. Canadian Journal of Fisheries and Aquatic Sciences **73**:1787–1799.

Hurtado-Ferro F et al. 2015. Looking in the rear-view mirror: bias and retrospective patterns in integrated, age-structured stock assessment models. ICES Journal of Marine Science **72**:99–110.

Kapur M, Fitchett MD, Yau A, Carvalho F. 2019. 2018 benchmark stock assessment of Main Hawaiian Islands Kona crab. Page 114. NOAA technical memorandum NMFS-PIFSC 76.

Kenchington TJ. 2014. Natural mortality estimators for information-limited fisheries. Fish and Fisheries **15**:533–562.

Kittinger JN, Pandolfi JM, Blodgett JH, Hunt TL, Jiang H, Maly K, McClenachan LE, Schultz JK, Wilcox BA. 2011. Historical reconstruction reveals recovery in Hawaiian coral reefs. PLoS ONE **6**:e25460.

Langseth B, Syslo J, Yau A, Kapur M, Brodziak J. 2018. Stock assessment for the Main Hawaiian Islands Deep 7 bottomfish complex in 2018, with catch projections through 2022. U.S. Dept. of Commerce, NOAA Technical Memorandum NOAA-TM-NMFS-PIFSC-69, 217 p.

Lee H-H, Maunder MN, Piner KR, Methot RD. 2012. Can steepness of the stock–recruitment relationship be estimated in fishery stock assessment models? Fisheries Research **125–126**:254–261.

Lee H-H, Piner KR, Methot RD, Maunder MN. 2014. Use of likelihood profiling over a global scaling parameter to structure the population dynamics model: an example using blue marlin in the Pacific Ocean. Fisheries Research **158**:138–146.

Ma H. 2013. Catch estimates for major pelagic species from the Hawaii Marine Recreational Fishing Survey (2003-2011). PIFSC internal report IR-13-006.

Ma H, Ogawa TK. 2016. Hawaii Marine Recreational Fishing Survey: a summary of current sampling, estimation and data analyses. U.S. Dep. Commer., NOAA Tech. Memo., NOAA-TM-NMFS-PIFSC-55, 43p.

Maunder MN, Punt AE. 2004. Standardizing catch and effort data: a review of recent approaches. Fisheries Research **70**:141–159.

Methot RD. 2000. Technical description of the Stock Synthesis assessment program. U.S. Dept. Commer., NOAA Tech. Memo. NMFS-NWFSC-43, 46 p.

Methot RD, Taylor IG. 2011. Adjusting for bias due to variability of estimated recruitments in fishery assessment models. Canadian Journal of Fisheries and Aquatic Sciences **68**:1744–1760.

Methot RD, Wetzel CR. 2013. Stock Synthesis: A biological and statistical framework for fish stock assessment and fishery management. Fisheries Research **142**:86–99.

Meyer CG, Papastamatiou YP, Holland KN. 2007. Seasonal, diel, and tidal movements of green jobfish (*Aprion virescens*, Lutjanidae) at remote Hawaiian atolls: implications for marine protected area design. Marine Biology **151**:2133–2143.

Mohn R. 1999. The retrospective problem in sequential population analysis: an investigation using cod fishery and simulated data. ICES Journal of Marine Science **56**:473–488.

Nadon MO. 2017. Stock assessment of the coral reef fishes of Hawaii, 2016. Page 212. NOAA Tech. Memo. NOAA-TM-NMFS-PIFSC-60.

Nadon MO, Ault JS, Williams ID, Smith SG, DiNardo GT. 2015. Length-based assessment of coral reef fish populations in the Main and Northwestern Hawaiian Islands. PLoS ONE **10**:e0133960.

NMFS Office of Science and Technology. 2020. Marine Recreational Information Program, https://inport.nmfs.noaa.gov/inport/item/10906.

Pacific Islands Fisheries Science Center. 2020a. Hawaii DAR Fisherman Reporting System Data, https://inport.nmfs.noaa.gov/inport/item/5609.

Pacific Islands Fisheries Science Center. 2020b. Pacific Reef Assessment and Monitoring Program: Rapid Ecological Assessments of Fish Belt Transect Surveys (BLT) at Coral

Reef Sites across the Pacific Ocean from 2000 to 2009, https://inport.nmfs.noaa.gov/inport/item/5565.

Pacific Islands Fisheries Science Center. 2020c. Pacific Reef Assessment and Monitoring Program: Stratified Random Surveys (StRS) of Reef Fish, including Benthic Estimate Data at Coral Reef Sites across the Pacific Ocean from 2007 to 2012, https://inport.nmfs.noaa.gov/inport/item/34515.

Pelletier D, Ferraris J. 2000. A multivariate approach for defining fishing tactics from commercial catch and effort data. Canadian Journal of Fisheries and Aquatic Sciences **57**:51–65.

Pyle RL et al. 2016. A comprehensive investigation of mesophotic coral ecosystems in the Hawaiian Archipelago. PeerJ **4**:e2475.

Raîche G, Walls TA, Magis D, Riopel M, Blais J-G. 2013. Non-graphical solutions for Cattell's scree Test. Methodology **9**:23–29.

Restrepo VR et al. 1998. Technical guidance on the use of precautionary approaches in implementing national standard 1 of the Magnuson-Stevens Fishery Conservation and Management Act. NOAA Technical Memorandum NMFSF/ SPO-031, NOAA, USA: 54 pp.

Sabater MG, Kleiber P. 2013. Improving specification of acceptable biological catches of data-poor reef fish stocks using a biomass-augmented catch-MSY approach. Western Pacific Regional Fishery Management Council, Honolulu, HI.

Schnute J. 1981. A versatile growth model with statistically stable parameters. Canadian Journal of Fisheries and Aquatic Sciences **38**:1128–1140.

Sundberg M, Underkoffler K. 2011. Size composition and length-weight data for bottomfish and pelagic species in Honolulu, Hawaii. Admin report 11-04.

Then AY, Hoenig JM, Hall NG, Hewitt DA. 2015. Evaluating the predictive performance of empirical estimators of natural mortality rate using information on over 200 fish species. ICES Journal of Marine Science **72**:82–92.

Thorson JT. 2019. Predicting recruitment density dependence and intrinsic growth rate for all fishes worldwide using a data-integrated life-history model. Fish and Fisheries:10.1111/faf.12427.

Thorson JT, Jensen OP, Zipkin EF. 2014. How variable is recruitment for exploited marine fishes? A hierarchical model for testing life history theory. Canadian Journal of Fisheries and Aquatic Sciences **71**:973–983.

Toonen RJ et al. 2011. Defining boundaries for ecosystem-based management: a multispecies case study of marine connectivity across the Hawaiian Archipelago. Journal of Marine Biology **2011**:1–13.

Williamson DH et al. 2016. Large-scale, multidirectional larval connectivity among coral reef fish populations in the Great Barrier Reef Marine Park. Molecular Ecology **25**:6039–6054.

Winker H, Carvalho F, Kapur M. 2018. JABBA: Just Another Bayesian Biomass Assessment. Fisheries Research **204**:275–288.

Winker H, Kerwath SE, Attwood CG. 2013. Comparison of two approaches to standardize catch-per-unit-effort for targeting behaviour in a multispecies hand-line fishery. Fisheries Research **139**:118–131.

Winker H, Kerwath SE, Attwood CG. 2014. Proof of concept for a novel procedure to standardize multispecies catch and effort data. Fisheries Research **155**:149–159.

WPRFMC. 2009. Western Pacific Fishery Management Council [WPRFMC] - Fishery Ecosystem Plan for the Hawaii Archipelago. Available at: http://www.wpcouncil.org/fishery-plans-policies-reports/hawaii-fishery-ecosystem-plan.

Wren JLK, Kobayashi DR, Jia Y, Toonen RJ. 2016. Modeled Population Connectivity across the Hawaiian Archipelago. PLOS ONE **11**:e0167626.

Yau A. 2018. Report from Hawaii bottomfish commercial fishery data workshops, 2015-2016. NOAA Tech. Memo. NMFS-PIFSC-68, 105 p.

6 Tables

Table 1. Key model parameters, including some estimated by Stock Synthesis.

Parameter	Value	Comment	Source
Natural mortality (M)	0.10 yr^{-1}	Fixed. Assumes S=0.04	Derived from A_{max}
Reference age (A_{min})	3 yr	Model structure	O'Malley – pers. comm.
Maximum age (A_{max})	32 yr	Model structure	O'Malley – pers. comm.
Length at Amin (L_{Amin})	51.6 cm	Fixed	O'Malley – pers. comm.
Length at Amax (L_{Amax})	76.5 cm	Fixed	O'Malley – pers. comm.
Growth rate (K)	0.136 yr^{-1}	Fixed	O'Malley – pers. comm.
CV of length < L_{Amin}	0.12	Fixed	O'Malley – pers. comm.
CV of length > L_{Amin}	0.12	Fixed	O'Malley – pers. comm.
Length-weight σ	1.18e-05	Fixed	Sundberg & Underkoffler (2011)
Length-weight β	3.043	Fixed	Sundberg & Underkoffler (2011)
Length-at-50% maturity	44.8 cm	Fixed	Everson & Williams (1989)
Slope of maturity ogive	−3.44	Fixed	Everson & Williams (1989)
Spawner-recruit steepness (h)	0.81	Fixed	FishLife 2 - Thorson (2019)
Recruitment variability (σ_R)	0.39	Fixed	FishLife 2 - Thorson (2019)
Unfished log-scale recruitment (Log(R_0))	4.31	Estimated	Stock Synthesis model
Length 50% selectivity deep-sea handline	53.7 cm	Estimated	Stock Synthesis model
Length 95% selectivity deep-sea handline	74.6 cm	Estimated	Stock Synthesis model
Length 50% selectivity inshore handline	36.4 cm	Fixed	LBSPR model
Length 95% selectivity inshore handline	47.8 cm	Fixed	LBSPR model
Length 50% selectivity trolling	45.9 cm	Fixed	LBSPR model
Length 95% selectivity trolling	61.6 cm	Fixed	LBSPR model
Length 50% selectivity other	48.9 cm	Fixed	LBSPR model
Length 95% selectivity other	62.2 cm	Fixed	LBSPR model
Length 50% selectivity recreational	35.0 cm	Fixed	LBSPR model
Length 95% selectivity recreational	50.0 cm	Fixed	LBSPR model
Length 50% selectivity diver survey	45.9 cm	Fixed (trolling)	LBSPR model
Length 95% selectivity diver survey	61.6 cm	Fixed (trolling)	LBSPR model

Note: all lengths are fork lengths (FL)

Table 2. Main assumptions of the uku Stock Synthesis model with links to relevant report sections.

Model structure and assumptions	Report section
Single stock area corresponding to the entire main Hawaiian Islands (MHI)	1.2, 2.2.5
No sex differences in life history and abundance	2.2.5
Time-invariant life history parameters	-
Fecundity proportional to female biomass	2.2.5
Single spawning and recruitment period during the first month of the year	2.2.5
Beverton-Holt stock-recruitment curve with estimated lognormal annual deviations	2.2.5, 3.2
Steepness (h) fixed, not estimated within the model	2.2.5, 2.3.5, 3.2
Natural mortality (M) constant with age and linked to longevity with $S_{max\ age}$ = 0.04	2.2.5, 2.3.5, 3.2
Initial conditions derived from equilibrium catch and estimated in Stock Synthesis	2.2.5
Time-invariant selectivity	2.2.6
Multinomial error distribution for size-frequency data in Stock Synthesis	2.2.6, 2.3.5, 3.2
Size observations are random and representative of population size-frequency	2.2.6, 2.3.5
Time-invariant catchability	2.2.6, 2.3.5, 3.2
Fishing mortality estimated as continuous full parameters	2.2.6
Recreational catch is highly uncertain, commercial catch has greater certainty	2.2.6, 2.3.5, 3.2
CPUE tied to population abundance	2.2.2, 2.3.5, 3.2
Diver survey index tied to population abundance	2.2.4, 2.3.5, 3.2
CPUE coefficients of variation (CV) artificially low and increased by 10% in model	2.2.6, 2.3.5, 3.2
Projection recruitment: 60% S-R curve, 20% recent, and 20% long-term	2.5, 3.3

Table 3. Summary of commercial and recreational catch data for uku (table continued on next page).

Year	Commercial (metric tons)				Recreational (metric tons)
	Deep-sea handline	Inshore handline	Trolling	Other gears	
1948	40.4	4.33	0.04	1.27	23.7
1949	33.0	3.42	0.24	1.02	23.7
1950	22.8	2.83	0.00	0.65	23.1
1951	16.1	3.43	0.02	0.92	24.2
1952	25.0	3.81	0.02	0.62	23.8
1953	22.6	9.22	0.00	1.00	23.6
1954	16.6	10.09	0.00	1.45	23.8
1955	14.3	12.30	0.01	7.93	25.5
1956	19.2	12.15	0.00	0.75	26.4
1957	37.3	5.93	0.00	0.53	27.3
1958	28.8	3.56	0.00	0.54	28.0
1959	18.4	1.90	0.00	0.61	28.9
1960	17.2	2.35	0.00	1.02	30.2
1961	15.8	2.86	0.00	0.48	30.5
1962	23.4	3.43	0.02	2.06	32.2
1963	24.8	3.10	0.02	0.87	31.5
1964	40.0	0.48	0.00	0.31	32.3
1965	22.2	0.24	0.00	0.23	33.2
1966	26.1	0.01	0.00	0.14	33.7
1967	26.0	0.38	0.04	0.13	33.9
1968	22.1	0.03	0.03	0.37	33.7
1969	25.5	0.02	0.01	0.61	36.5
1970	21.3	0.01	0.00	0.25	36.6
1971	21.8	0.01	0.02	0.30	36.7
1972	21.5	0.02	0.12	0.21	38.6
1973	30.0	0.05	0.10	0.18	39.1
1974	34.9	0.09	0.16	0.19	41.2
1975	26.6	0.75	0.52	0.30	41.8
1976	23.6	3.20	0.62	0.73	43.0
1977	25.0	3.58	0.82	1.64	43.3
1978	28.0	8.29	0.16	1.72	43.0
1979	36.1	1.85	0.42	1.18	45.7
1980	31.8	0.55	0.69	0.83	45.2
1981	36.7	0.27	0.30	1.35	46.6
1982	43.9	0.31	0.61	0.96	46.4
1983	56.3	0.61	1.33	1.86	47.1
1984	61.5	0.11	0.51	0.87	48.4
1985	21.7	0.25	0.12	0.33	49.4
1986	36.8	4.20	0.68	5.56	51.2

| Year | Commercial (metric tons) | | | | Recreational (metric tons) |
	Deep-sea handline	Inshore handline	Trolling	Other gears	
1987	21.4	2.85	0.67	0.86	49.7
1988	145.2	4.81	2.64	3.62	51.3
1989	90.9	1.34	1.59	0.69	51.3
1990	39.3	2.07	2.83	0.99	52.3
1991	32.0	5.11	2.64	1.24	53.3
1992	31.2	6.76	0.91	0.97	53.6
1993	27.8	2.19	0.64	1.12	54.2
1994	26.3	5.18	0.33	0.78	54.6
1995	23.7	2.19	0.73	0.61	56.5
1996	18.6	3.91	0.82	0.84	55.4
1997	21.6	7.97	0.61	0.63	56.2
1998	20.0	6.37	0.48	0.85	56.3
1999	34.0	5.31	0.57	0.90	55.5
2000	30.5	5.87	0.78	0.64	57.1
2001	17.5	6.97	1.47	0.59	58.4
2002	19.2	4.36	0.60	1.38	57.3
2003	14.4	2.93	2.46	1.06	50.2
2004	26.1	3.57	3.71	1.52	65.8
2005	20.3	2.44	4.23	1.89	84.8
2006	17.4	4.33	3.23	2.03	48.7
2007	20.7	5.21	3.81	1.67	30.0
2008	28.6	5.89	5.80	1.66	19.8
2009	30.2	4.84	2.52	2.33	25.1
2010	37.8	7.83	4.22	4.97	45.2
2011	34.8	8.29	2.88	3.64	58.6
2012	34.4	8.98	4.82	4.82	93.8
2013	34.6	8.60	5.46	6.28	26.9
2014	25.8	5.51	5.53	7.11	47.9
2015	29.5	5.71	3.92	7.10	32.7
2016	33.3	5.23	6.56	8.99	26.8
2017	38.8	7.70	6.91	6.44	58.6
2018	15.4	7.74	4.18	6.54	90.7

Table 4. List of predictor variables considered for the logistic and lognormal regression models used for CPUE standardization. Dashes represent variables not available for a model and "Errors" indicate variables resulting in model convergence errors.

| | 1948-2002 | | 2003-2018 | | | | | |
| | Deep-sea handline | | Deep-sea handline | | Inshore handline | | Trolling | |
Predictor	Logistic	Lognormal	Logistic	Lognormal	Logistic	Lognormal	Logistic	Lognormal
Year	Y	Y	Y	Y	Y	Y	Y	Y
Fisher	Errors	Y	Errors	Y	Errors	Y	Errors	Y
Area	Y	Y	Y	Y	Y	Y	Y	Y
Month	Y	Y	Y	Y	Y	Y	Y	Y
Log(cumulative experience)	N	N	Y	N	N	N	Y	N
Wind speed	-	-	N	Y	N	Y	Y	Y
PC1	Y	Y	Y	Y	Y	Y	Y	Y
PC1^2	Y	Y	Y	Y	Y	Y	Y	Y
PC2	Y	N	Y	N	Y	Y	Y	Y
PC2^2	Y	N	Y	N	Y	Y	Y	Y
Area:month	N	Y	N	N	N	N	N	N
Year:Area	Errors	Errors	Errors	Errors	Errors	Errors	Errors	Errors

Table 5. Akaike information criterion (AIC), delta AIC, and percent AIC change from the previous model, used for CPUE standardization model selection (deep-sea handline). The final selected model is shown in bold.

Model	AIC	ΔAIC	AIC change (%)
1948-2002 Lognormal			
log(CPUE) ~ 1	145484	19559	
log(CPUE) ~ YEAR	145030	19105	0.3
log(CPUE) ~ YEAR + (1|FISHER)	132459	6534	8.7
log(CPUE) ~ YEAR + (1|FISHER) + AREA	129512	3587	2.2
log(CPUE) ~ YEAR + (1|FISHER) + AREA + MONTH	128031	2106	1.1
log(CPUE) ~ YEAR + (1|FISHER) + AREA*MONTH	127518	1593	0.4
log(CPUE) ~ YEAR + (1|FISHER) + AREA + MONTH + log(CUM_EXP)	127945	2020	-0.3
log(CPUE) ~ YEAR + (1|FISHER) + AREA + MONTH + log(CUM_EXP) + PC1	126253	328	1.3
log(CPUE) ~ YEAR + (1|FISHER) + AREA + MONTH + log(CUM_EXP) + poly(PC1,2)	126127	202	0.1
log(CPUE) ~ YEAR + (1|FISHER) + AREA + MONTH + log(CUM_EXP) + poly(PC1,2) + PC2	126132	207	0.0
log(CPUE) ~ YEAR + (1|FISHER) + AREA + MONTH + log(CUM_EXP) + poly(PC1,2) + poly(PC2,2)	126125	200	0.0
log(CPUE) ~ YEAR + (1|FISHER) + AREA*MONTH + poly(PC1,2)	125925	0	
1948-2002 Logistic			
PRES ~ 1	94464	34603	0.0
PRES ~ YEAR	90175	30313	4.5
PRES ~ YEAR + AREA	81257	21395	9.9
PRES ~ YEAR + AREA + MONTH	81159	21297	0.1
PRES ~ YEAR + AREA + MONTH + log(CUM_EXP)	81158	21297	0.0
PRES ~ YEAR + AREA + MONTH + log(CUM_EXP) + PC1	70351	10489	13.3
PRES ~ YEAR + AREA + MONTH + log(CUM_EXP) + poly(PC1,2)	64959	5098	7.7
PRES ~ YEAR + AREA + MONTH + log(CUM_EXP) + poly(PC1,2) + PC2	62247	2386	4.2
PRES ~ YEAR + AREA + MONTH + log(CUM_EXP) + poly(PC1,2) + poly(PC2,2)	59862	0	3.8
PRES ~ YEAR + AREA + MONTH + poly(PC1,2) + poly(PC2,2)	59885	24	
2003-2018 Lognormal			
log(CPUE) ~ 1	37236	6822	
log(CPUE) ~ YEAR	37206	6792	0.1
log(CPUE) ~ YEAR + (1|FISHER)	32867	2453	11.7
log(CPUE) ~ YEAR + (1|FISHER) + AREA	32760	2346	0.3
log(CPUE) ~ YEAR + (1|FISHER) + AREA + MONTH	31908	1494	2.6
log(CPUE) ~ YEAR + (1|FISHER) + AREA * MONTH	31996	1582	-0.3
log(CPUE) ~ YEAR + (1|FISHER) + AREA + MONTH + SPEED	31911	1497	0.3
log(CPUE) ~ YEAR + (1|FISHER) + AREA + MONTH + SPEED + log(CUM_EXP)	31919	1506	0.0
log(CPUE) ~ YEAR + (1|FISHER) + AREA + MONTH + SPEED + log(CUM_EXP) + PC1	30443	29	4.6
log(CPUE) ~ YEAR + (1|FISHER) + AREA + MONTH + SPEED + log(CUM_EXP) + poly(PC1,2)	30418	5	0.1
log(CPUE) ~ YEAR + (1|FISHER) + AREA + MONTH + SPEED + log(CUM_EXP) + poly(PC1,2) + PC2	30414	0	0.0
log(CPUE) ~ YEAR + (1|FISHER) + AREA + MONTH + SPEED + log(CUM_EXP) + poly(PC1,2) + poly(PC2,2)	30422	8	0.0
log(CPUE) ~ YEAR + (1|FISHER) + AREA + MONTH + SPEED + poly(PC1,2)	30417	3	
2003-2018 Logistic			
PRES ~ 1	53875	13001	
PRES ~ YEAR	53688	12814	0.3
PRES ~ YEAR + AREA	49111	8237	8.5
PRES ~ YEAR + AREA + MONTH	46898	6024	4.5
PRES ~ YEAR + AREA + MONTH + SPEED	46872	5998	0.1
PRES ~ YEAR + AREA + MONTH + SPEED + log(CUM_EXP)	46538	5664	0.7
PRES ~ YEAR + AREA + MONTH + SPEED + log(CUM_EXP) + PC1	43214	2340	7.1
PRES ~ YEAR + AREA + MONTH + SPEED + log(CUM_EXP) + poly(PC1,2)	42860	1986	0.8
PRES ~ YEAR + AREA + MONTH + SPEED + log(CUM_EXP) + poly(PC1,2) + PC2	41141	267	4.0
PRES ~ YEAR + AREA + MONTH + SPEED + log(CUM_EXP) + poly(PC1,2) + poly(PC2,2)	40874	1	0.6
PRES ~ YEAR + AREA + MONTH + log(CUM_EXP) + poly(PC1,2) + poly(PC2,2)	40874	0	

Table 6. Akaike information criterion (AIC), delta AIC, and percent AIC change from the previous model, used for CPUE standardization model selection (inshore handline). The final selected model is shown in bold.

Model	AIC	ΔAIC	AIC change (%)
2003-2018 Lognormal			
log(CPUE) ~ 1	13075	2468	
log(CPUE) ~ YEAR	12971	2364	0.8
log(CPUE) ~ YEAR + (1|FISHER)	10964	356	15.5
log(CPUE) ~ YEAR + (1|FISHER) + AREA	10874	267	0.8
log(CPUE) ~ YEAR + (1|FISHER) + AREA + MONTH	10913	305	-0.4
log(CPUE) ~ YEAR + (1|FISHER) + AREA * MONTH	10963	356	-0.5
log(CPUE) ~ YEAR + (1|FISHER) + AREA + MONTH + SPEED	10919	312	0.4
log(CPUE) ~ YEAR + (1|FISHER) + AREA + MONTH + SPEED + log(CUM_EXP)	10927	319	-0.1
log(CPUE) ~ YEAR + (1|FISHER) + AREA + MONTH + SPEED + log(CUM_EXP) + PC1	10765	157	1.5
log(CPUE) ~ YEAR + (1|FISHER) + AREA + MONTH + SPEED + log(CUM_EXP) + poly(PC1,2)	10773	165	-0.1
log(CPUE) ~ YEAR + (1|FISHER) + AREA + MONTH + SPEED + log(CUM_EXP) + poly(PC1,2) + PC2	10778	170	0.0
log(CPUE) ~ YEAR + (1|FISHER) + AREA + MONTH + SPEED + log(CUM_EXP) + poly(PC1,2) + poly(PC2,2)	10615	8	1.5
log(CPUE) ~ YEAR + (1|FISHER) + AREA + MONTH + SPEED + poly(PC1,2) + poly(PC2,2)	10607	0	
2003-2018 Logistic			
PRES ~ 1	28932	9538	
PRES ~ YEAR	28681	9287	0.9
PRES ~ YEAR + AREA	23041	3647	19.7
PRES ~ YEAR + AREA + MONTH	23021	3627	0.1
PRES ~ YEAR + AREA + MONTH + SPEED	23000	3606	0.1
PRES ~ YEAR + AREA + MONTH + SPEED + log(CUM_EXP)	22983	3590	0.1
PRES ~ YEAR + AREA + MONTH + SPEED + log(CUM_EXP) + PC1	21971	2577	4.4
PRES ~ YEAR + AREA + MONTH + SPEED + log(CUM_EXP) + poly(PC1,2)	21094	1700	4.0
PRES ~ YEAR + AREA + MONTH + SPEED + log(CUM_EXP) + poly(PC1,2) + PC2	20055	661	4.9
PRES ~ YEAR + AREA + MONTH + SPEED + log(CUM_EXP) + poly(PC1,2) + poly(PC2,2)	19394	0	3.3
PRES ~ YEAR + AREA + MONTH + poly(PC1,2) + poly(PC2,2)	19556	163	

Table 7. Akaike information criterion (AIC), delta AIC, and percent AIC change from the previous model, used for CPUE standardization model selection (trolling). The final selected model is shown in bold.

Model	AIC	ΔAIC	AIC change (%)
2003-2018 Lognormal			
log(CPUE) ~ 1	7676	1592	
log(CPUE) ~ YEAR	7686	1602	-0.1
log(CPUE) ~ YEAR + (1|FISHER)	6192	108	19.4
log(CPUE) ~ YEAR + (1|FISHER) + AREA	6167	83	0.4
log(CPUE) ~ YEAR + (1|FISHER) + AREA + MONTH	6210	126	-0.7
log(CPUE) ~ YEAR + (1|FISHER) + AREA * MONTH	6264	180	-0.9
log(CPUE) ~ YEAR + (1|FISHER) + AREA + MONTH + SPEED	6206	122	0.9
log(CPUE) ~ YEAR + (1|FISHER) + AREA + MONTH + SPEED + log(CUM_EXP)	6214	130	-0.1
log(CPUE) ~ YEAR + (1|FISHER) + AREA + MONTH + SPEED + log(CUM_EXP) + PC1	6211	127	0.0
log(CPUE) ~ YEAR + (1|FISHER) + AREA + MONTH + SPEED + log(CUM_EXP) + poly(PC1,2)	6147	62	1.0
log(CPUE) ~ YEAR + (1|FISHER) + AREA + MONTH + SPEED + log(CUM_EXP) + poly(PC1,2) + PC2	6150	66	-0.1
log(CPUE) ~ YEAR + (1|FISHER) + AREA + MONTH + SPEED + log(CUM_EXP) + poly(PC1,2) + poly(PC2,2)	6134	50	0.3
log(CPUE) ~ YEAR + (1|FISHER) + AREA + SPEED + poly(PC1,2) + poly(PC2,2)	6084	0	
2003-2018 Logistic			
PRES ~ 1	31174	6275	
PRES ~ YEAR	30861	5961	1.0
PRES ~ YEAR + AREA	26217	1317	15.0
PRES ~ YEAR + AREA + MONTH	25921	1021	1.1
PRES ~ YEAR + AREA + MONTH + SPEED	25893	993	0.1
PRES ~ YEAR + AREA + MONTH + SPEED + log(CUM_EXP)	25865	966	0.1
PRES ~ YEAR + AREA + MONTH + SPEED + log(CUM_EXP) + PC1	25741	841	0.5
PRES ~ YEAR + AREA + MONTH + SPEED + log(CUM_EXP) + poly(PC1,2)	25257	357	1.9
PRES ~ YEAR + AREA + MONTH + SPEED + log(CUM_EXP) + poly(PC1,2) + PC2	25241	341	0.1
PRES ~ YEAR + AREA + MONTH + SPEED + log(CUM_EXP) + poly(PC1,2) + poly(PC2,2)	24900	0	1.4
PRES ~ YEAR + AREA + MONTH + SPEED + log(CUM_EXP) + poly(PC1,2) + poly(PC2,2)	24900	0	

Table 8. Mean and CV of CPUE relative abundance indices used in the base-case model for MHI uku. CVs are estimated from the standardization process (not variance adjusted). Table continued on next page.

Year	Deep-sea Handline Old		Deep-Sea Handline Recent		Inshore Handline Recent		Trolling Recent		Diver Survey	
	Mean	CV	Mean	CV	Mean	CV	Mean	CV	Mean	CV
1948	9.70	0.07	-	-	-	-	-	-	-	-
1949	9.43	0.07	-	-	-	-	-	-	-	-
1950	8.80	0.09	-	-	-	-	-	-	-	-
1951	8.55	0.10	-	-	-	-	-	-	-	-
1952	9.00	0.10	-	-	-	-	-	-	-	-
1953	12.13	0.10	-	-	-	-	-	-	-	-
1954	11.81	0.10	-	-	-	-	-	-	-	-
1955	11.31	0.11	-	-	-	-	-	-	-	-
1956	10.07	0.12	-	-	-	-	-	-	-	-
1957	11.54	0.11	-	-	-	-	-	-	-	-
1958	13.15	0.10	-	-	-	-	-	-	-	-
1959	7.95	0.10	-	-	-	-	-	-	-	-
1960	7.37	0.10	-	-	-	-	-	-	-	-
1961	7.75	0.10	-	-	-	-	-	-	-	-
1962	8.73	0.11	-	-	-	-	-	-	-	-
1963	9.62	0.09	-	-	-	-	-	-	-	-
1964	9.01	0.09	-	-	-	-	-	-	-	-
1965	8.55	0.09	-	-	-	-	-	-	-	-
1966	8.49	0.08	-	-	-	-	-	-	-	-
1967	7.18	0.09	-	-	-	-	-	-	-	-
1968	8.53	0.09	-	-	-	-	-	-	-	-
1969	8.00	0.08	-	-	-	-	-	-	-	-
1970	7.95	0.09	-	-	-	-	-	-	-	-
1971	7.99	0.09	-	-	-	-	-	-	-	-
1972	9.40	0.09	-	-	-	-	-	-	-	-
1973	9.97	0.08	-	-	-	-	-	-	-	-
1974	11.11	0.08	-	-	-	-	-	-	-	-
1975	10.32	0.09	-	-	-	-	-	-	-	-
1976	9.41	0.62	-	-	-	-	-	-	-	-
1977	7.63	0.08	-	-	-	-	-	-	-	-
1978	11.89	0.08	-	-	-	-	-	-	-	-
1979	10.73	0.08	-	-	-	-	-	-	-	-
1980	9.12	0.07	-	-	-	-	-	-	-	-
1981	8.53	0.07	-	-	-	-	-	-	-	-
1982	7.93	0.07	-	-	-	-	-	-	-	-
1983	8.05	0.07	-	-	-	-	-	-	-	-
1984	7.18	0.07	-	-	-	-	-	-	-	-

Year	Deep-sea Handline Old		Deep-Sea Handline Recent		Inshore Handline Recent		Trolling Recent		Diver Survey	
	Mean	CV	Mean	CV	Mean	CV	Mean	CV	Mean	CV
1985	6.34	0.08	-	-	-	-	-	-	-	-
1986	8.09	0.08	-	-	-	-	-	-	-	-
1987	6.82	0.08	-	-	-	-	-	-	-	-
1988	11.74	0.07	-	-	-	-	-	-	-	-
1989	8.21	0.08	-	-	-	-	-	-	-	-
1990	6.42	0.08	-	-	-	-	-	-	-	-
1991	6.56	0.08	-	-	-	-	-	-	-	-
1992	7.08	0.08	-	-	-	-	-	-	-	-
1993	7.29	0.08	-	-	-	-	-	-	-	-
1994	6.59	0.08	-	-	-	-	-	-	-	-
1995	6.19	0.08	-	-	-	-	-	-	-	-
1996	6.11	0.08	-	-	-	-	-	-	-	-
1997	6.75	0.08	-	-	-	-	-	-	-	-
1998	6.01	0.08	-	-	-	-	-	-	-	-
1999	7.37	0.08	-	-	-	-	-	-	-	-
2000	7.29	0.08	-	-	-	-	-	-	-	-
2001	7.03	0.08	-	-	-	-	-	-	-	-
2002	6.10	0.09	-	-	-	-	-	-	-	-
2003	-	-	0.79	0.07	0.60	0.12	0.03	0.16	-	-
2004	-	-	1.06	0.06	0.95	0.11	0.04	0.16	-	-
2005	-	-	1.04	0.07	0.90	0.12	0.05	0.16	0.01	0.54
2006	-	-	1.02	0.07	1.26	0.12	0.03	0.16	-	-
2007	-	-	1.20	0.06	1.38	0.11	0.04	0.17	-	-
2008	-	-	1.19	0.06	1.08	0.11	0.05	0.16	0.12	0.50
2009	-	-	0.91	0.07	0.83	0.11	0.04	0.16	-	-
2010	-	-	1.32	0.06	1.15	0.11	0.08	0.16	0.08	0.43
2011	-	-	1.20	0.06	1.31	0.11	0.07	0.16	-	-
2012	-	-	1.10	0.07	1.35	0.10	0.07	0.15	0.04	0.21
2013	-	-	1.39	0.06	1.37	0.11	0.12	0.15	-	-
2014	-	-	1.25	0.07	1.54	0.12	0.11	0.15	-	-
2015	-	-	1.64	0.07	1.76	0.11	0.09	0.16	0.04	0.36
2016	-	-	1.60	0.07	1.92	0.12	0.09	0.17	0.05	0.30
2017	-	-	1.73	0.07	2.82	0.14	0.10	0.18	-	-
2018	-	-	1.47	0.09	3.27	0.12	0.06	0.21	-	-

Table 9. Negative log-likelihoods (NLL) of data components in the base case model over a range of fixed levels of virgin recruitment in thousands of recruits in log-scale, $\log(R_0)$. Likelihoods are relative to the minimum NLL (best-fit) for each respective data component. Colors indicate relative likelihood (green: low NLL and better-fit; red: high NLL and poorer-fit). The maximum likelihood estimate of $\log(R_0)$ was 4.31.

Log(R0)	Total	Recruitment	Catch	SizeFreq	Survey
3.6	125.00	56.00	44.35	17.48	7.47
3.7	90.64	36.01	36.23	12.70	6.00
3.8	60.97	20.63	26.46	9.72	4.45
3.9	37.24	10.60	16.35	7.87	2.71
4	20.05	4.98	8.25	5.91	1.21
4.1	8.88	2.04	3.25	3.57	0.31
4.2	2.64	0.64	0.83	1.46	0.00
4.3	0.16	0.09	0.04	0.19	0.14
4.33491	0.00	0.02	0.00	0.00	0.28
4.4	0.50	0.00	0.14	0.02	0.64
4.5	2.91	0.19	0.63	0.96	1.43
4.6	6.78	0.53	1.17	2.90	2.48
4.7	11.62	0.95	1.53	5.64	3.78
4.8	17.01	1.41	1.62	9.00	5.28
4.9	22.63	1.85	1.43	12.73	6.91
5	28.23	2.27	1.03	16.62	8.59

Table 10. Negative log-likelihoods (NLL) of abundance index data components in the base case model over a range of fixed levels of virgin recruitment in thousands of recruits in log-scale, $\log(R_0)$. Likelihoods are relative to the minimum NLL (best-fit) for each respective data component. Colors indicate relative likelihood (green: low NLL and better-fit; red: high NLL and poorer-fit). The maximum likelihood estimate of $\log(R_0)$ was 4.31.

Log(R_0)	Total	DSH_old	DSH_recent	ISH_recent	Trol_recent	Divers
3.6	7.47	2.37	1.12	3.38	1.24	0.01
3.7	6.00	1.71	0.93	3.10	0.90	0.00
3.8	4.45	1.06	0.75	2.64	0.63	0.01
3.9	2.71	0.48	0.54	1.92	0.36	0.05
4	1.21	0.11	0.36	1.12	0.15	0.11
4.1	0.31	0.00	0.24	0.51	0.04	0.16
4.2	0.00	0.13	0.15	0.16	0.00	0.20
4.3	0.14	0.45	0.09	0.02	0.00	0.22
4.335	0.28	0.61	0.07	0.00	0.01	0.22
4.4	0.64	0.95	0.05	0.01	0.04	0.23
4.5	1.43	1.59	0.02	0.11	0.12	0.24
4.6	2.48	2.37	0.00	0.28	0.23	0.24
4.7	3.78	3.29	0.00	0.52	0.37	0.24
4.8	5.28	4.32	0.02	0.79	0.53	0.24
4.9	6.91	5.43	0.06	1.09	0.71	0.24
5	8.59	6.57	0.11	1.40	0.90	0.24

Table 11. Mean input log standard error (SE), additional variance added within the model with resulting total log(SE), and root-mean-square-errors (RMSE) for the relative abundance indices used in the base-case model.

Fleet	N	Input log(SE)	Variance adjustment	Total log(SE) in model	RMSE
CPUE_DSH_old	55	0.09	0.1	0.19	0.13
CPUE_DSH_recent	16	0.07	0.1	0.17	0.12
CPUE_ISH_recent	16	0.12	0.1	0.22	0.28
CPUE_Trol_recent	16	0.16	0.1	0.26	0.30
OPUE_Divers	6	0.28	0.1	0.38	0.35

Table 12. Time series of total biomass (age 1 and older), spawning biomass, age-0 recruitment, and instantaneous fishing mortality estimated in the base-case model. CV = coefficient of variation. Table continued on next page.

Year	Age 1+ biomass (mt) Mean	Spawning Biomass (mt) Mean	CV	Recruitment (1000s recruits) Mean	CV	Fishing mortality (yr^-1) Mean	CV
1948	1243	589	0.16	71	0.35	0.06	0.21
1949	1291	617	0.15	65	0.35	0.05	0.22
1950	1326	637	0.15	66	0.35	0.04	0.25
1951	1364	657	0.14	63	0.35	0.03	0.28
1952	1397	674	0.14	56	0.34	0.04	0.24
1953	1416	685	0.14	53	0.33	0.04	0.23
1954	1420	689	0.14	48	0.33	0.04	0.25
1955	1417	689	0.14	48	0.32	0.04	0.24
1956	1397	680	0.14	51	0.32	0.04	0.25
1957	1371	668	0.14	48	0.32	0.05	0.23
1958	1331	647	0.14	49	0.32	0.05	0.27
1959	1300	632	0.14	51	0.33	0.04	0.31
1960	1278	621	0.14	52	0.32	0.04	0.31
1961	1256	610	0.14	52	0.32	0.04	0.32
1962	1239	601	0.14	51	0.32	0.05	0.28
1963	1213	588	0.14	56	0.32	0.05	0.29
1964	1187	575	0.14	62	0.32	0.07	0.26
1965	1152	556	0.15	60	0.32	0.05	0.32
1966	1142	550	0.15	56	0.33	0.06	0.30
1967	1136	547	0.15	67	0.33	0.06	0.30
1968	1129	544	0.14	71	0.33	0.05	0.32
1969	1128	540	0.14	72	0.34	0.06	0.30
1970	1136	543	0.14	99	0.32	0.05	0.32
1971	1157	552	0.14	90	0.32	0.06	0.32
1972	1188	561	0.14	63	0.33	0.05	0.32
1973	1241	589	0.14	55	0.33	0.06	0.29
1974	1267	609	0.13	70	0.32	0.07	0.29
1975	1256	606	0.13	89	0.29	0.06	0.32
1976	1249	599	0.13	65	0.31	0.06	0.33
1977	1257	599	0.13	62	0.30	0.07	0.30
1978	1271	611	0.13	74	0.27	0.07	0.30
1979	1254	603	0.13	63	0.27	0.08	0.30
1980	1231	590	0.13	76	0.25	0.08	0.32
1981	1219	586	0.13	63	0.26	0.08	0.30
1982	1199	574	0.13	109	0.21	0.09	0.28
1983	1183	566	0.13	86	0.26	0.10	0.25

Year	Age 1+ biomass (mt) Mean	Spawning Biomass (mt) Mean	CV	Recruitment (1000s recruits) Mean	CV	Fishing mortality (yr⁻¹) Mean	CV
1984	1160	545	0.13	73	0.28	0.10	0.23
1985	1172	555	0.13	51	0.30	0.06	0.31
1986	1203	574	0.13	53	0.28	0.08	0.24
1987	1189	574	0.13	70	0.27	0.06	0.29
1988	1177	568	0.12	133	0.21	0.19	0.17
1989	1047	497	0.14	54	0.32	0.16	0.21
1990	1006	464	0.15	60	0.30	0.10	0.26
1991	1045	499	0.14	64	0.30	0.10	0.27
1992	1027	491	0.14	58	0.30	0.10	0.28
1993	1012	483	0.14	54	0.32	0.09	0.30
1994	1004	481	0.14	65	0.31	0.09	0.30
1995	985	472	0.14	85	0.29	0.09	0.31
1996	976	464	0.14	74	0.30	0.08	0.32
1997	986	465	0.14	64	0.32	0.09	0.29
1998	1005	476	0.14	65	0.32	0.08	0.29
1999	1018	485	0.14	59	0.33	0.10	0.27
2000	1008	481	0.14	60	0.34	0.09	0.28
2001	998	477	0.14	66	0.35	0.08	0.32
2002	991	473	0.15	95	0.36	0.09	0.32
2003	987	470	0.15	142	0.35	0.06	0.30
2004	1024	479	0.15	101	0.39	0.09	0.28
2005	1081	496	0.16	81	0.37	0.09	0.30
2006	1163	545	0.16	71	0.35	0.06	0.28
2007	1231	584	0.15	74	0.36	0.05	0.24
2008	1284	614	0.15	93	0.36	0.05	0.20
2009	1325	634	0.15	91	0.37	0.05	0.20
2010	1370	653	0.15	111	0.38	0.07	0.21
2011	1402	667	0.15	102	0.39	0.07	0.23
2012	1436	680	0.15	90	0.41	0.08	0.24
2013	1463	695	0.15	149	0.36	0.06	0.20
2014	1516	722	0.15	109	0.38	0.06	0.24
2015	1574	739	0.15	71	0.37	0.05	0.22
2016	1674	797	0.15	70	0.38	0.05	0.20
2017	1722	831	0.15	73	0.39	0.07	0.26
2018	1693	819	0.15	74	0.40	0.08	0.37

Table 13. Estimated biological reference points derived from the Stock Synthesis base-case model where F is the instantaneous annual fishing mortality rate, SPR is spawning potential ratio, SSB is spawning stock biomass, $MSST$ indicates minimum stock size threshold, and MSY indicates maximum sustainable yield.

Reference Point	Estimate
F_{MSY} (age 5−30)	0.14
F_{2018} (age 5−30)	0.08
F_{2018}/F_{MSY}	0.57
SSB_{MSY}	334 mt
SSB_{MSST}	301 mt
SSB_{2018}	819 mt
SSB_{2018}/SSB_{MSST}	2.7
MSY	93 mt
Catch$_{2016-2018}$	108 mt
SPR_{MSY}	31%
SPR_{2018}	40%

Table 14. Summary table of key model output for all sensitivity model runs.

Model	F_{2018}	F_{msy}	F_{2018}/F_{msy}	SSB_{msy}	SSB_{2018}	SSB_{2018}/SSB_{msy}	MSY
Base case	0.08	0.14	0.57	334	819	2.45	93
M equals 0.09	0.08	0.12	0.67	347	754	2.17	87
M equals 0.11	0.07	0.15	0.47	327	876	2.68	98
L_{Amax} equals 68.9 cm	0.07	0.15	0.47	316	914	2.89	101
L_{Amax} equals 84.2 cm	0.19	0.12	1.58	343	324	0.94	85
L_{mat} equals 40.3 cm	0.08	0.14	0.57	337	827	2.45	93
L_{mat} equals 49.3 cm	0.08	0.13	0.62	323	794	2.46	92
Sigma R = 0.35	0.08	0.14	0.57	331	787	2.38	92
Sigma R = 0.43	0.07	0.14	0.5	334	847	2.54	93
Steepness = 0.73	0.07	0.11	0.64	384	828	2.16	88
Steepness = 0.89	0.08	0.17	0.47	286	811	2.84	97
Rec. catch using ratios	0.04	0.14	0.29	327	859	2.63	93
Rec. catch phone corrected	0.07	0.14	0.5	351	879	2.5	98
Rec. catch -30%	0.09	0.14	0.64	289	727	2.52	80
Rec. catch +30%	0.07	0.14	0.5	376	914	2.43	105
Original CPUE CVs	0.07	0.14	0.5	336	891	2.65	93
CPUE: DSH+DSH	0.09	0.14	0.64	328	674	2.05	91
CPUE: DSH+ISH	0.08	0.14	0.57	331	759	2.29	92
CPUE: DSH+TROL	0.09	0.14	0.64	326	662	2.03	91
Size frequency lambda=0.1	0.09	0.14	0.64	319	671	2.1	89
ISH 1992-2018 single *q*	0.07	0.14	0.5	336	860	2.56	93
M from Lorenzen	0.07	0.15	0.47	321	843	2.63	96
DSH 1948-2018 single *q*	0.09	0.14	0.64	326	707	2.17	91
ISH 1992-2018 two *q*s	0.08	0.14	0.57	334	825	2.47	93
Long DSH+ISH and *M* Lorenzen	0.08	0.15	0.53	314	757	2.41	94
Model starts in 1970	0.07	0.14	0.5	388	892	2.3	108
Estimated sigma *R*	0.06	0.14	0.43	349	967	2.77	97
Time-varying *q*	0.08	0.14	0.57	333	816	2.45	93
Effective N from SS	0.07	0.14	0.5	335	834	2.49	93
Exclude diver surveys	0.08	0.14	0.57	334	822	2.46	93

Table 15. Projection results for the median probability of overfishing (F/F_{MSY}>1) at different annual catch values. The median probability the stock is overfished (SSB/SSB_{MSST}<1), median fishing mortality, and median biomass are the values in each year that correspond to the specified catch values. Catch values for a given probability of overfishing in a given year were applied in all previous years (i.e., 2020 to the year of interest).

Probability of overfishing (F/F_{MSY} >1)										
	0.05	0.1	0.15	0.2	0.25	0.3	0.35	0.4	0.45	0.5
Total catch (mt)										
2020	122	129	134	139	143	145	147	149	151	154
2021	119	125	130	135	137	140	142	144	146	148
2022	117	124	128	132	134	136	138	140	142	144
2023	116	122	126	129	132	134	136	138	139	141
2024	116	121	124	127	129	132	134	135	137	139
2025	115	120	123	126	128	130	132	133	135	137
2026	114	119	122	124	126	128	130	132	134	135
Probability stock is overfished (SSB/SSB_{MSST}<1)										
2020	0	0	0	0	0	0	0	0	0	0
2021	0	0	0	0	0	0	0	0	0	0
2022	0	0	0	0	0	0	0	0	0	0
2023	0	0	0	0	0	0	0	0	0	0
2024	0	0	0	0	0	0	0	0	0	0
2025	0	0	0	0	0	0	0	0	0	0
2026	0	0	0	0	0	0	0	0	0	0
Fishing Mortality										
2020	0.11	0.11	0.12	0.12	0.13	0.13	0.13	0.13	0.13	0.14
2021	0.11	0.11	0.12	0.12	0.12	0.13	0.13	0.13	0.13	0.14
2022	0.10	0.11	0.12	0.12	0.12	0.13	0.13	0.13	0.13	0.14
2023	0.10	0.11	0.12	0.12	0.12	0.13	0.13	0.13	0.13	0.14
2024	0.10	0.11	0.12	0.12	0.12	0.13	0.13	0.13	0.13	0.14
2025	0.10	0.11	0.11	0.12	0.12	0.13	0.13	0.13	0.13	0.14
2026	0.10	0.11	0.11	0.12	0.12	0.12	0.13	0.13	0.13	0.14
Spawning biomass (metric tons)										
2020	635	635	635	635	635	635	635	635	635	635
2021	618	615	613	611	610	608	607	606	605	604
2022	615	608	604	600	598	596	595	593	591	589
2023	612	604	598	594	589	587	584	581	579	577
2024	609	600	594	588	585	579	575	573	570	566
2025	609	597	590	583	578	574	569	567	562	557
2026	609	596	588	582	577	571	565	560	554	552

Table 16. Probability of overfishing (F/F_{MSY}>1) at different annual catch values (metric tons) by year. Catch values for a given probability of overfishing in a given year were applied in all previous years (i.e., 2020 to the year of interest). Table continued on next page.

Probability of overfishing	Total catch in metric tons						
	2020	2021	2022	2023	2024	2025	2026
0.50	154	148	144	141	139	137	135
0.49	153	148	144	141	139	137	135
0.48	153	147	144	141	138	136	135
0.47	152	147	143	140	138	136	134
0.46	152	146	143	140	138	136	134
0.45	151	146	142	139	137	135	134
0.44	151	145	142	139	137	135	133
0.43	151	145	142	139	136	135	133
0.42	150	145	141	138	136	134	133
0.41	150	144	141	138	136	134	132
0.40	149	144	140	138	135	133	132
0.39	149	143	140	137	135	133	132
0.38	148	143	140	137	135	133	131
0.37	148	143	139	136	134	132	131
0.36	148	142	139	136	134	132	131
0.35	147	142	138	136	134	132	130
0.34	147	141	138	135	133	131	130
0.33	146	141	138	135	133	131	130
0.32	146	141	137	135	132	131	129
0.31	145	140	137	134	132	130	129
0.30	145	140	136	134	132	130	128
0.29	145	139	136	133	131	129	128
0.28	144	139	135	133	131	129	128
0.27	144	138	135	132	130	129	127
0.26	143	138	135	132	130	128	127
0.25	143	137	134	132	129	128	126
0.24	142	137	134	131	129	127	126
0.23	142	136	133	131	129	127	126
0.22	141	136	133	130	128	127	125
0.21	140	135	132	130	128	126	125
0.20	139	135	132	129	127	126	124
0.19	139	134	131	129	127	125	124
0.18	138	133	130	128	126	125	123
0.17	136	132	130	127	126	124	123
0.16	135	131	129	127	125	124	122
0.15	134	130	128	126	124	123	122
0.14	133	129	127	125	124	122	121

Probability of overfishing	Total catch in metric tons						
	2020	2021	2022	2023	2024	2025	2026
0.13	132	128	126	125	123	122	121
0.12	131	127	126	124	122	121	120
0.11	130	126	125	123	122	121	120
0.10	129	125	124	122	121	120	119
0.09	127	124	122	121	120	119	118
0.08	126	123	121	120	119	118	117
0.07	125	122	120	119	118	117	116
0.06	123	120	119	118	117	116	115
0.05	122	119	117	116	116	115	114
0.04	120	117	116	115	114	114	113
0.03	117	115	114	113	112	112	111
0.02	114	112	111	111	110	110	109
0.01	110	109	108	107	107	107	106

Table 17. Alternative (<u>not for management</u>) projection results for a low recruitment forecast scenario (i.e., recruitment sampled from the bottom 25th percentile of model-estimated recruitment between 1948 and 2018). The median probability the stock is overfished ($SSB/SSB_{MSST}<1$), median fishing mortality, and median biomass are the values in each year that correspond to the specified catch values.

Probability of overfishing ($F/F_{MSY} >1$)										
	0.05	0.1	0.15	0.2	0.25	0.3	0.35	0.4	0.45	0.5
Total catch (mt)										
2020	121	128	134	139	143	145	147	149	151	154
2021	117	123	129	133	136	138	140	142	144	146
2022	113	119	123	127	129	131	133	135	137	139
2023	109	114	118	122	124	126	127	129	131	132
2024	106	111	114	117	119	121	122	124	125	127
2025	103	108	111	113	115	117	118	119	120	122
2026	101	105	108	110	111	113	114	115	116	118
Probability stock is overfished ($SSB/SSB_{MSST}<1$)										
2020	0	0	0	0	0	0	0	0	0	0
2021	0	0	0	0	0	0	0	0	0	0
2022	0	0	0	0	0	0	0	0	0	0
2023	0	0	0	0	0	0	0	0	0	0
2024	0	0	0	0	0	0	0	0	0	0
2025	0	0	0	0	0	0	0	0	0	0
2026	0	0	0	0	0	0	0	0	0	0
Fishing Mortality										
2020	0.11	0.11	0.12	0.12	0.13	0.13	0.13	0.13	0.13	0.14
2021	0.11	0.11	0.12	0.12	0.13	0.13	0.13	0.13	0.13	0.14
2022	0.11	0.11	0.12	0.12	0.12	0.13	0.13	0.13	0.13	0.14
2023	0.10	0.11	0.12	0.12	0.12	0.13	0.13	0.13	0.13	0.14
2024	0.11	0.11	0.12	0.12	0.12	0.13	0.13	0.13	0.13	0.14
2025	0.11	0.11	0.12	0.12	0.12	0.13	0.13	0.13	0.13	0.14
2026	0.11	0.11	0.12	0.12	0.12	0.13	0.13	0.13	0.13	0.14
Spawning biomass (metric tons)										
2020	635	635	635	635	635	635	635	635	635	635
2021	619	616	613	611	610	609	608	607	606	605
2022	599	593	589	586	584	582	580	578	576	574
2023	580	573	568	562	559	556	555	552	549	548
2024	562	553	547	542	538	534	533	529	527	523
2025	546	535	528	524	519	515	512	510	508	503
2026	531	520	512	506	504	498	496	493	490	485

Note: This projection table is for an alternate recruitment scenario and not for the base case.
Do not use for determining official catch limits.

7 Figures
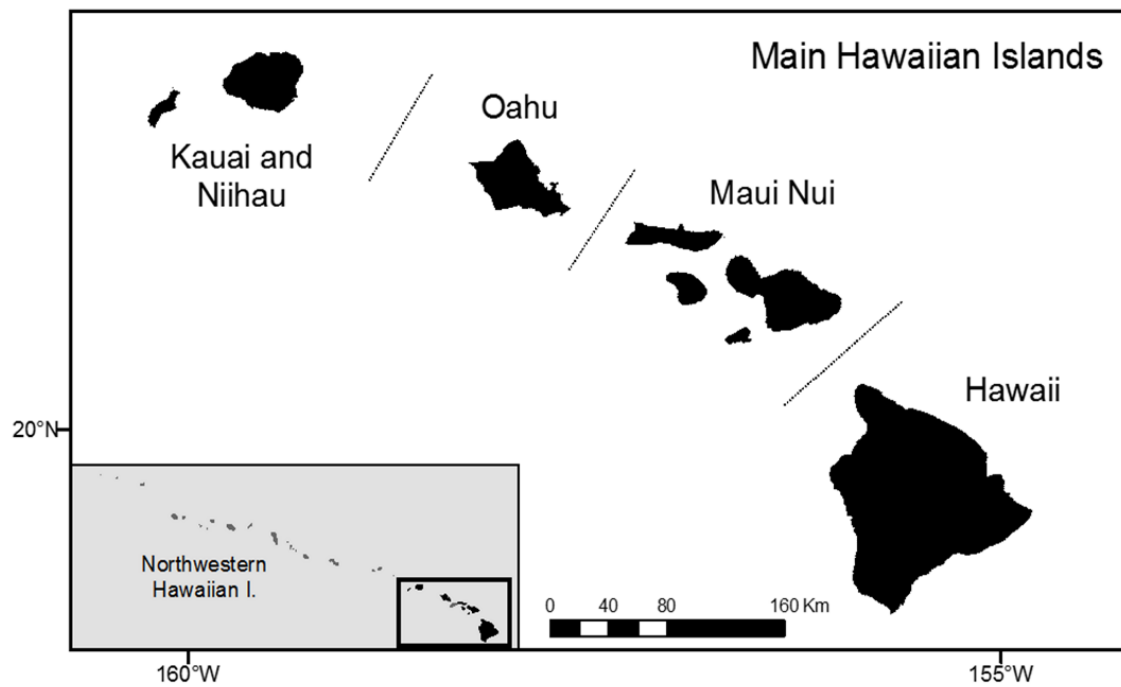
Figure 1. Map of the main Hawaiian Islands with its four sub-regions. The entire archipelago is visible in the inset, including the Northwestern Hawaiian Islands.
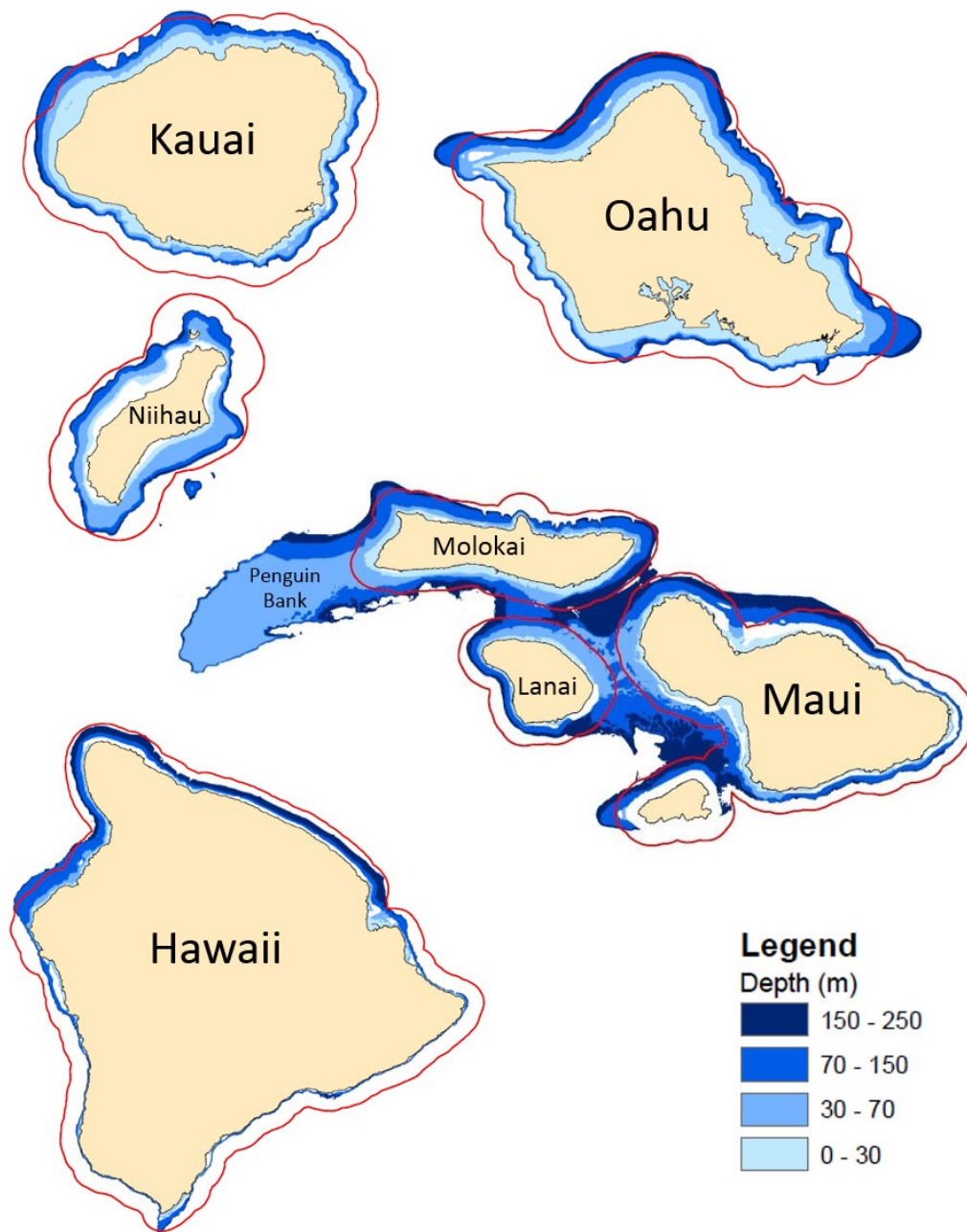
Figure 2. Map of the eight main Hawaiian Islands with depth zones (0 m to 250 m depths). Red contour lines represent the 3-nautical-mile state waters limit. Islands are not to scale and re-arranged to fit this page. Data source: CREP and Hawaii Mapping Research Group.
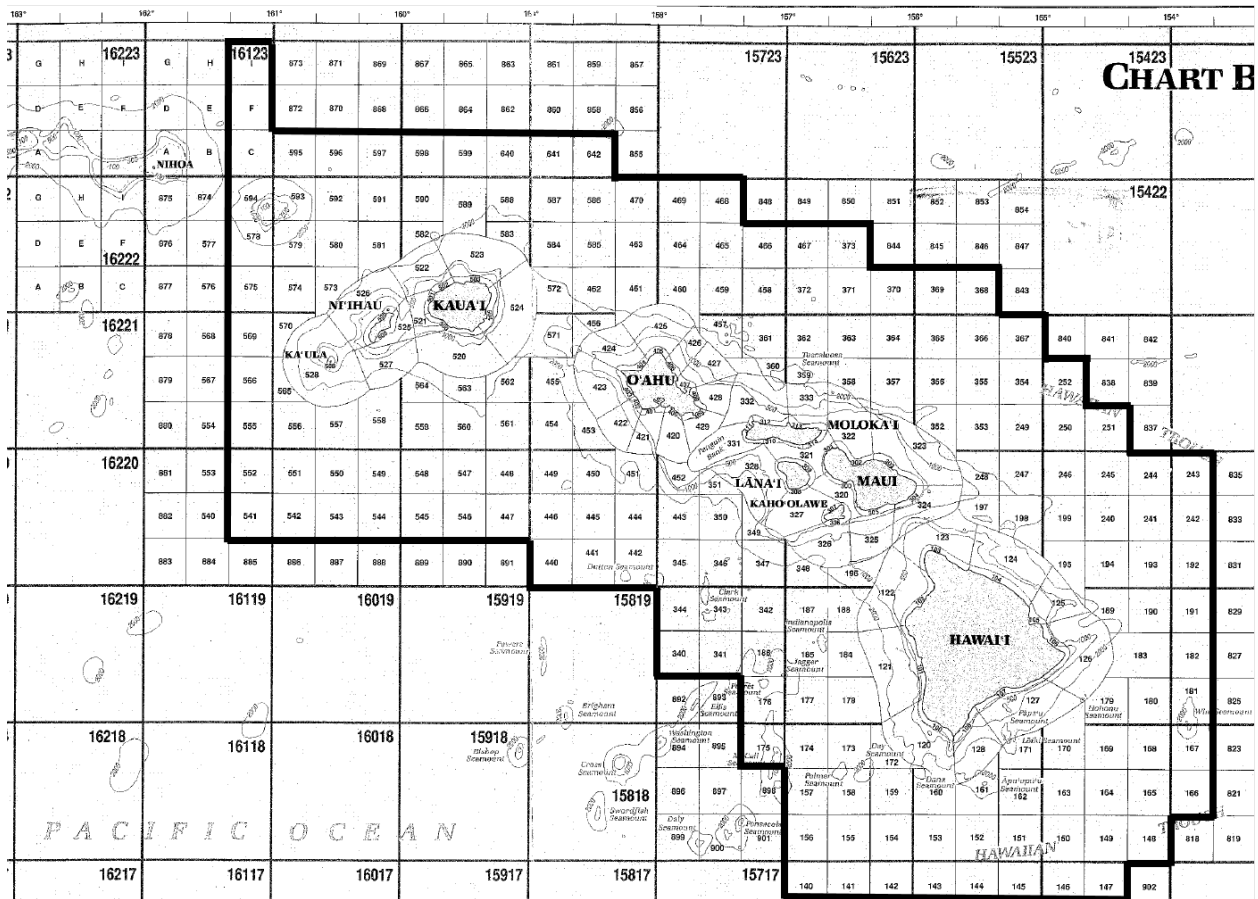
Figure 3. Boundary of the stock area in the main Hawaiian Islands used for the 2020 uku assessment.
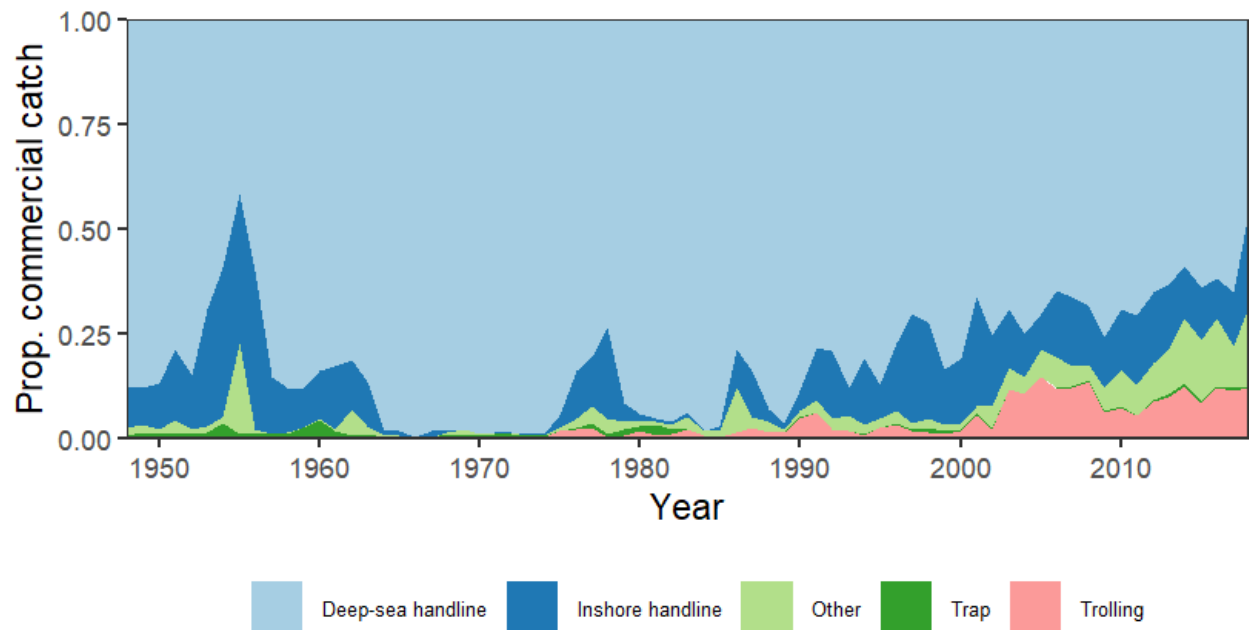
Figure 4. Proportion of total commercial catch caught by fishing gear type.
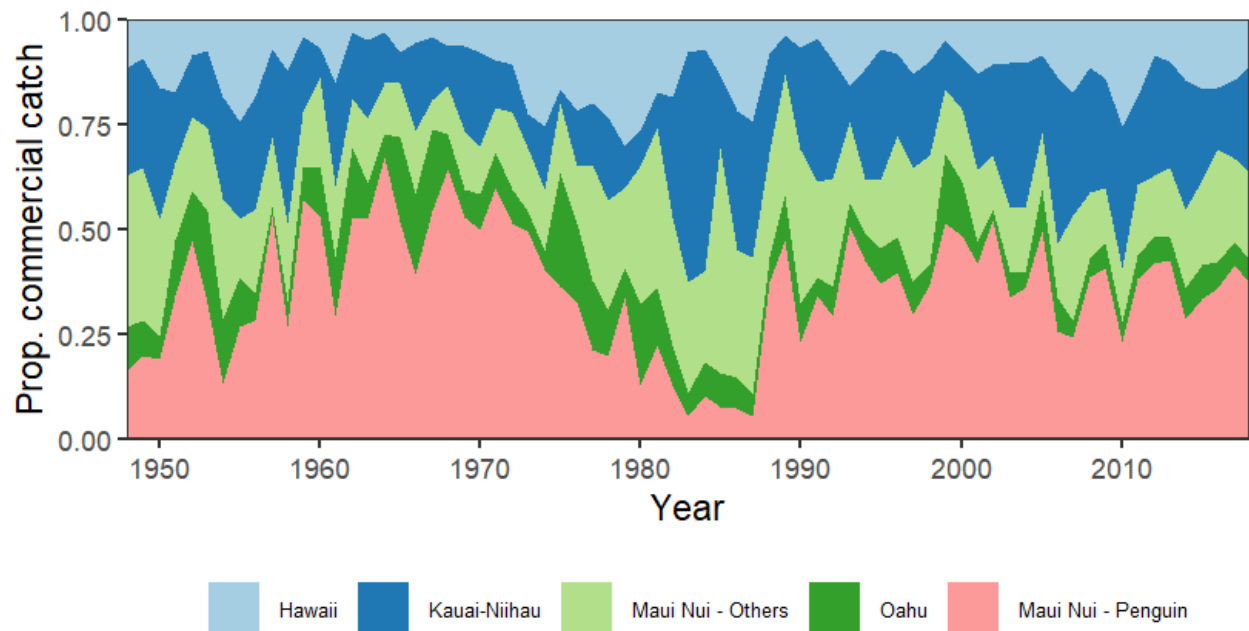
Figure 5. Proportion of total commercial catch caught by sub-region of the MHI, with Penguin Bank (part of the Maui Nui sub-region) listed separately.
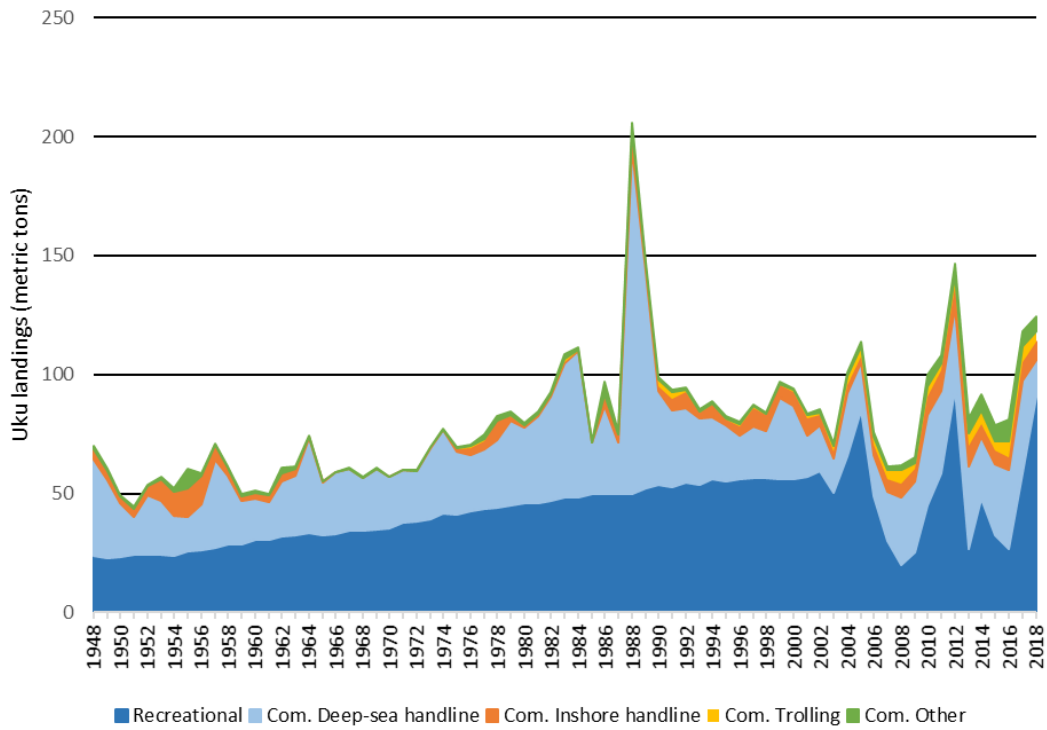
Figure 6. History of uku catch by sector (recreational and commercial), with the commercial catch further broken down by fishing gear type. Note that the recreational catch pre-2003 is reconstructed (see section 2.2.1 for details).
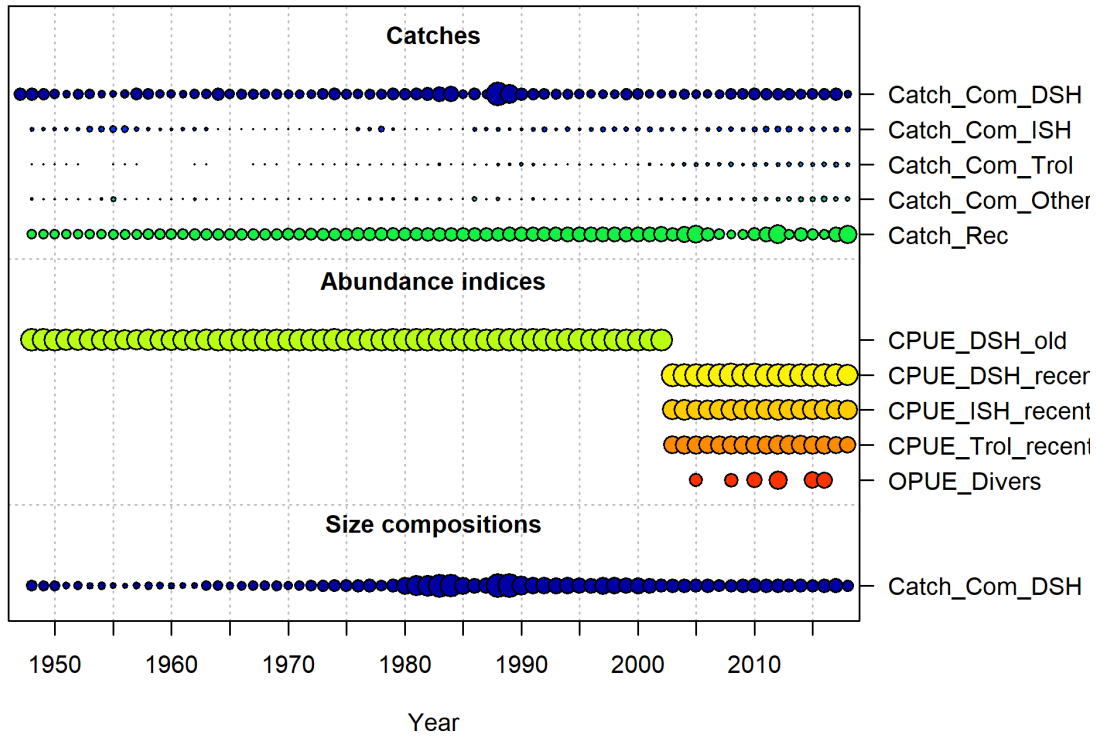
Figure 7. Summary of all datasets used in the Stock Synthesis model. DSH—deep-sea handline, ISH—inshore handline, Trol—trolling, Rec—recreational data, Divers—diver surveys.
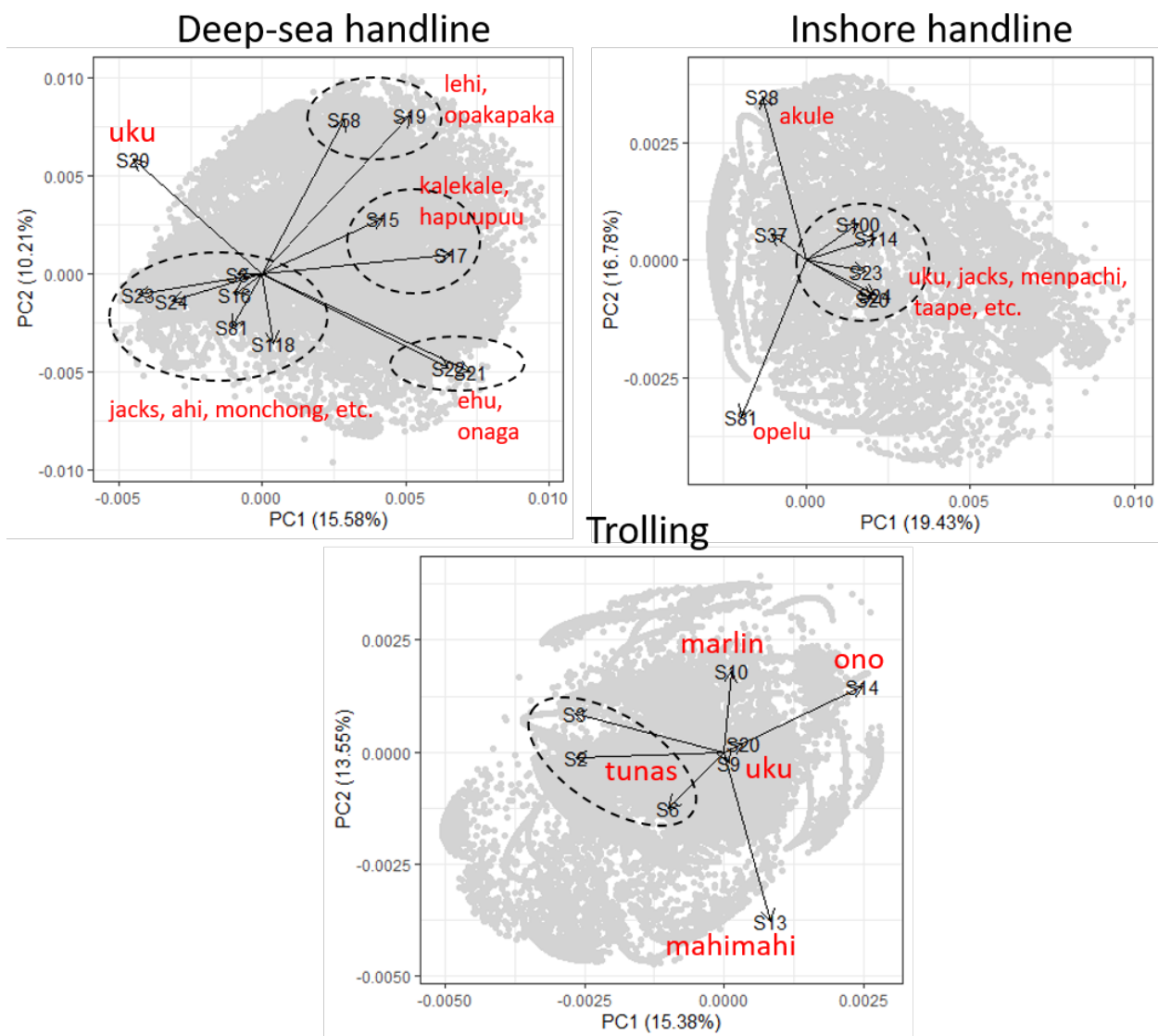
Figure 8. Principal Component Analysis (PCA) plots showing the principal axes included in the Direct Principal Component (DPC) analysis for the 3 gear types used for CPUE indices (note: uku are excluded from the actual DPC analyses but are presented here for reference).
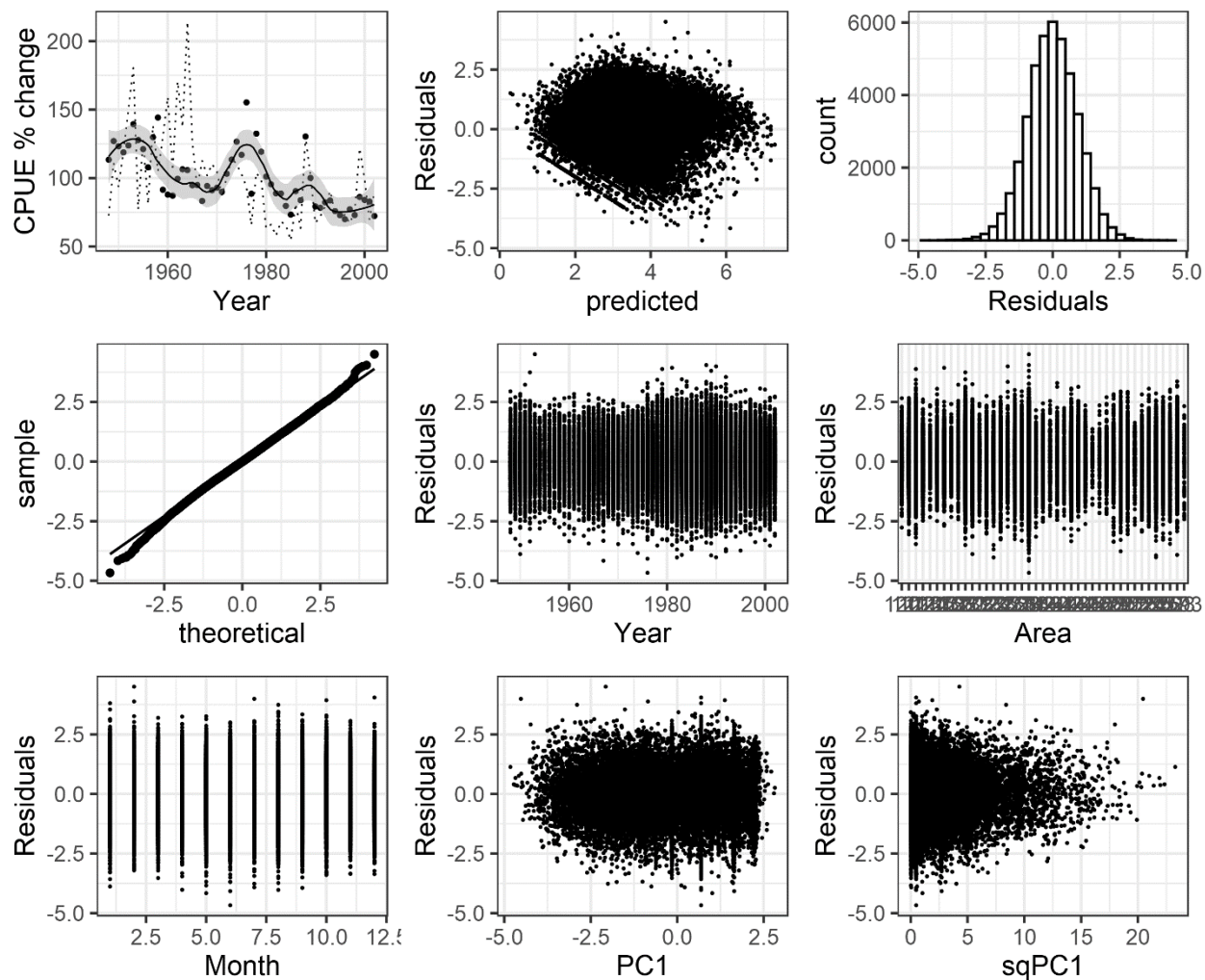
Figure 9. Diagnostics of the lognormal CPUE standardization model for the 1948−2002 period (deep-sea handline gear). Top left graph shows nominal vs. standardized CPUE trends as a percent of their respective overall mean (dashed line=nominal, dots with loess curve=standardized). All other graphs present overall or variable-specific residual patterns, including a quantile-quantile plot.
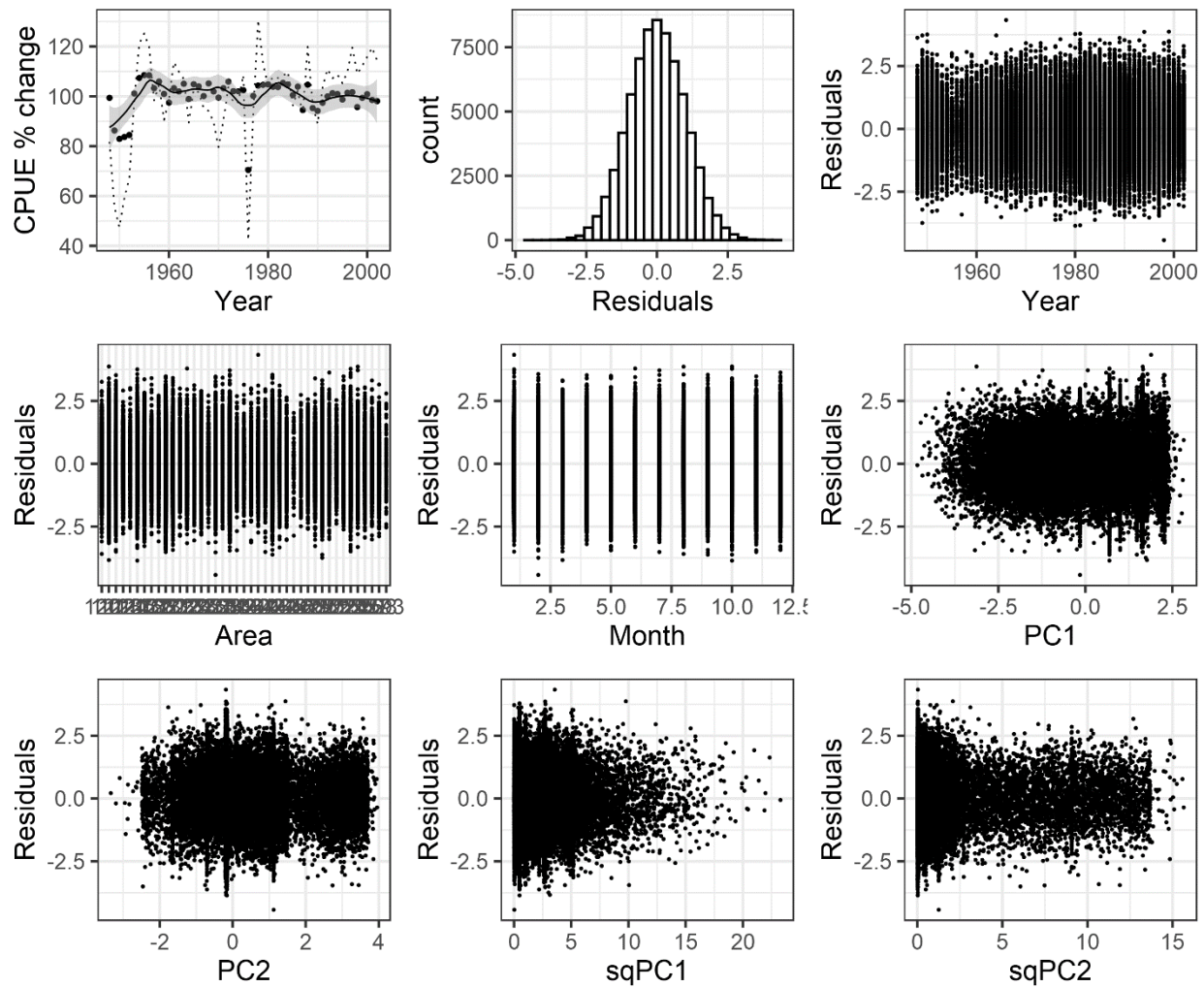
Figure 10. Diagnostics of the logistic CPUE standardization model for the 1948−2002 period (deep-sea handline gear). Top left graph shows nominal vs. standardized CPUE trends as a percent of their respective overall mean (dashed line=nominal, dots with loess curve=standardized). All other graphs present overall or variable-specific residual patterns.
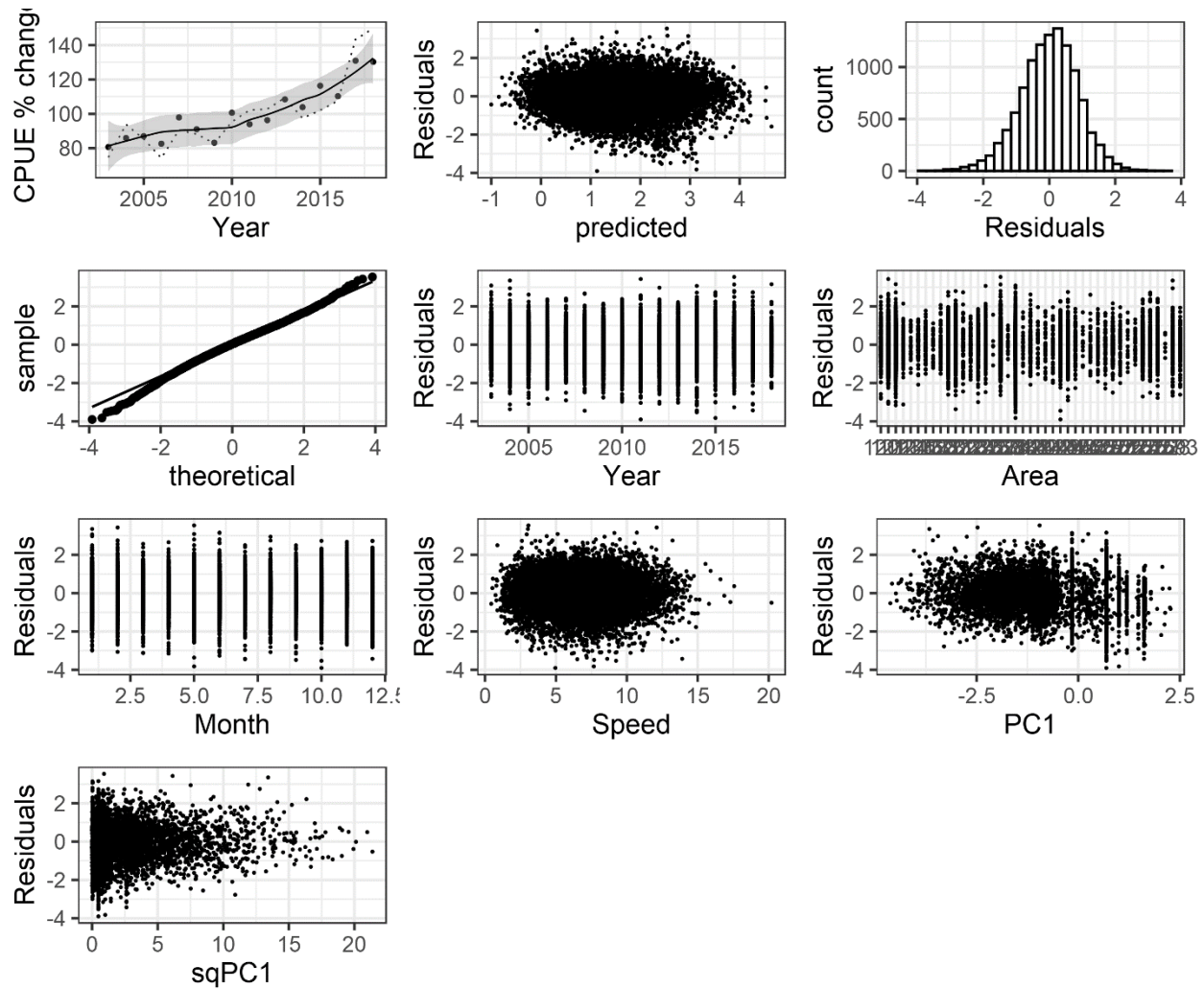
Figure 11. Diagnostics of the lognormal CPUE standardization model for the 2003−2018 period (deep-sea handline gear). Top left graph shows nominal vs. standardized CPUE trends as a percent of their respective overall mean (dashed line=nominal, dots with loess curve=standardized). All other graphs present overall or variable-specific residual patterns, including a quantile-quantile plot.
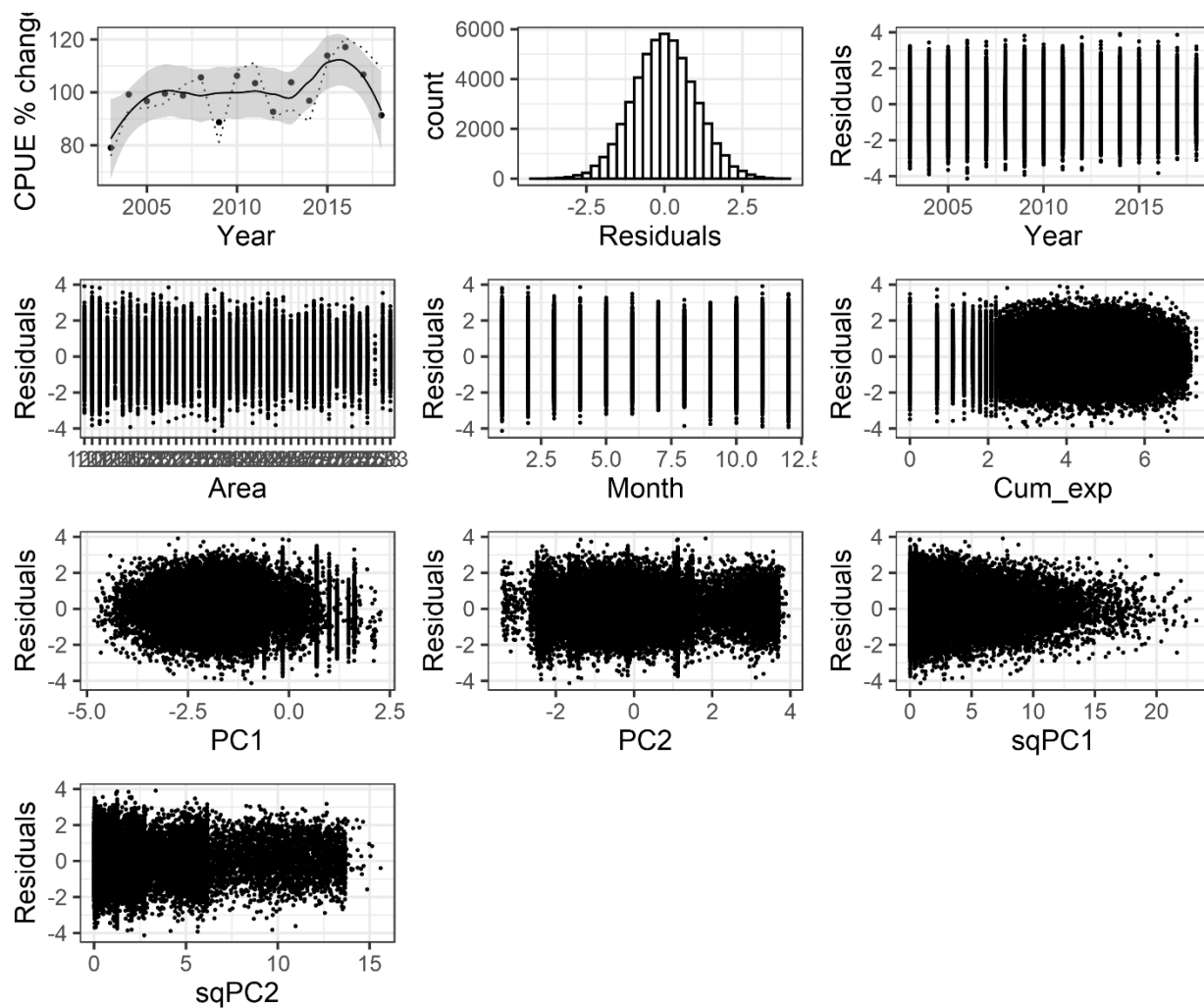
Figure 12. Diagnostics of the logistic CPUE standardization model for the 2003−2018 period (deep-sea handline gear). Top left graph shows nominal vs. standardized CPUE trends as a percent of their respective overall mean (dashed line=nominal, dots with loess curve=standardized). All other graphs present overall or variable-specific residual patterns.
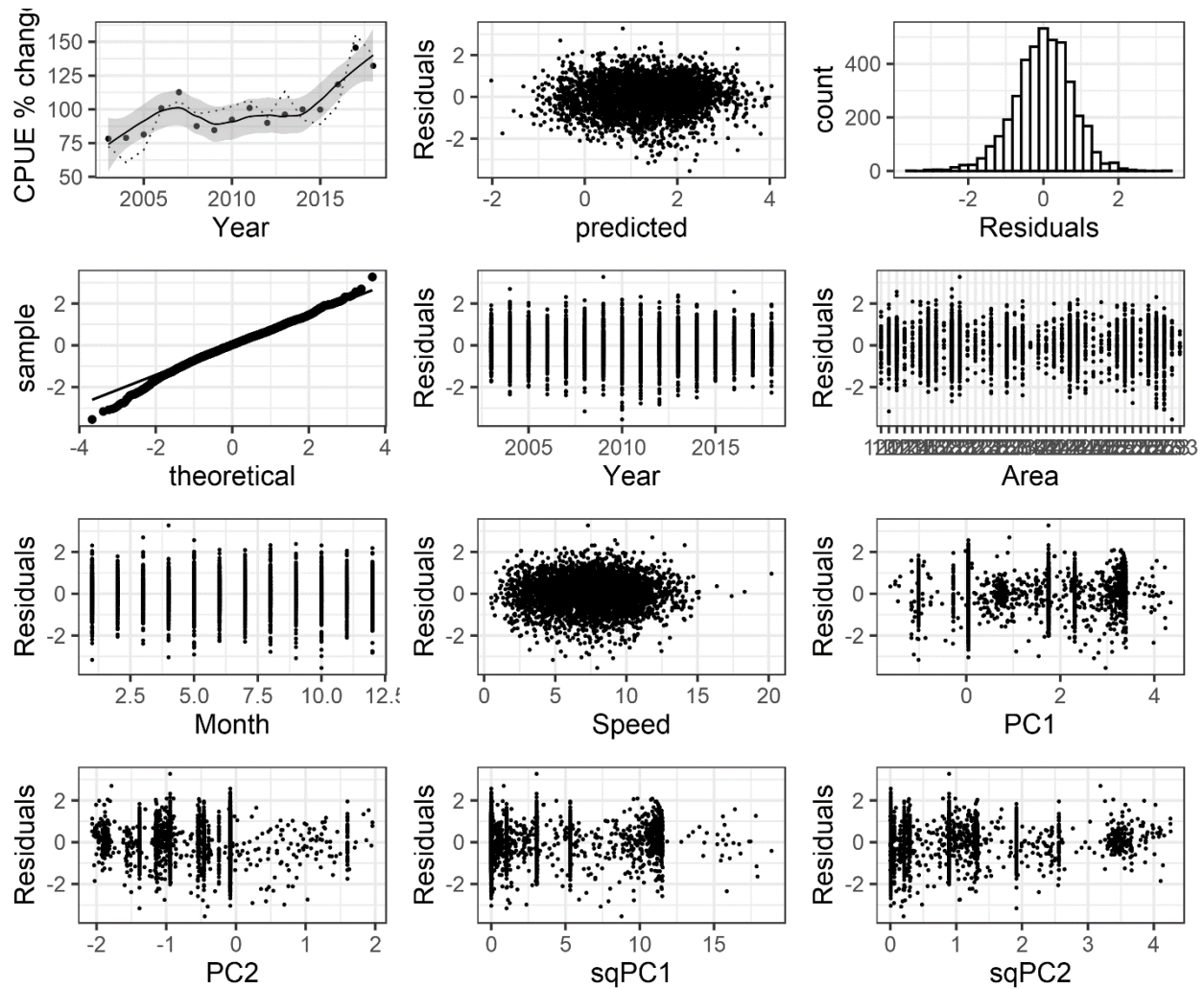
Figure 13. Diagnostics of the lognormal CPUE standardization model for the 2003−2018 period (inshore handline gear). Top left graph shows nominal vs. standardized CPUE trends as a percent of their respective overall mean (dashed line=nominal, dots with loess curve=standardized). All other graphs present overall or variable-specific residual patterns, including a quantile-quantile plot.
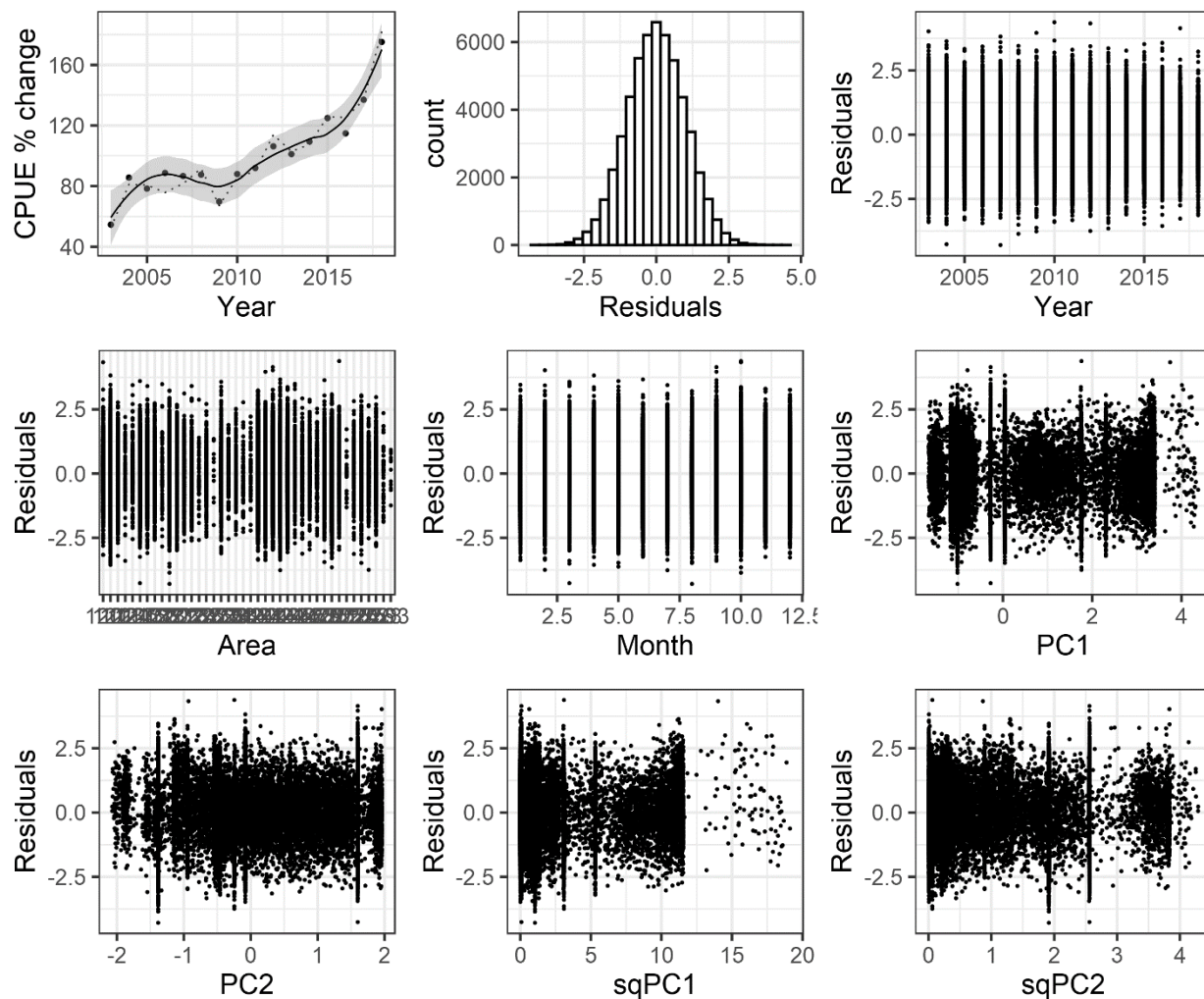
Figure 14. Diagnostics of the logistic CPUE standardization model for the 2003−2018 period (inshore handline gear). Top left graph shows nominal vs. standardized CPUE trends as a percent of their respective overall mean (dashed line=nominal, dots with loess curve=standardized). All other graphs present overall or variable-specific residual patterns.
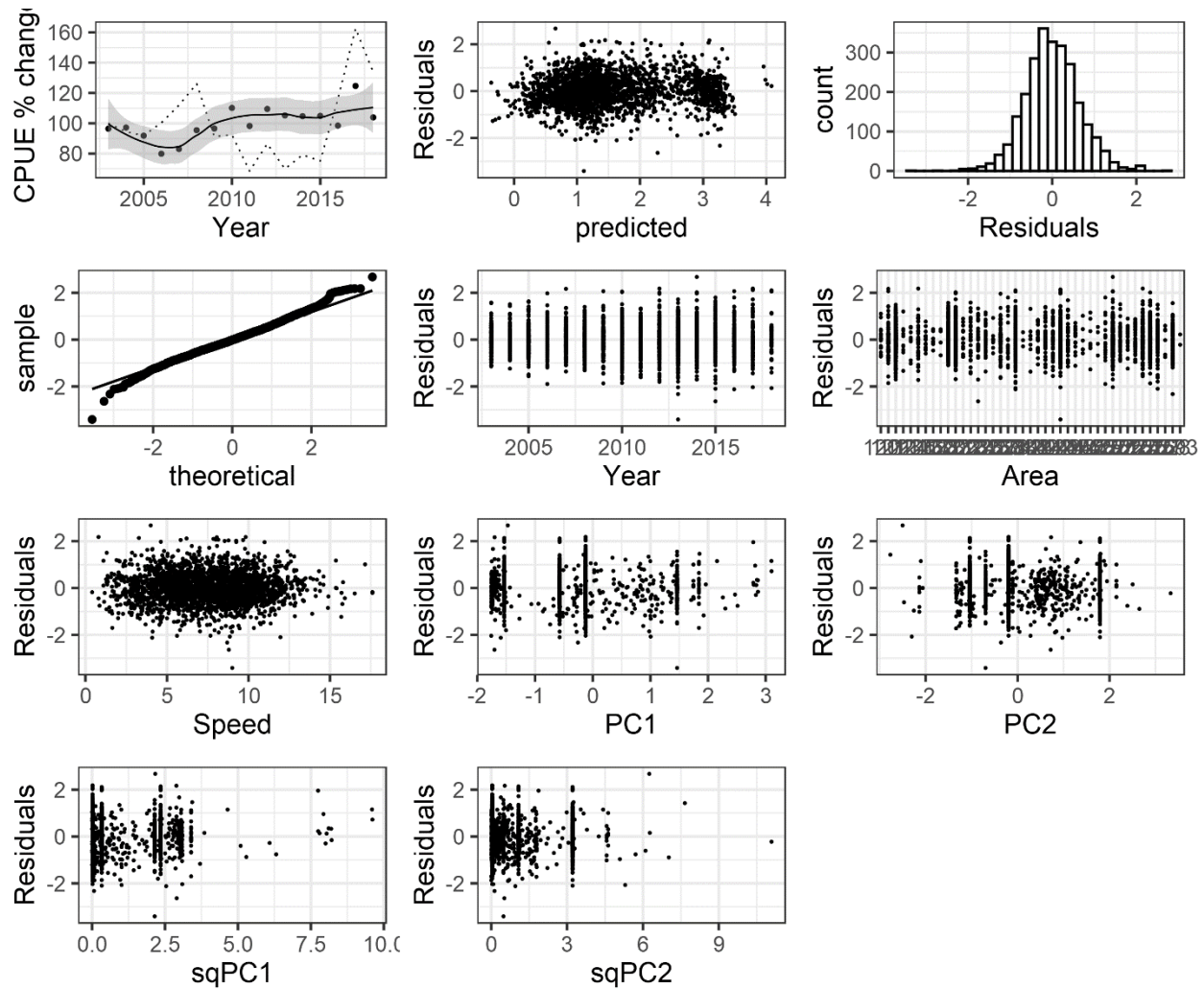
Figure 15. Diagnostics of the lognormal CPUE standardization model for the 2003−2018 period (trolling gear). Top left graph shows nominal vs. standardized CPUE trends as a percent of their respective overall mean (dashed line=nominal, dots with loess curve=standardized). All other graphs present overall or variable-specific residual patterns, including a quantile-quantile plot.

Figure 16. Diagnostics of the logistic CPUE standardization model for the 2003−2018 period (trolling gear). Top left graph shows nominal vs. standardized CPUE trends as a percent of their respective overall mean (dashed line=nominal, dots with loess curve=standardized). All other graphs present overall or variable-specific residual patterns.

Nominal (blue) vs standard. (red): 1948-2002

Nominal (blue) vs standard. (red): 2003-2018
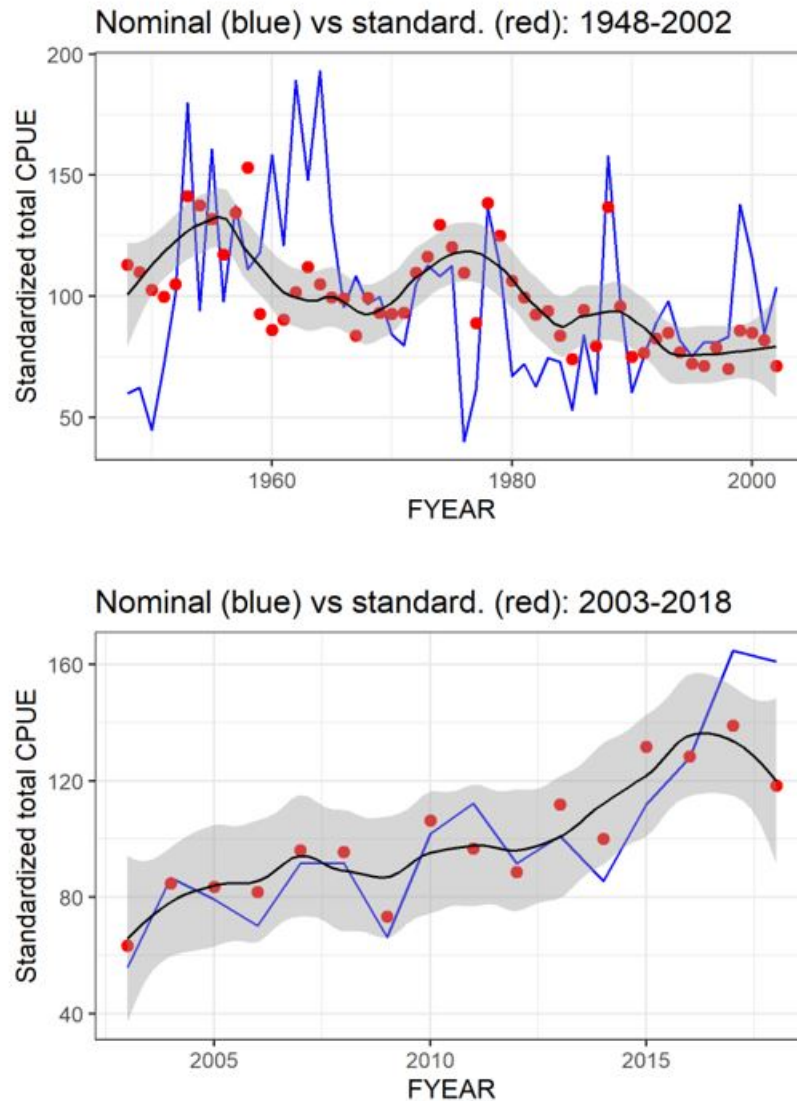
Figure 17. Overall nominal vs. standardized CPUE indices for deep-sea handline, generated by combining results from the lognormal and logistic standardization models.
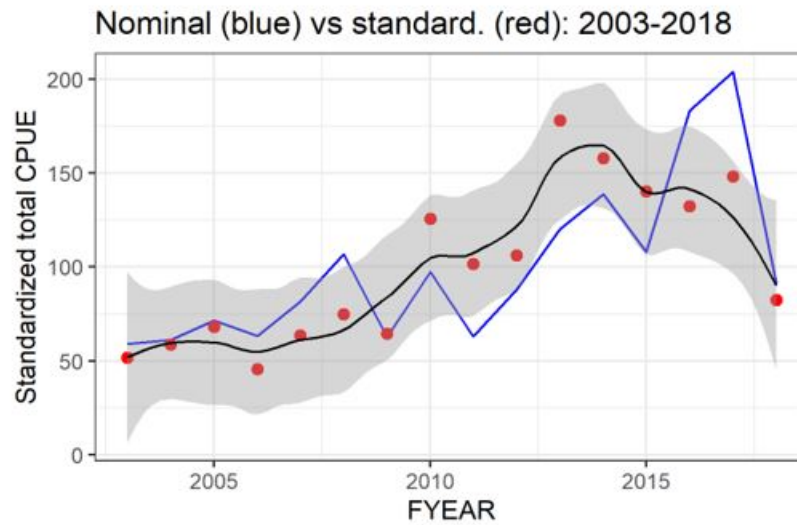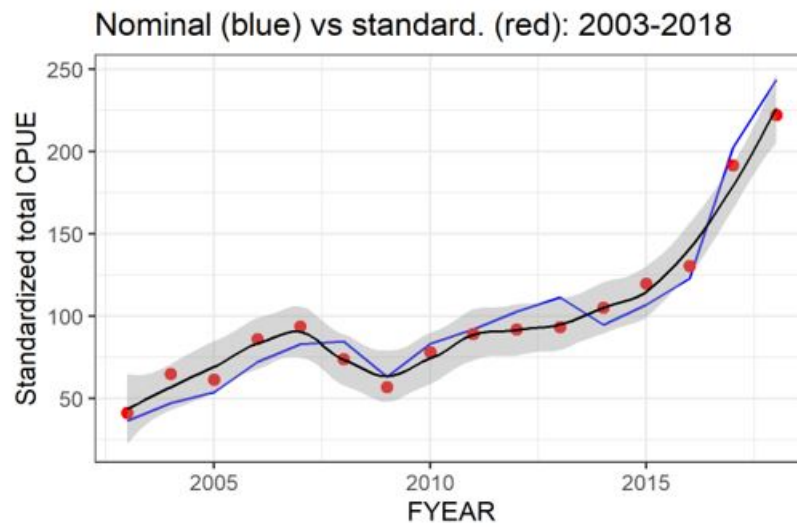
Figure 18. Overall nominal vs. standardized CPUE indices for inshore handline (top) and trolling (bottom) for the 2003−2018 period, generated by combining results from the lognormal and logistic standardization models.
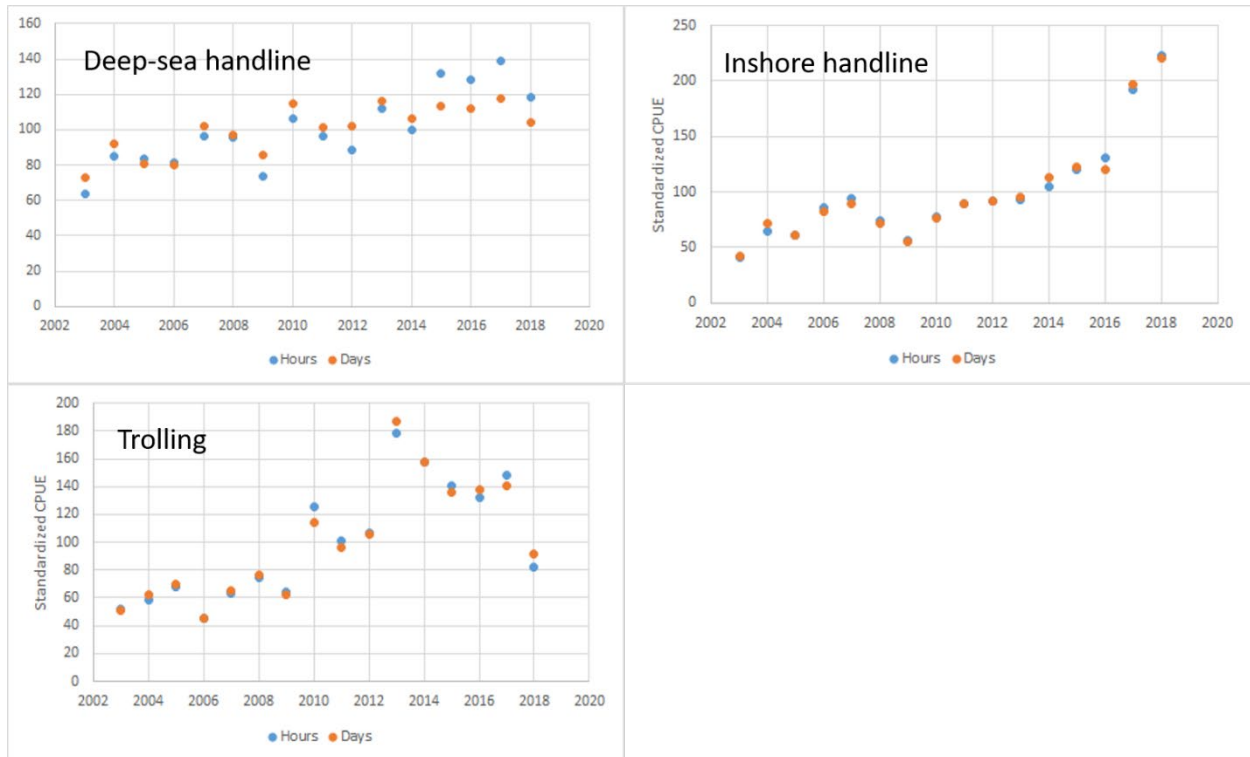
Figure 19. Standardized CPUE time series for the 2003−2018 period when using daily (orange dots) and hourly (blue dots) effort units. All CPUE series scaled to their mean value for comparison.
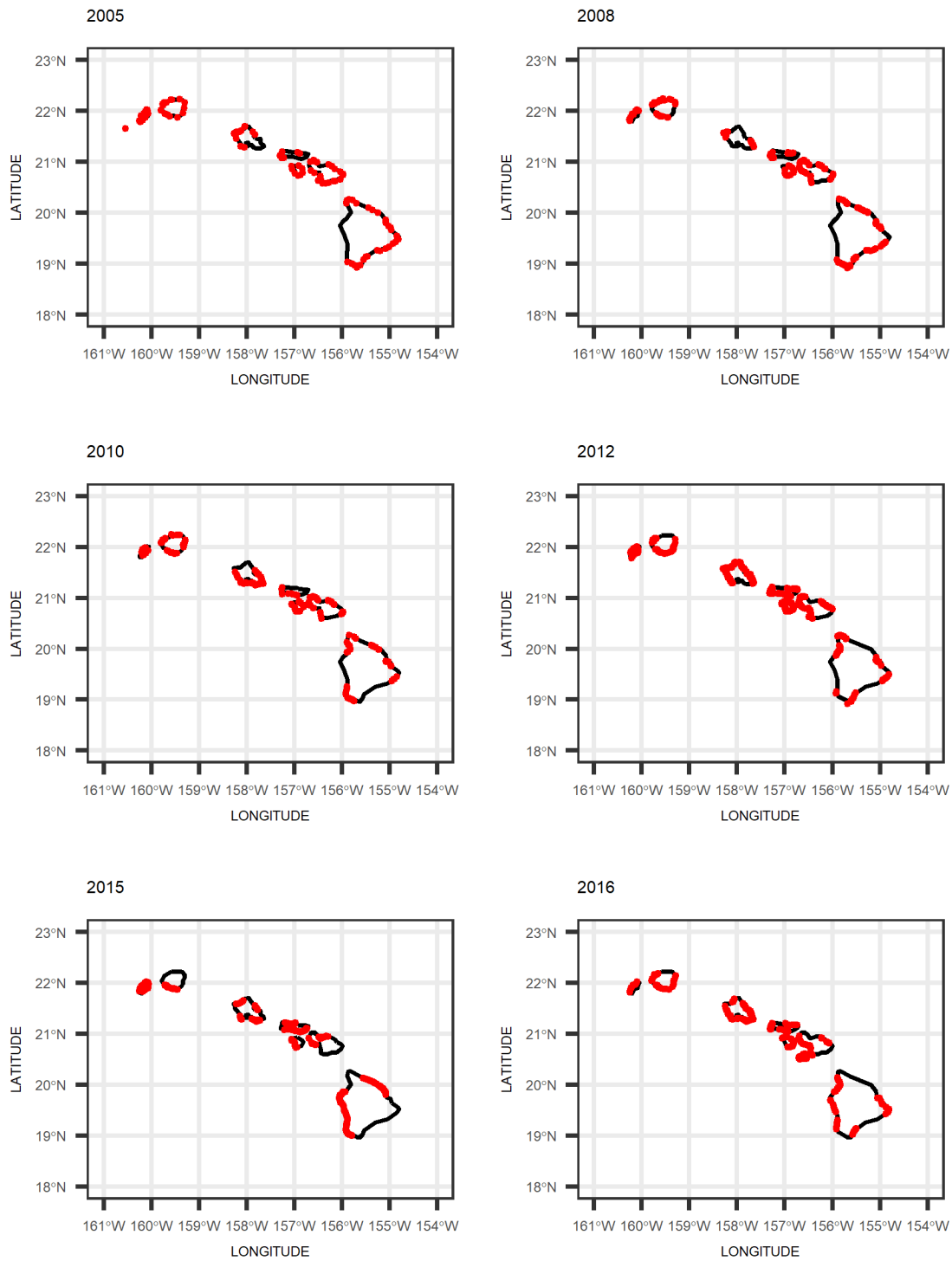
Figure 20. Distribution of survey sites (red dots) around the MHI for the NOAA diver surveys in each year.
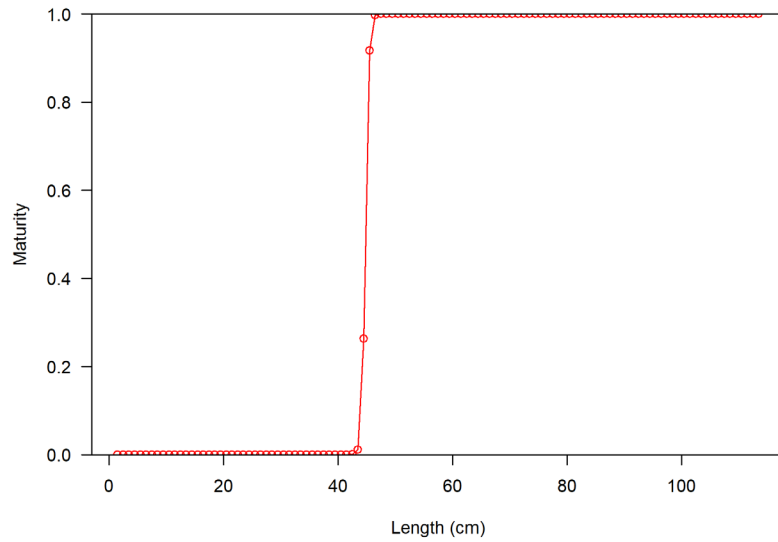
Figure 21. Maturity at length (FL) curve used in the stock assessment model, obtained from Everson and Williams (1989).
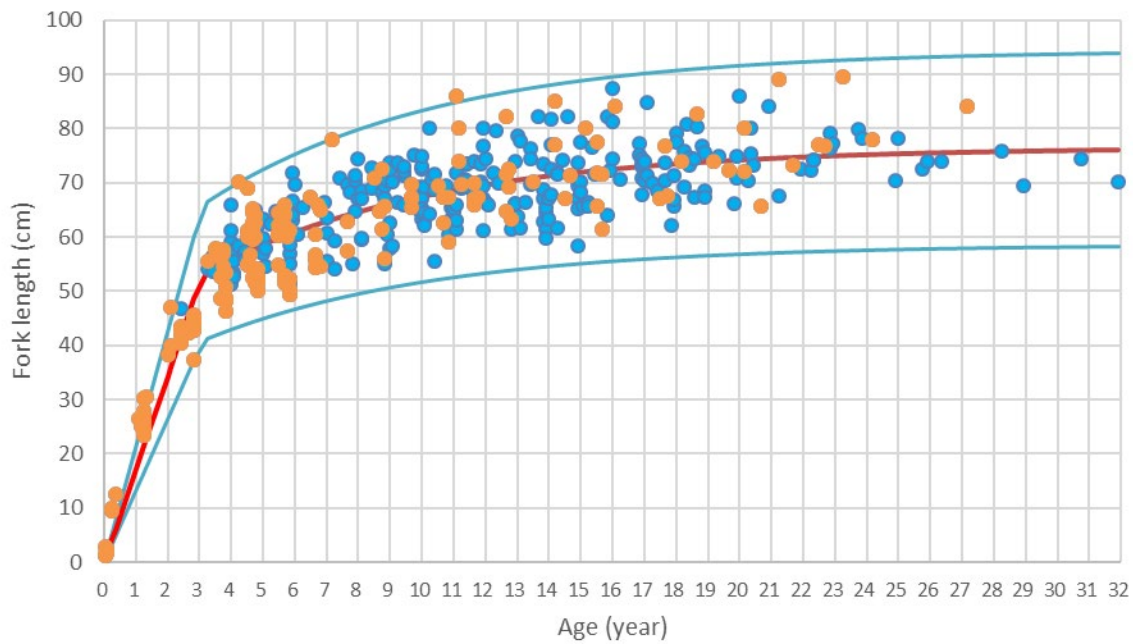
Figure 22. Age and length data collected in the MHI (orange points) and NWHI (blue points) with a two-stage von Bertalanffy curve, including the 95% confidence interval associated with the CV parameters (0.12 for both old and young individuals). Data provided by J. O'Malley, PIFSC.
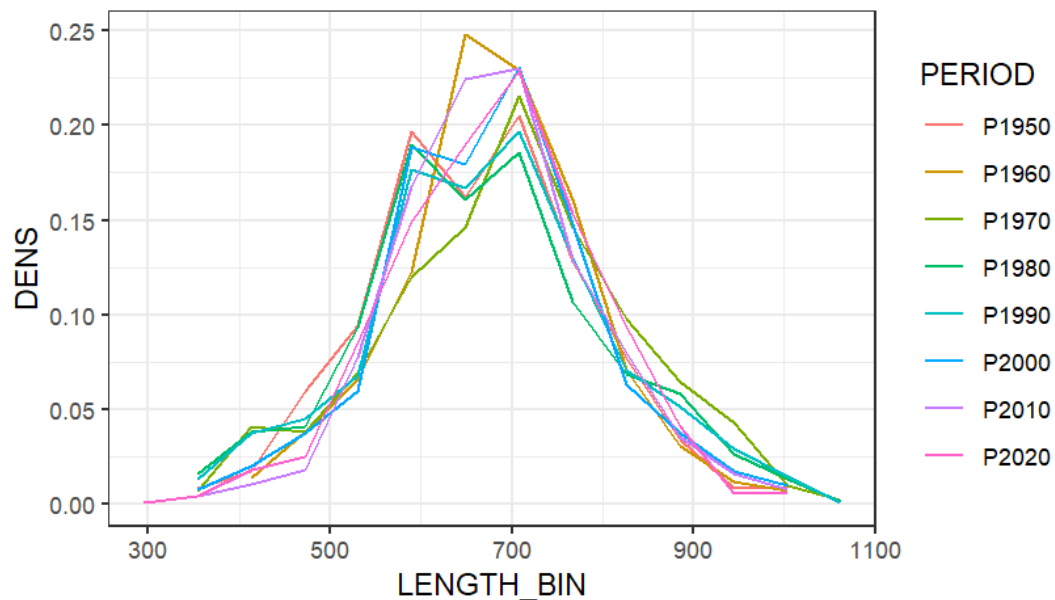
Figure 23. Size structures of uku from the FRS dataset and deep-sea handline gear summarized by decade.
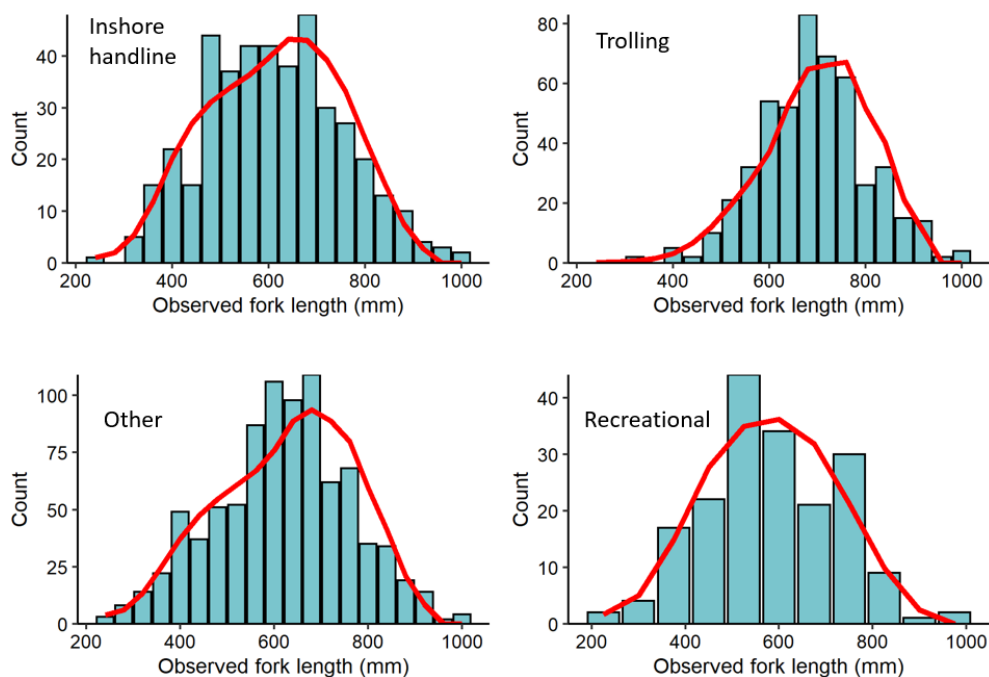
Figure 24. LBSPR model fit to size structure data for inshore handline, trolling, and "other" gear types from the FRS dataset (2008–2018), as well as for recreational landings reported in the HMRFS dataset (2003–2018).

Length-based selectivity by fleet in 2018
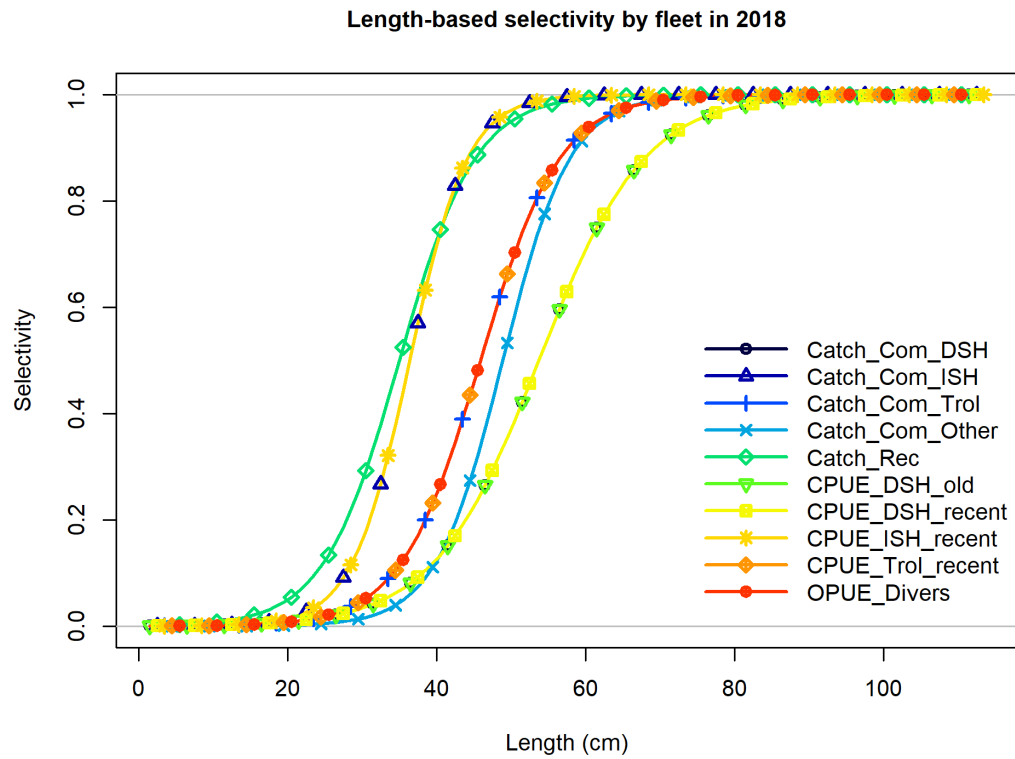
Figure 25. Length-based selectivity used in the Stock Synthesis model for all commercial fishing gear types and the recreational sector. Only the deep-sea handline selectivity was estimated in SS.

MFMT	MSST	B_{FLAG}
$F(B) = \dfrac{F_{MSY} B}{c \, B_{MSY}}$ for $B \le c \, B_{MSY}$ $F(B) = F_{MSY}$ for $B > c \, B_{MSY}$	$c \, B_{MSY}$	B_{MSY}
where $c = \max\,(1\text{-}M,\ 0.5)$		
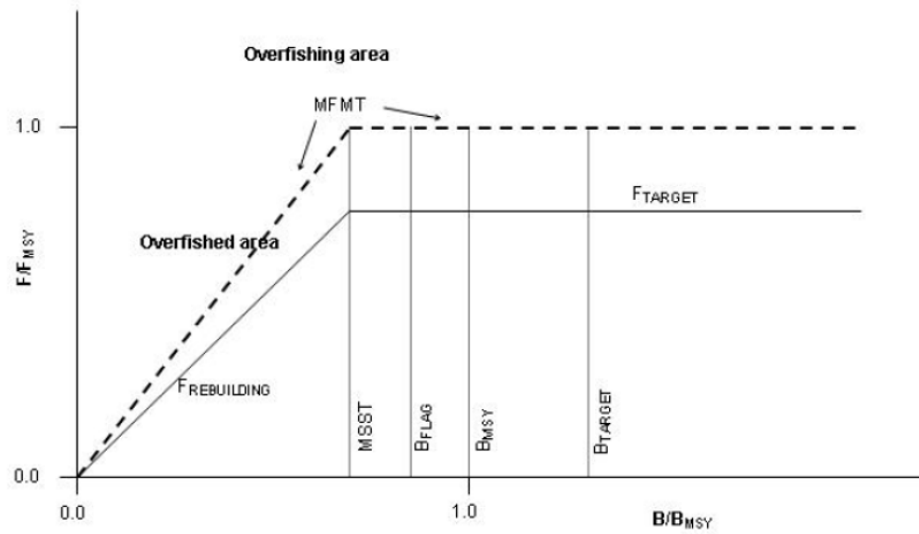
Figure 26. Fishery management control rules used for bottomfish in Hawaii.
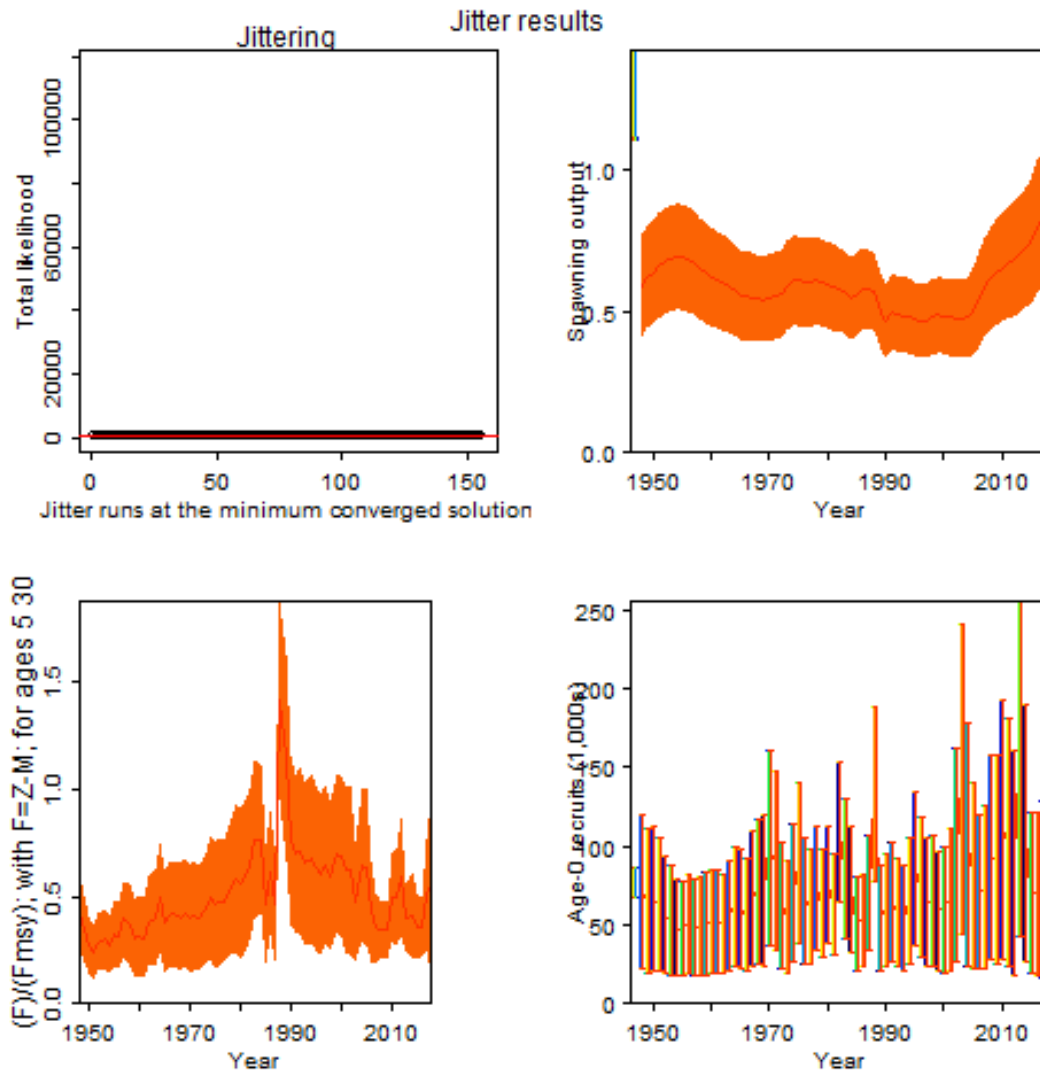
Figure 27. Jitter results for the base case model. The red line on the top left is the negative log-likelihood for the converged model.
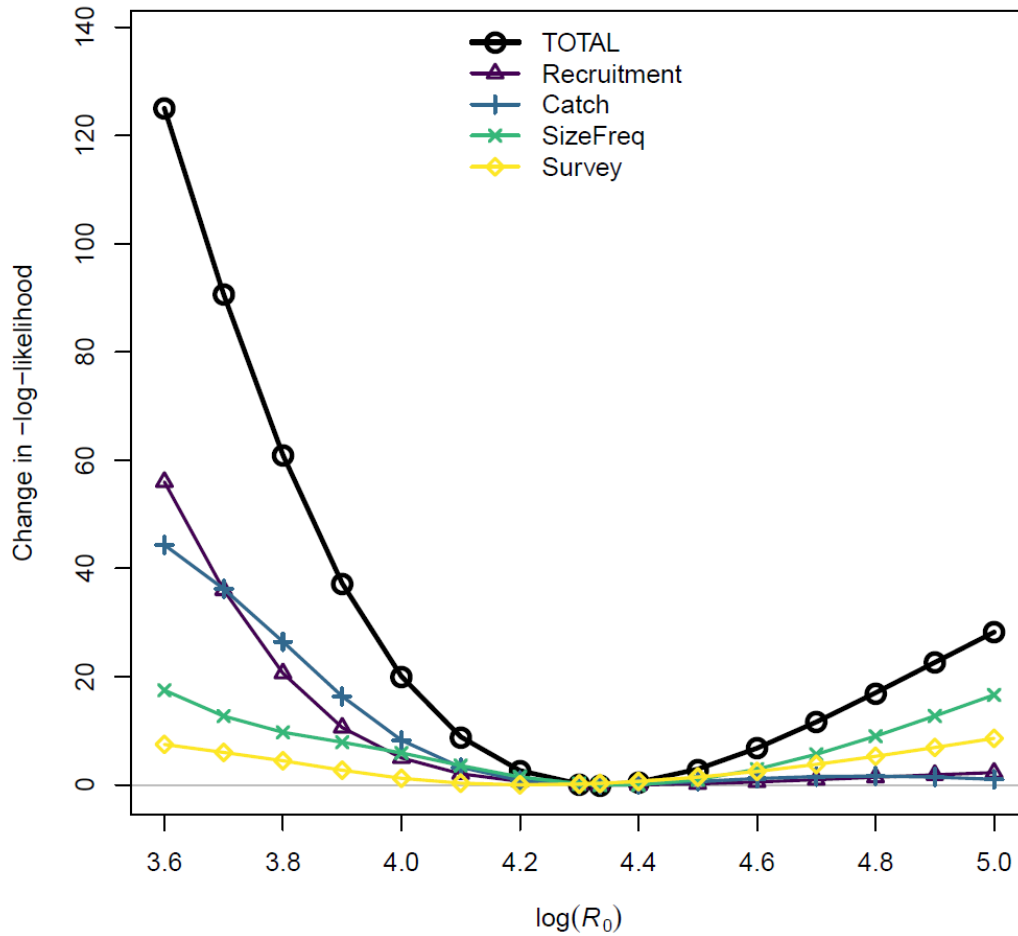
Figure 28. Profiles of the negative log-likelihoods relative to the minimum value of each component for the different likelihood components affecting the unfished recruitment parameter R_0 in log-scale for the base case model. Recruitment represents the likelihood component based on the deviations from the stock-recruitment curve, catch is the joint likelihood component based upon the estimated catch for each fleet, survey is the joint likelihood component based upon fitting to the CPUE and OPUE indices, and SizeFreq represents the likelihood component for the deep-sea handline fleet based on the fish size composition data.

Changes in index likelihood by fleet
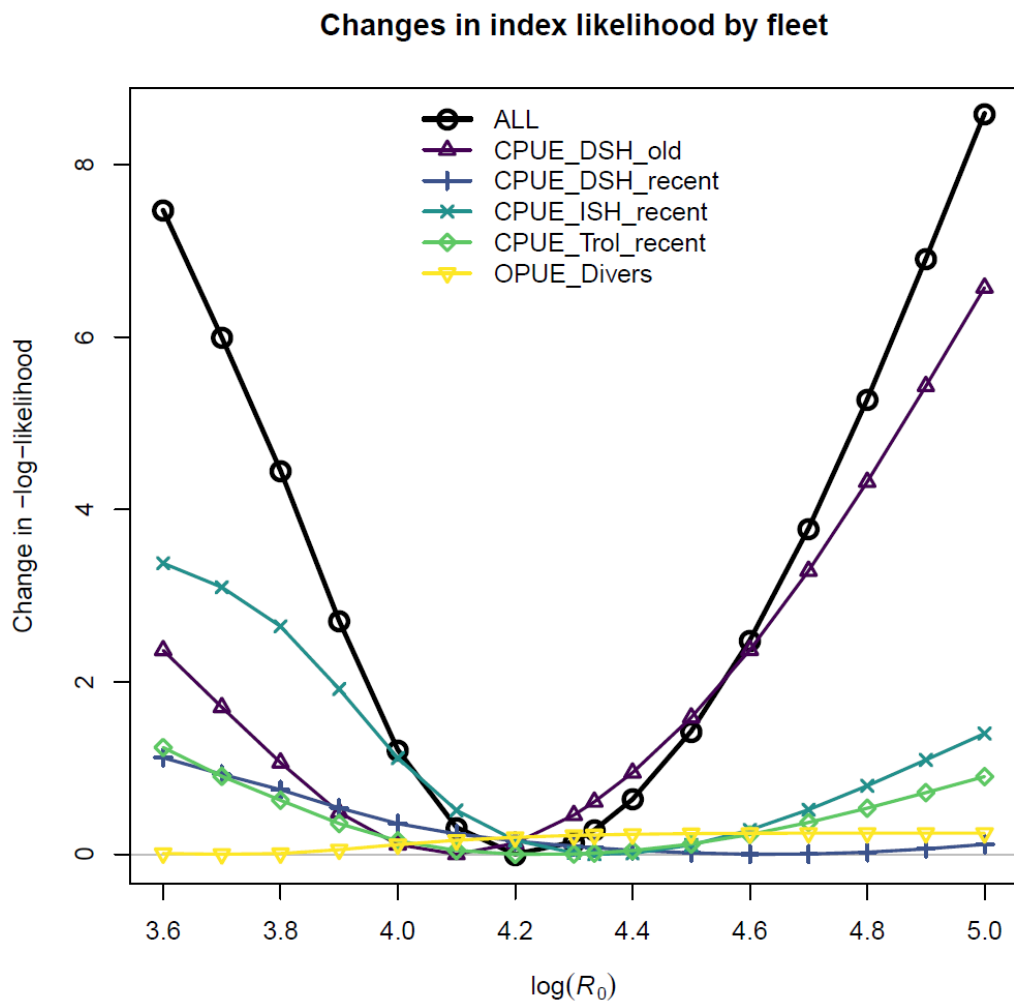
Figure 29. Profiles of the relative negative log-likelihoods by fleet-specific index likelihood components for the virgin recruitment in log-scale ($\log(R_0)$) ranged from 3.6 to 5.0 of the base case scenario. DSH—deep-sea handline, ISH—inshore handline, and Trol—trolling.
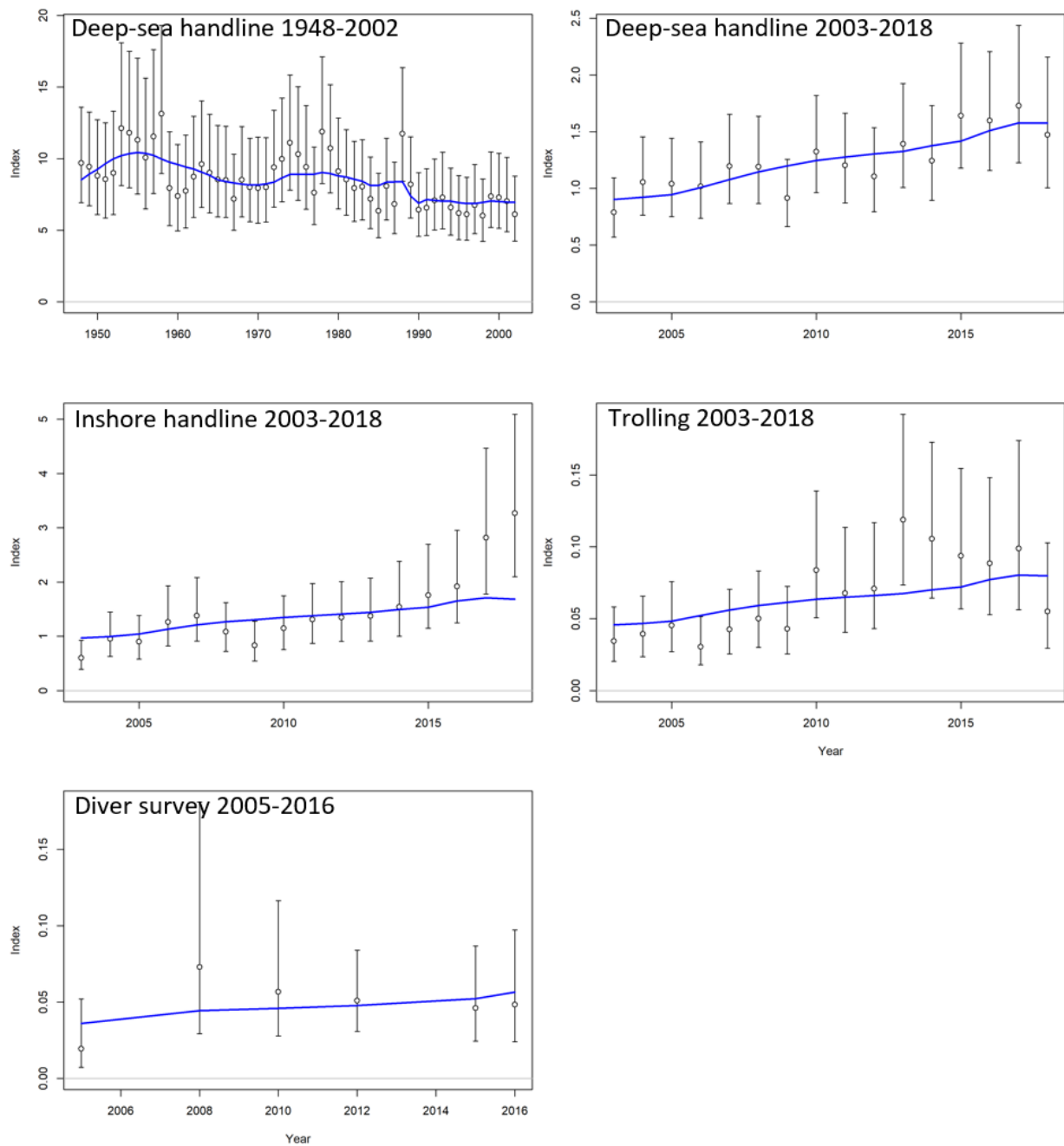
Figure 30. Plots of observed (open dots) and expected (blue lines) CPUE for the uku base case model for all abundance indices used in the model. Bars around each observed data point represent the sum of the input SE and additional SE added within the model.
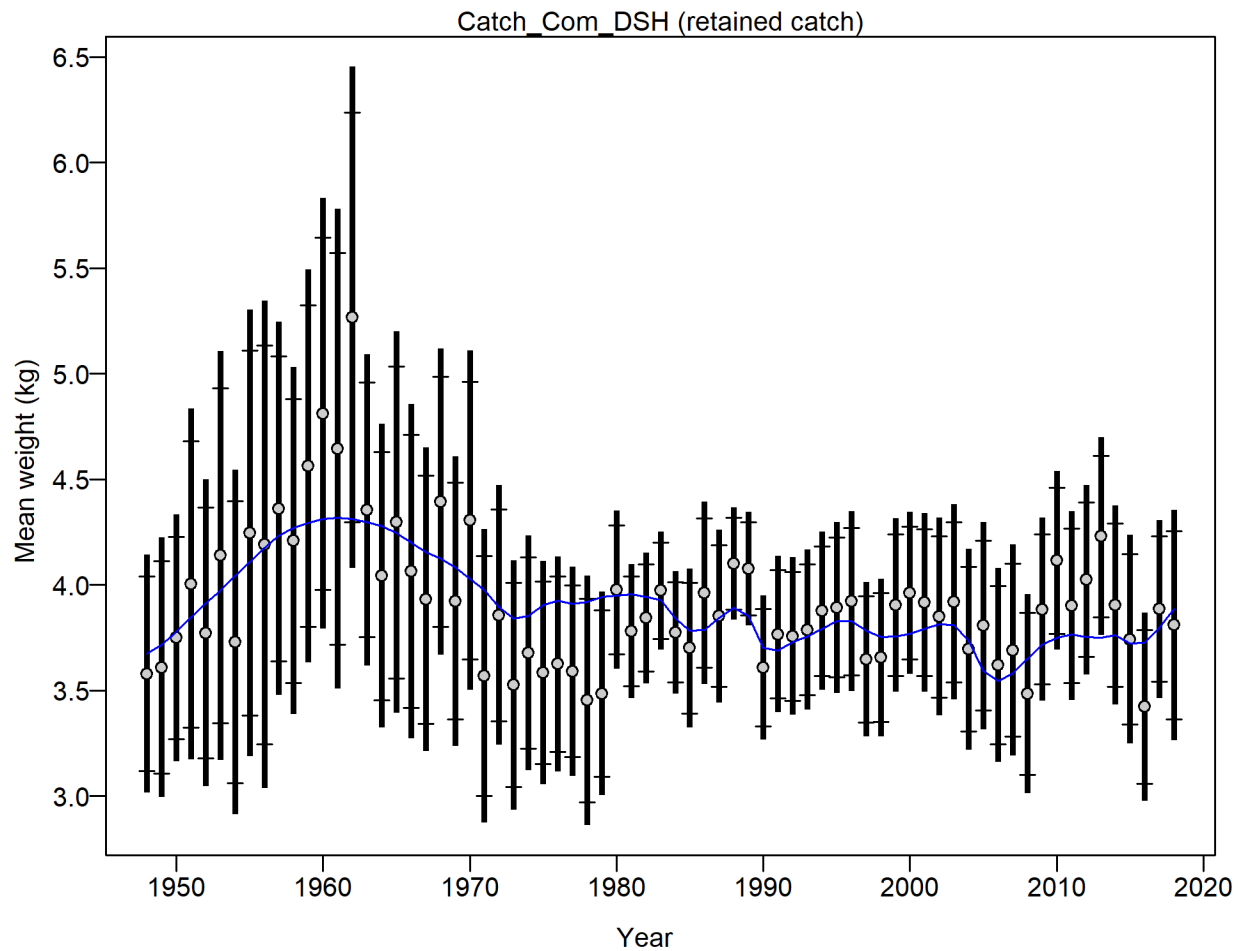
Figure 31. Model fit (lines) to mean weight (kg) of the composition data (points, showing the observed mean age and 95% credible limits around mean age (vertical lines).
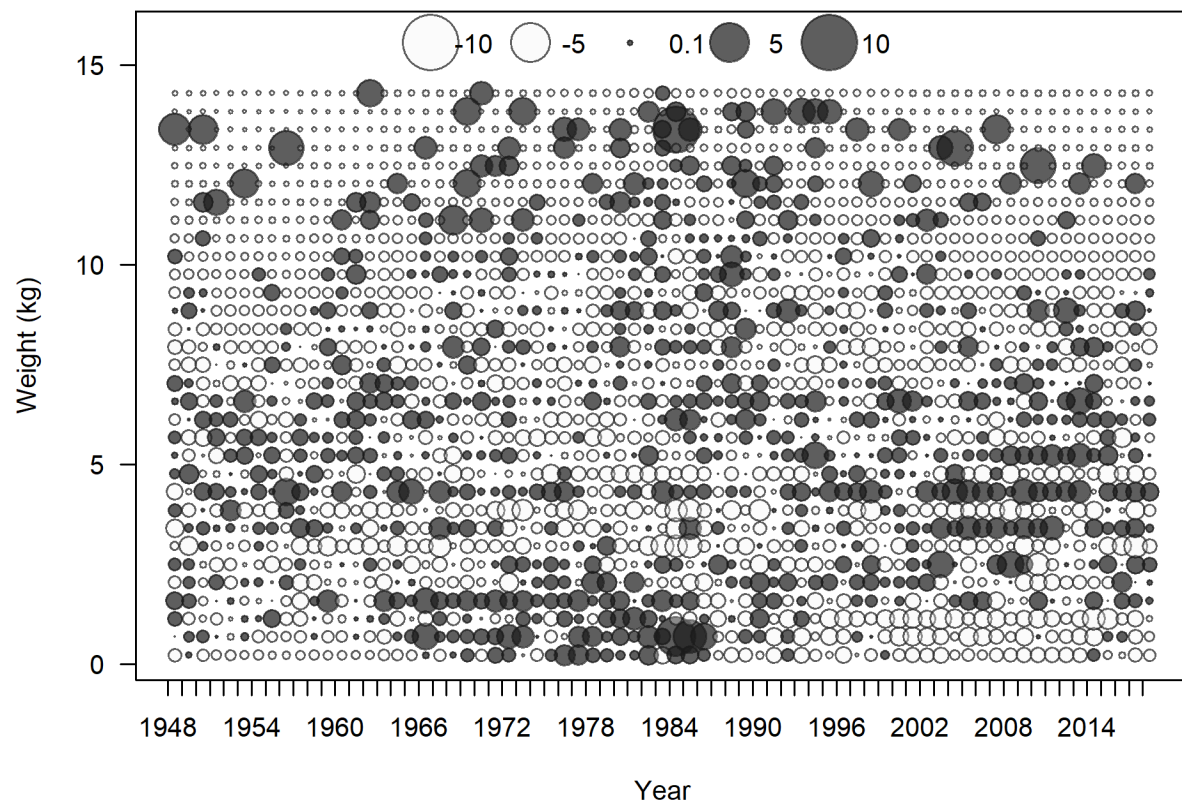
Figure 32. Pearson residual plots of model fits to the size composition data for deep-sea handline fishery targeting uku.
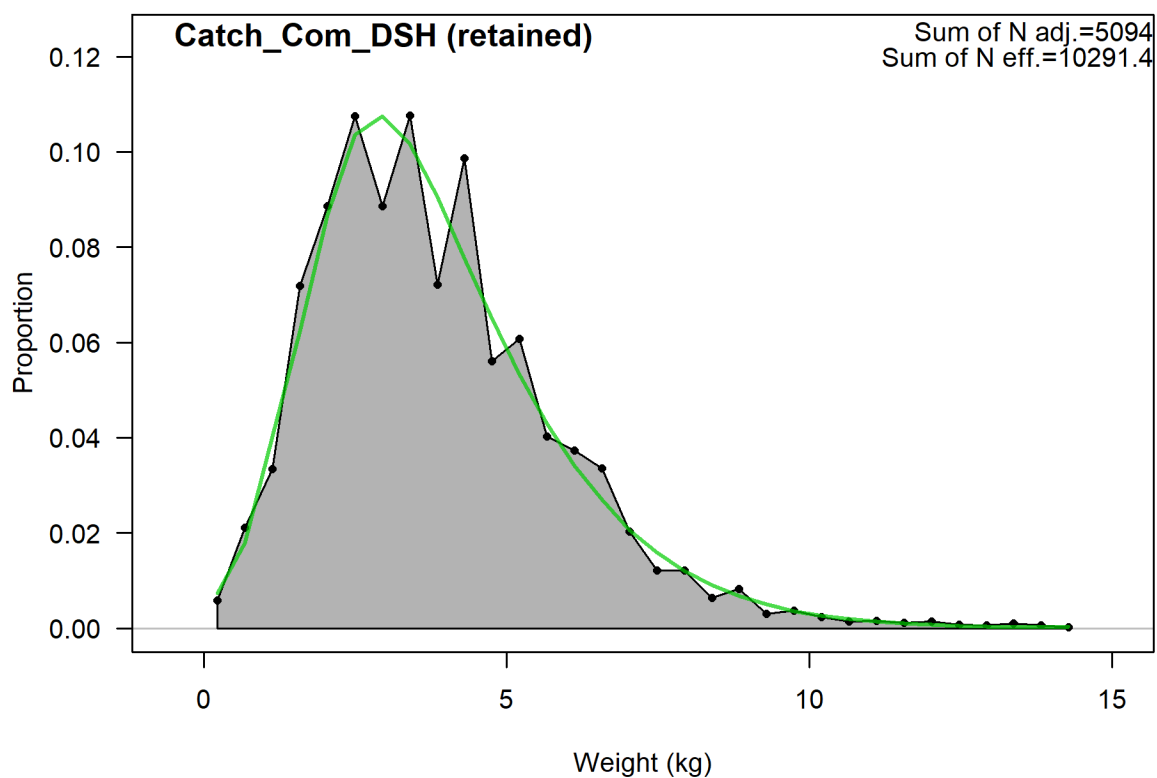
Figure 33. Comparison of observed (gray shaded area and black dots) and model predicted (green solid line) size composition data for the deep-sea handline fishery used in the stock assessment for uku.
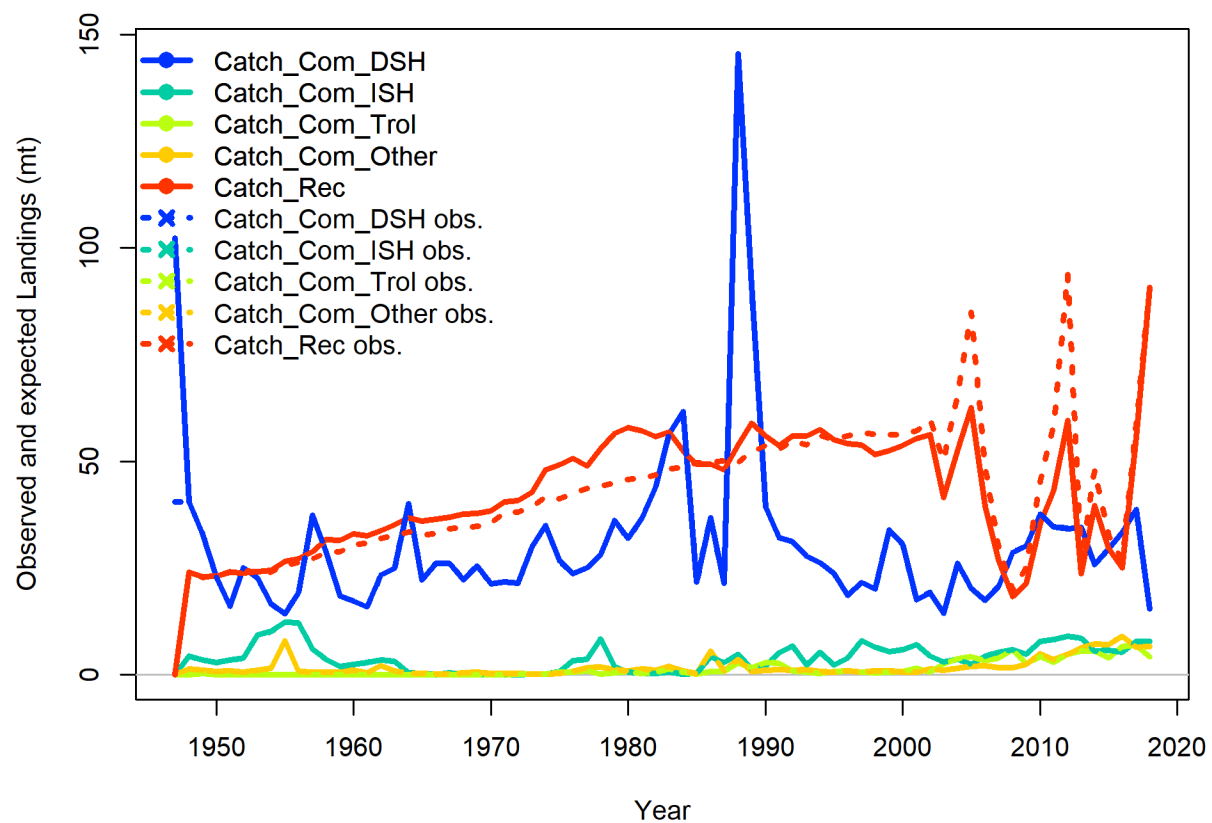
Figure 34. Observed (dashed line) versus estimated (full line) catch in the Stock Synthesis model.
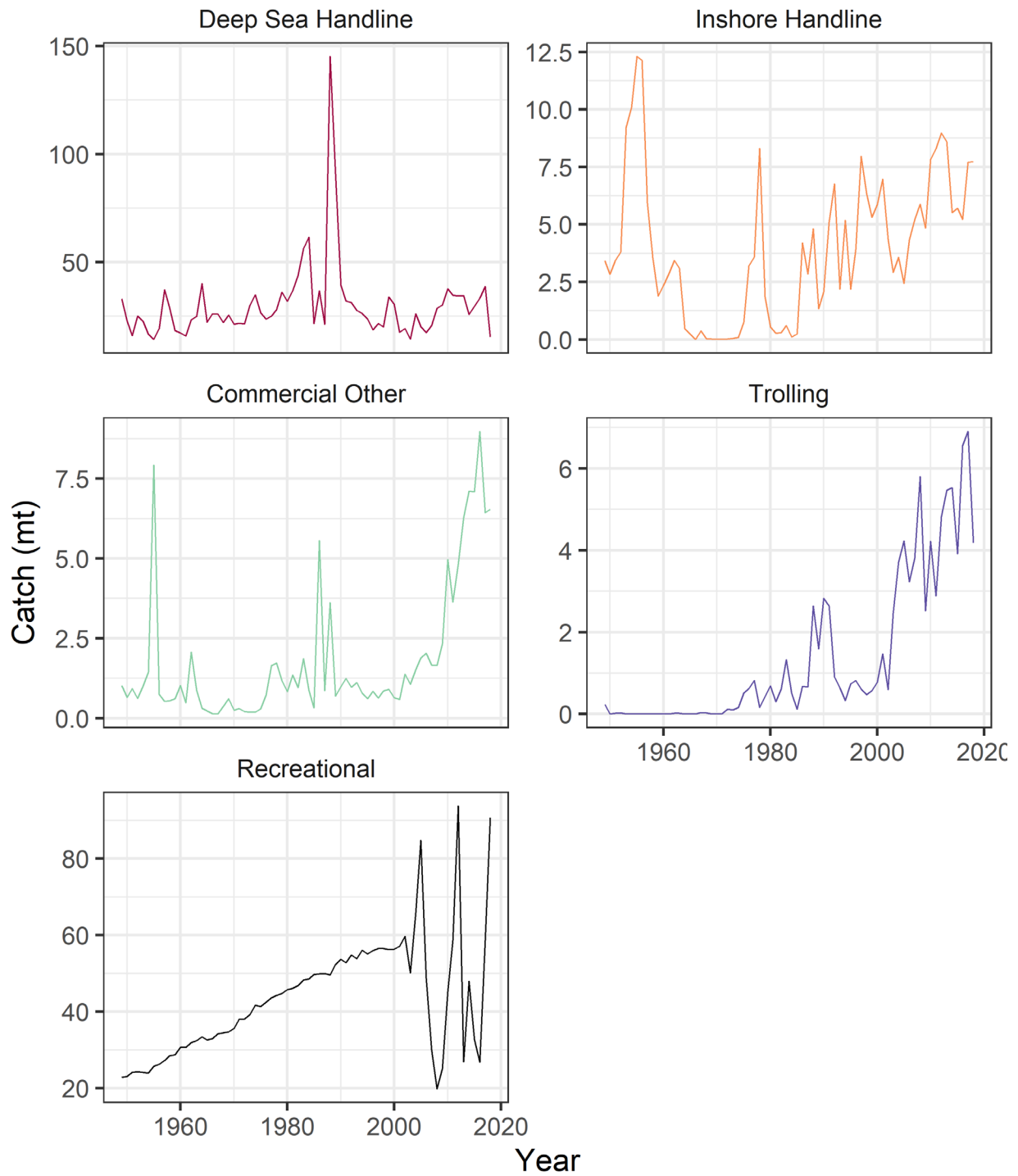
Figure 35. Observed catch by fishing gear.
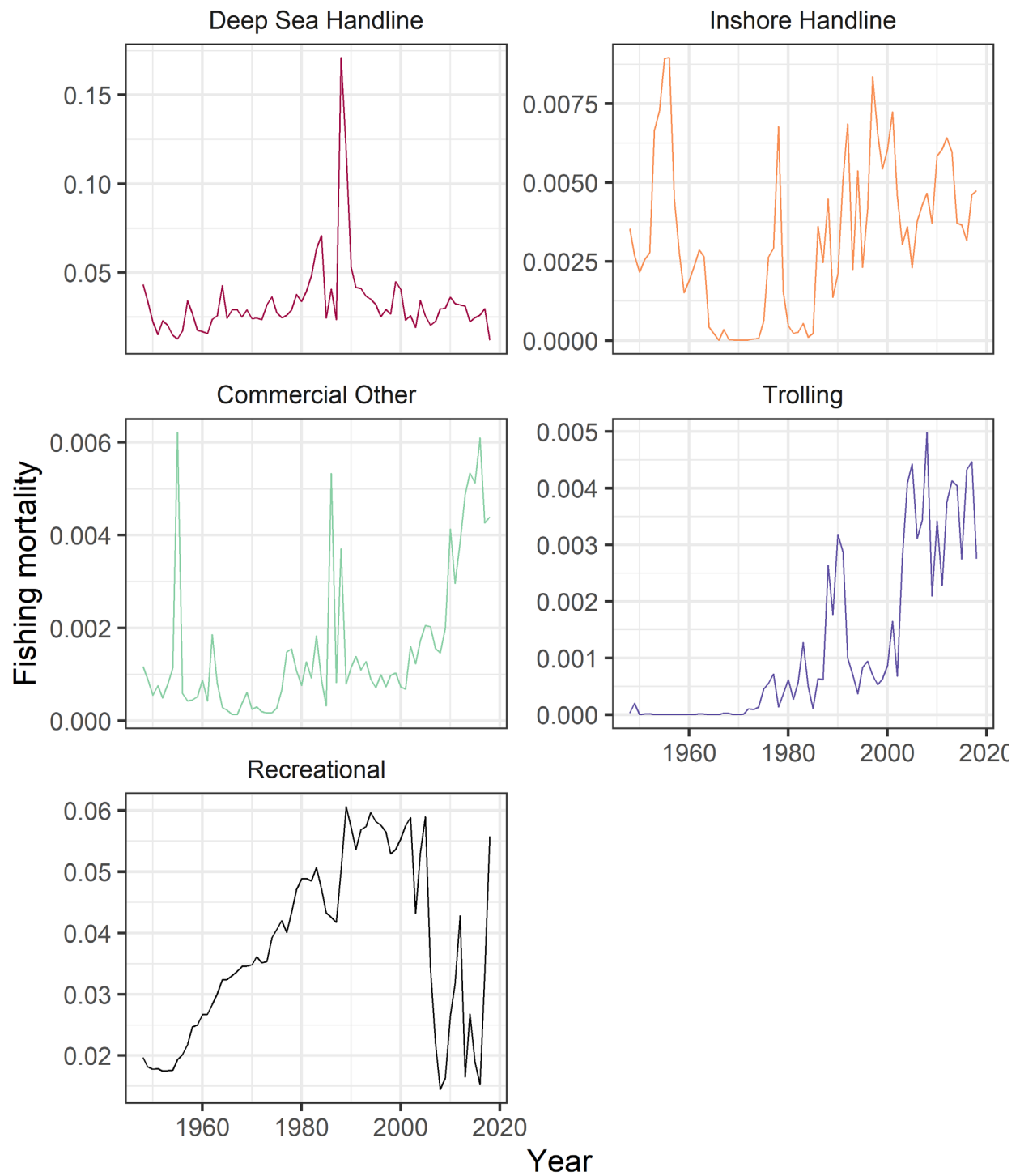
Figure 36. Annual fishing mortality estimated from the base-case model by fishing gear.
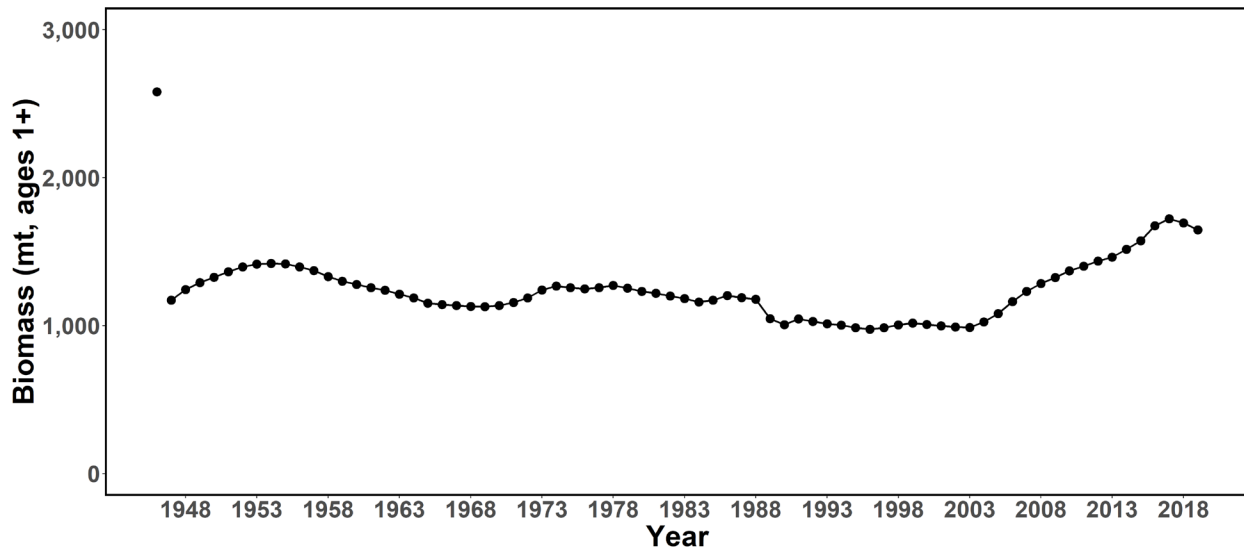
Figure 37. Time series of total biomass (age 1 and older, metric tons) for uku estimated in the base-case model. The first year indicates virgin biomass levels.
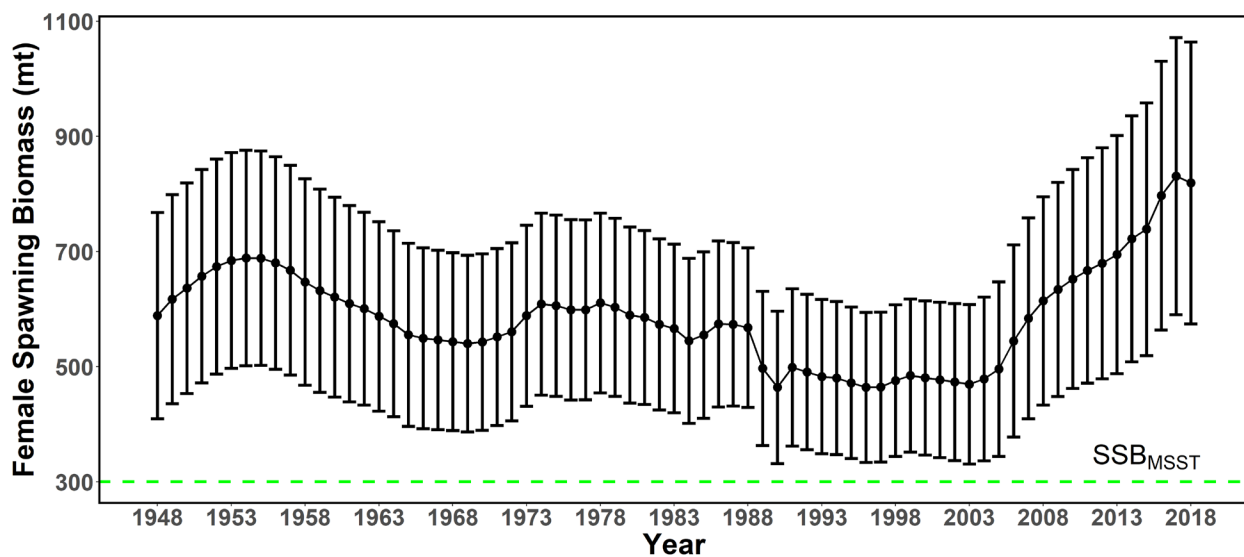
Figure 38. Time series of spawning biomass (metric tons) for uku estimated in the base-case model. The solid line with circles represents the maximum likelihood estimates and the error bars represent the uncertainty of the estimates (95% confidence intervals). The dashed horizontal line shows the spawning biomass to produce the MSST reference point (SSB_{MSST}).
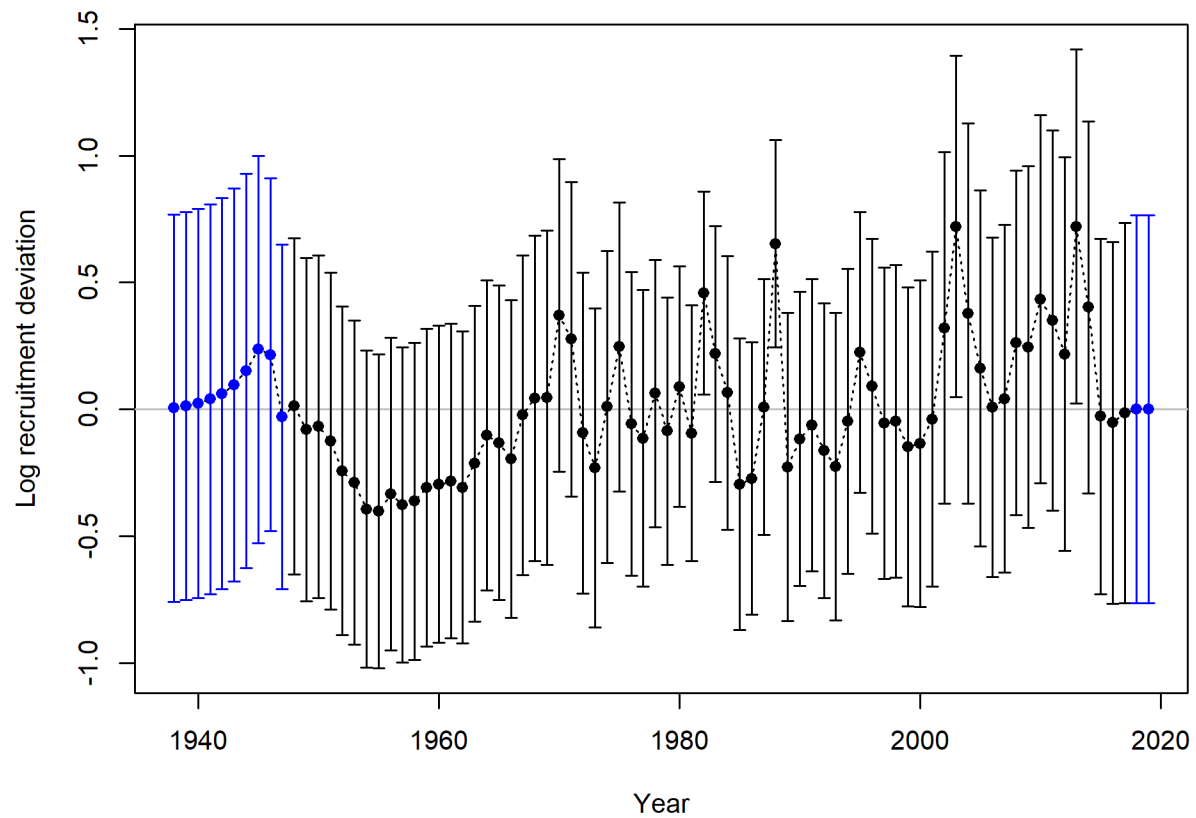
Figure 39. Estimated log recruitment deviations for the early (1938–1947, blue) and main (1948–2017, black) recruitment periods with associated 95% asymptotic confidence intervals.
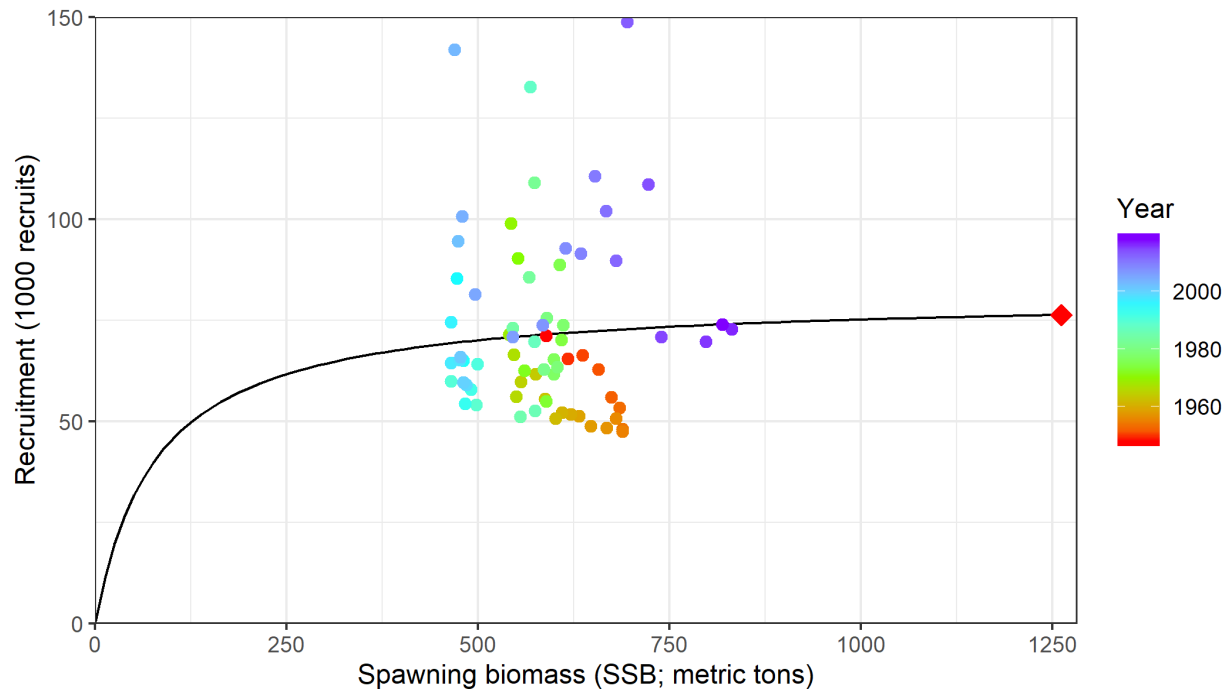
Figure 40. Expected recruitment from the stock-recruitment relationship (black line) and estimated annual recruitment (dots) from Stock Synthesis. Estimated virgin SSB and recruitment is indicated with a red diamond.
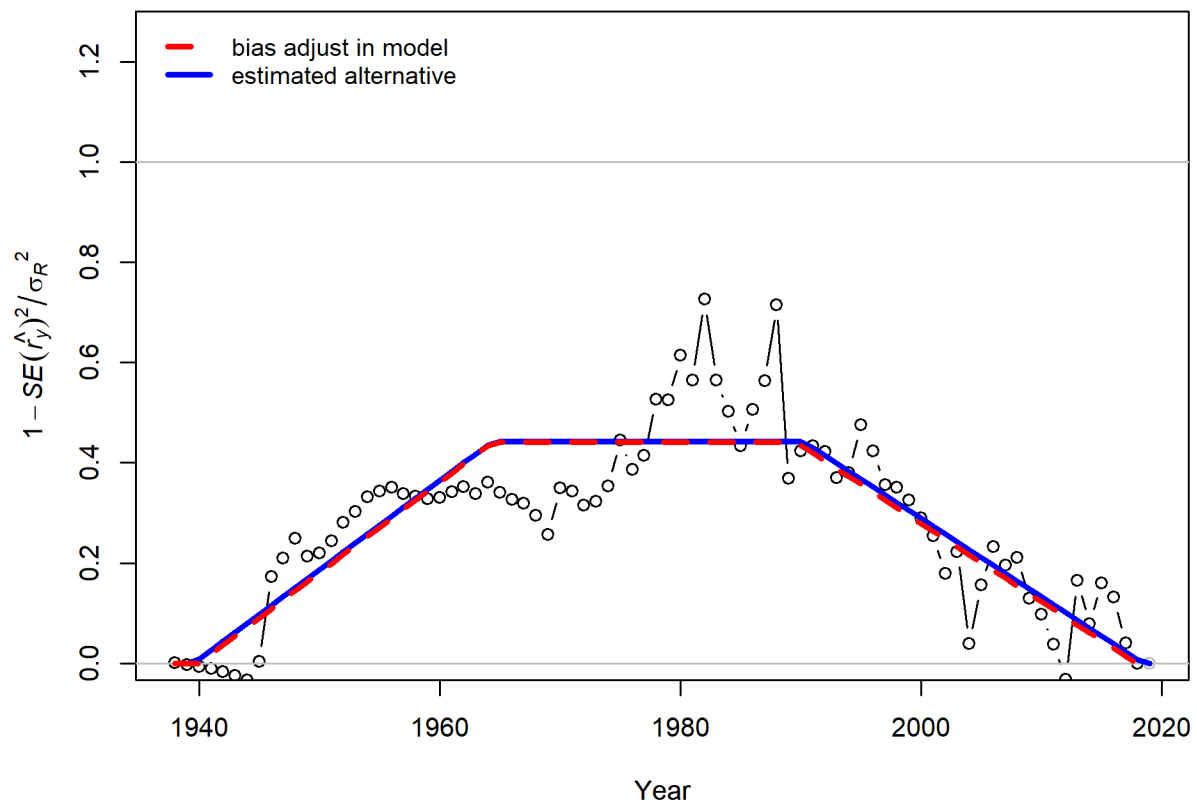
Figure 41. Bias adjustment applied to the stock-recruitment relationship (red stippled line) and the estimated alternative (blue line) obtained from the r4ss output.
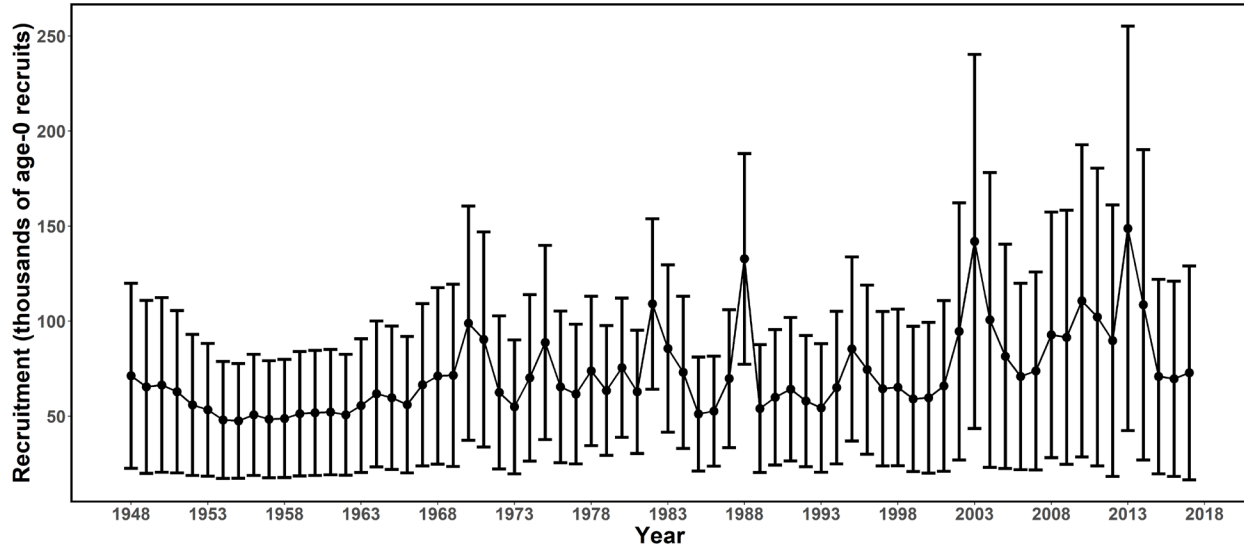
Figure 42. Time series of recruitment (thousands of age-0 fish) for uku estimated in the base-case model. The solid line with circles represents the maximum likelihood estimates and the error bars represent the uncertainty of the estimates (95% confidence intervals).
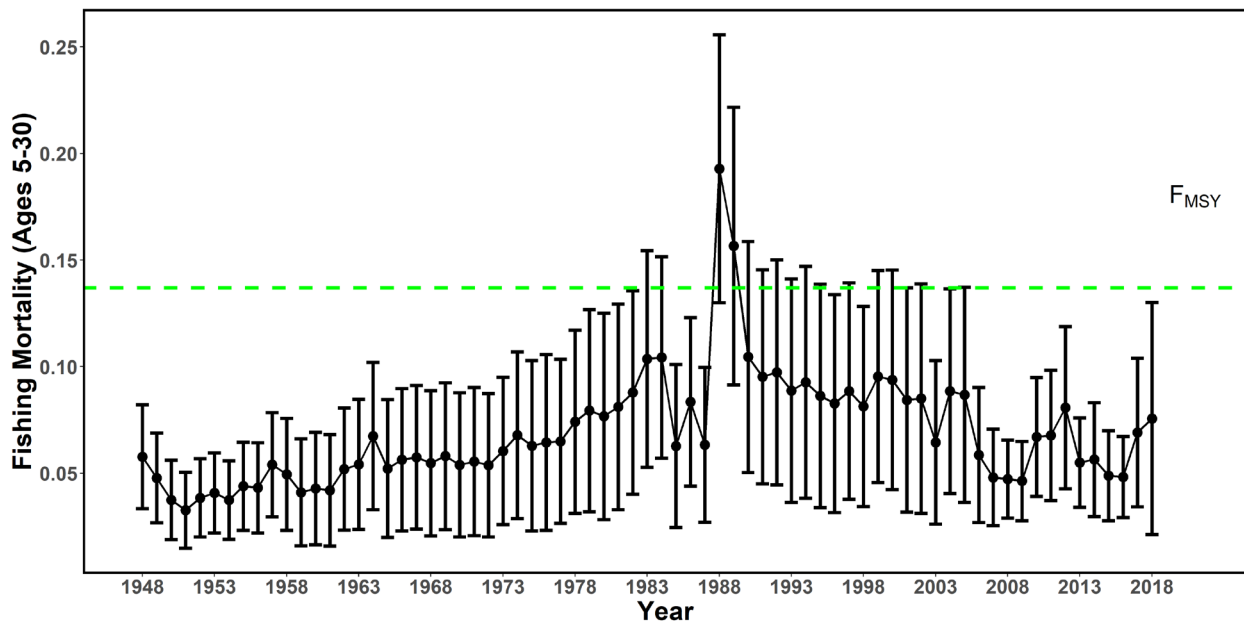
Figure 43. Time series of instantaneous fishing mortality (average for ages 5–30) for the uku estimated in the base-case model. The solid line with circles represents the maximum likelihood estimates and the error bars represent the uncertainty of the estimates (95% confidence interval). The dashed horizontal line shows the fishing mortality to produce the MSY reference point (F_{MSY}).
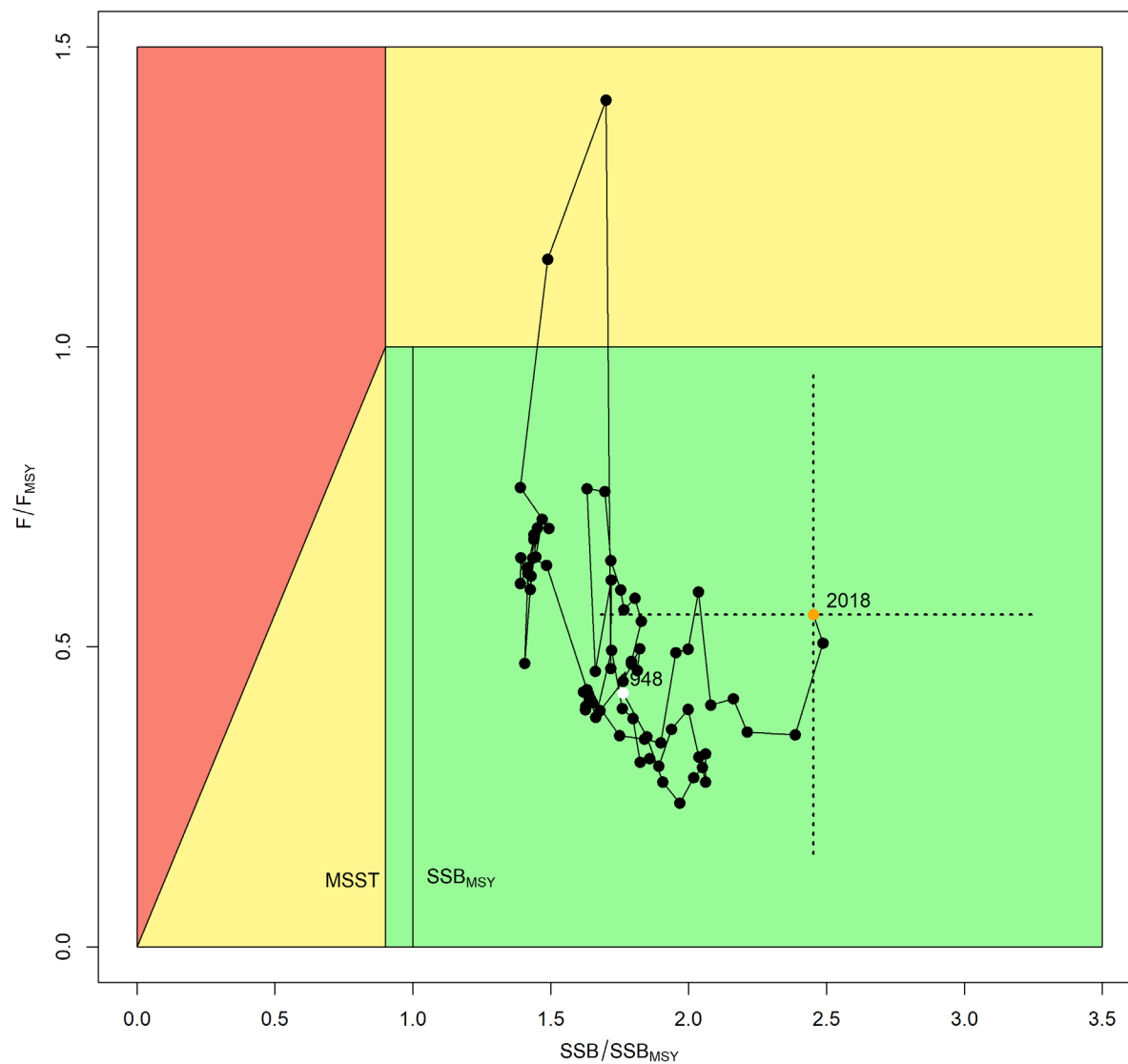
Figure 44. Kobe plot of the trends in estimates of relative fishing mortality (average of age 5–30) and spawning stock biomass of uku during 1948–2018. The white dot indicates 1948, the orange dot indicates 2018, and the dotted lines indicate the 95% confidence intervals around the final year values.
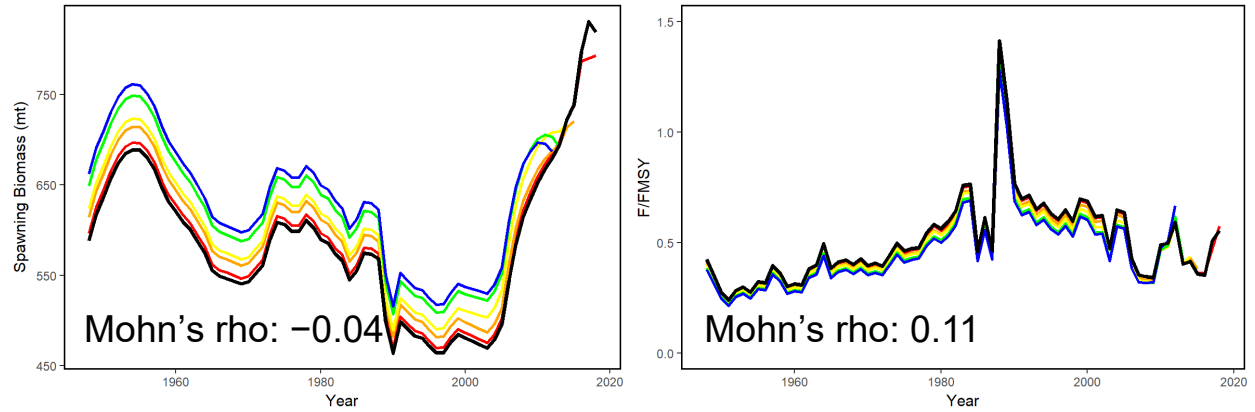
Figure 45. Retrospective analysis of spawning biomass (as $SSB/SSB\mathrm{M_{SST}}$, left) and fishing mortality (as F/F_{MSY}, right) consisting of 5 reruns of the base case model each fitted with one additional year of data removed from the base case model (black line, 1948-2018).
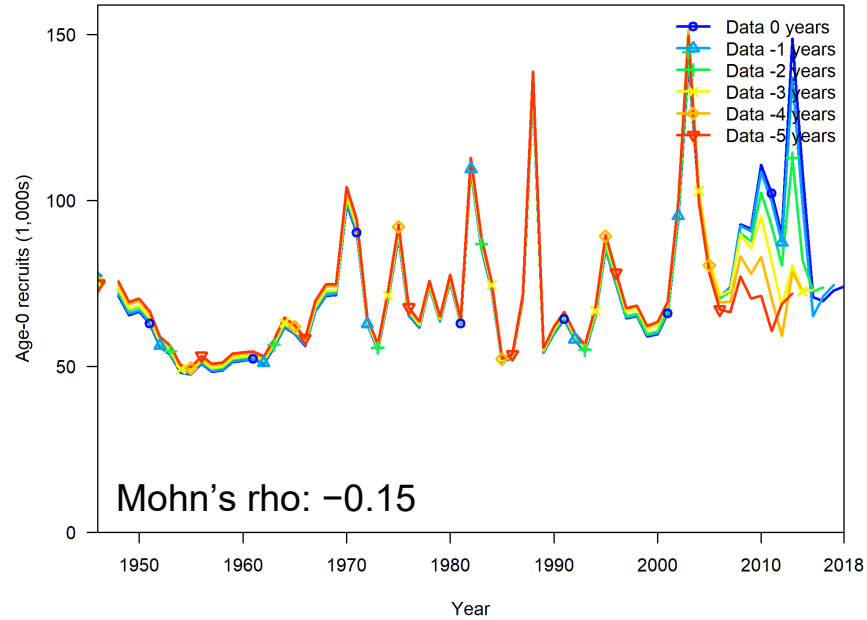
Figure 46. Plot of estimated Age-0 recruits (in 1000s of fish) for each run in the 5-year retrospective analysis. The dark blue line indicates the base-case model (1948–2018).
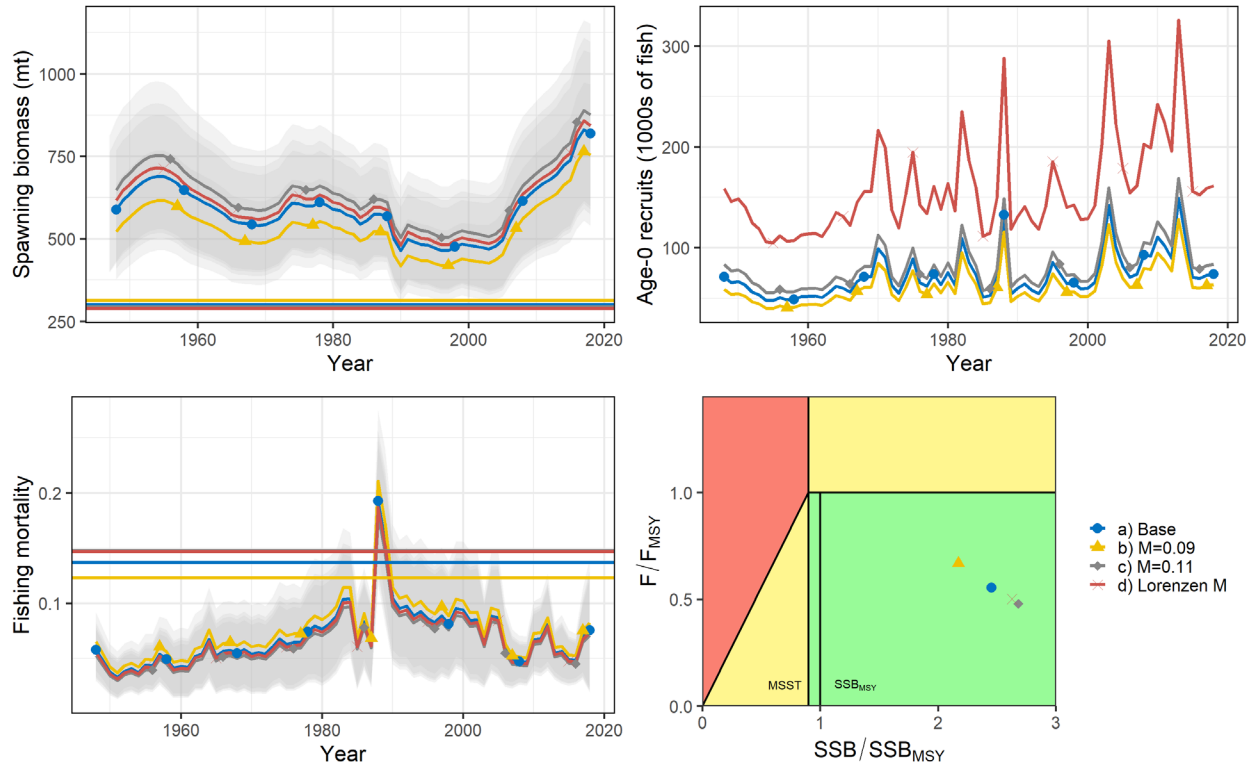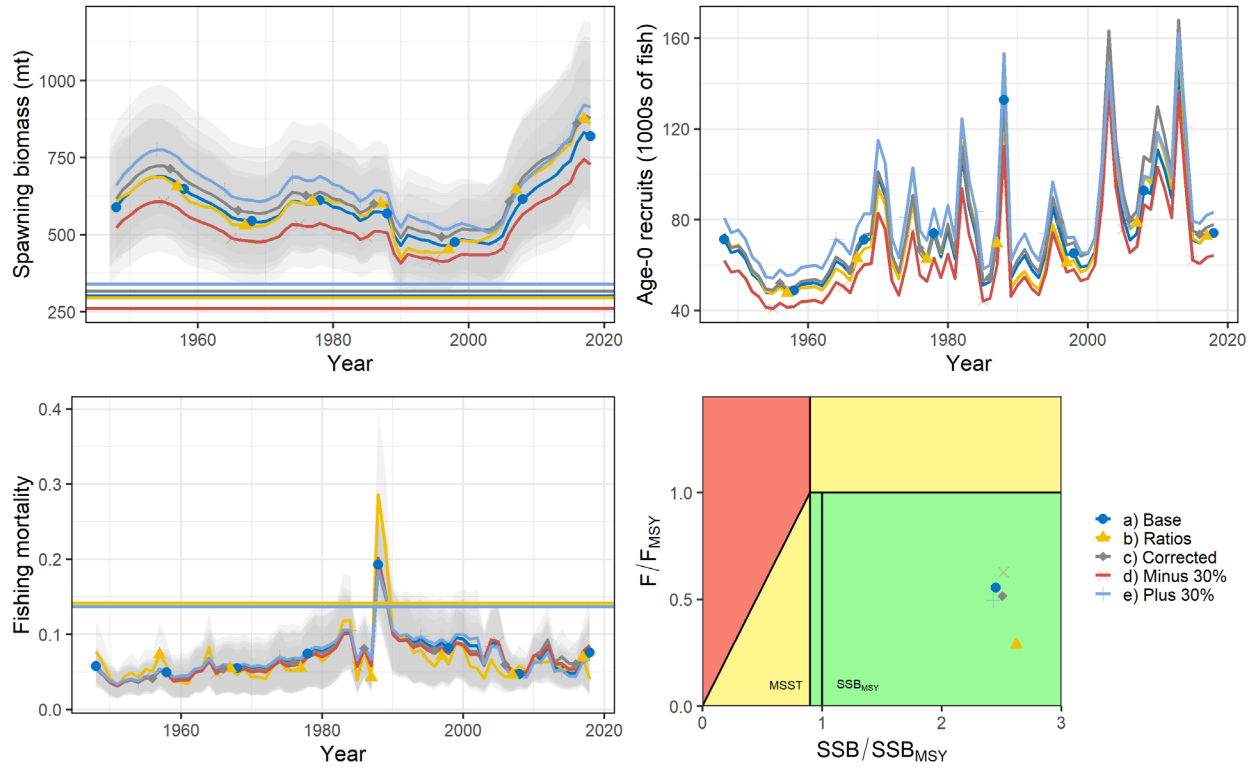
Figure 47. Sensitivity analyses showing differences in spawning biomass, fishing mortality, recruitment, and final year stock status (Kobe plot) under different natural mortality values (*M*).
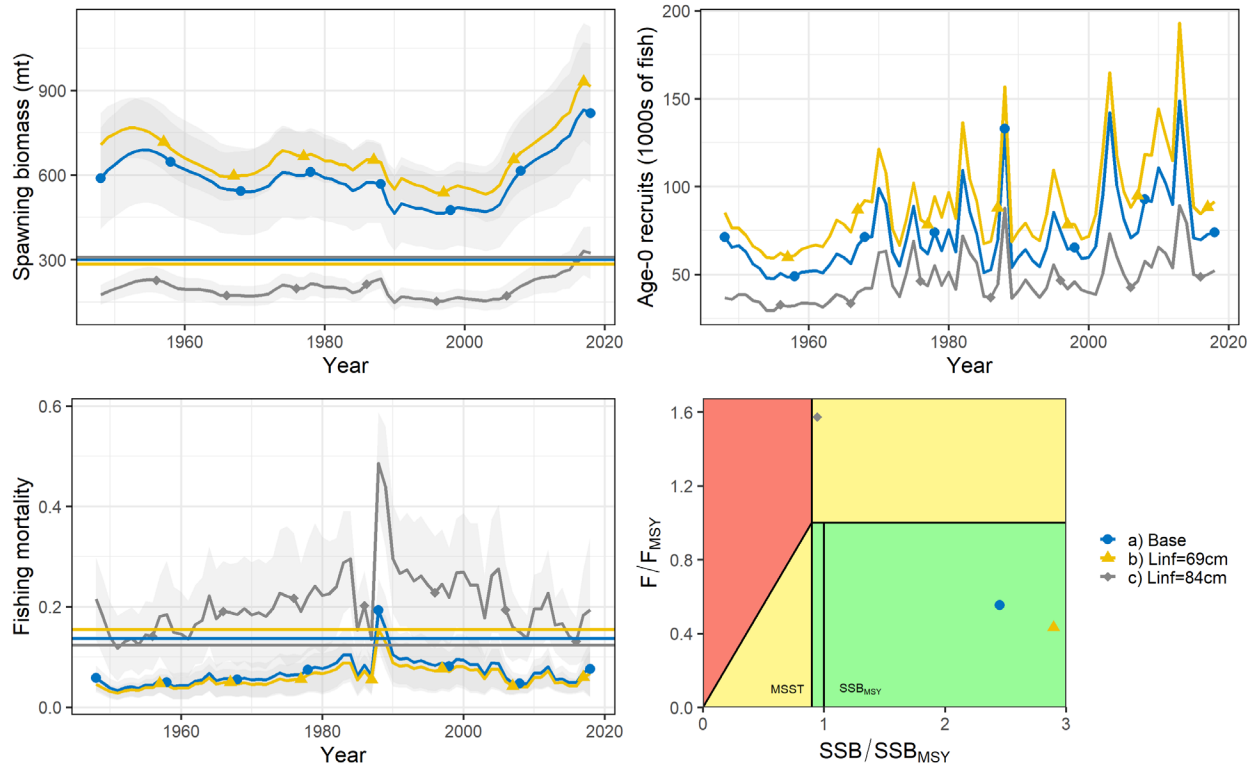
Figure 48. Sensitivity analyses showing differences in spawning biomass, fishing mortality, recruitment, and final year stock status (Kobe plot) under different length at maximum age (L_{Amax}) values.
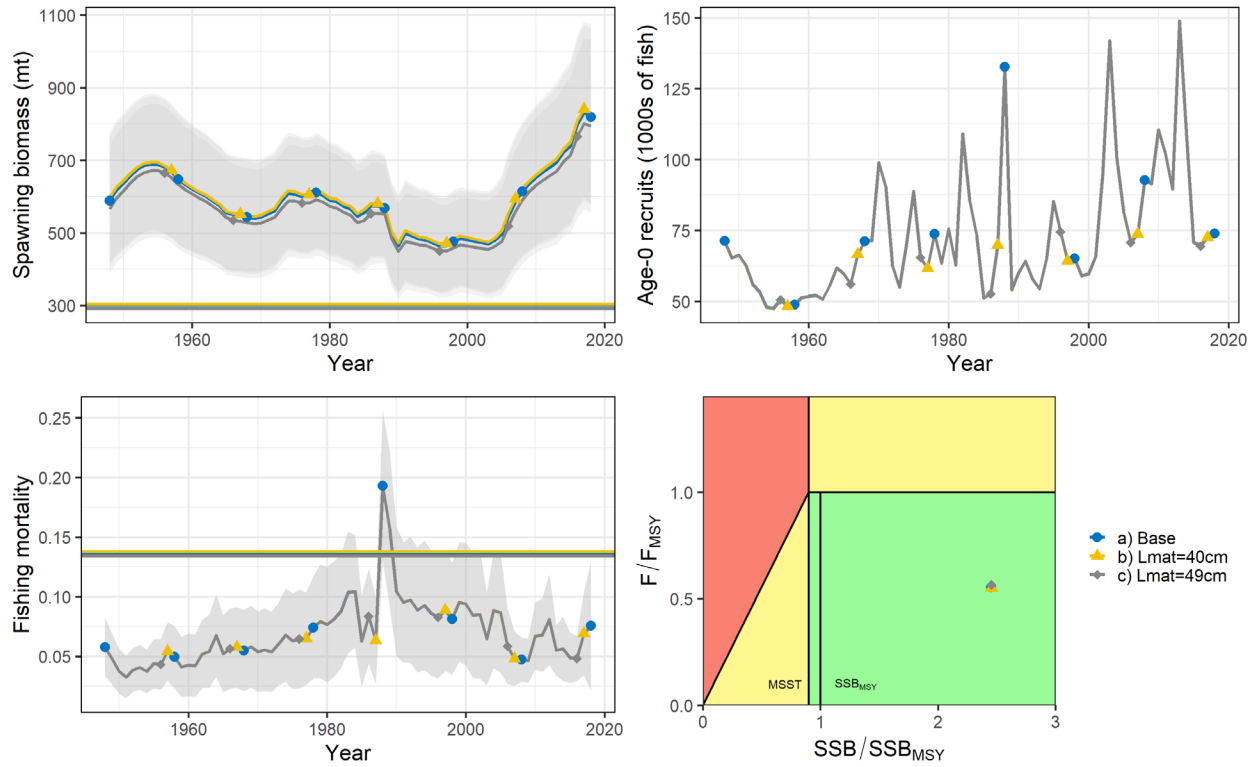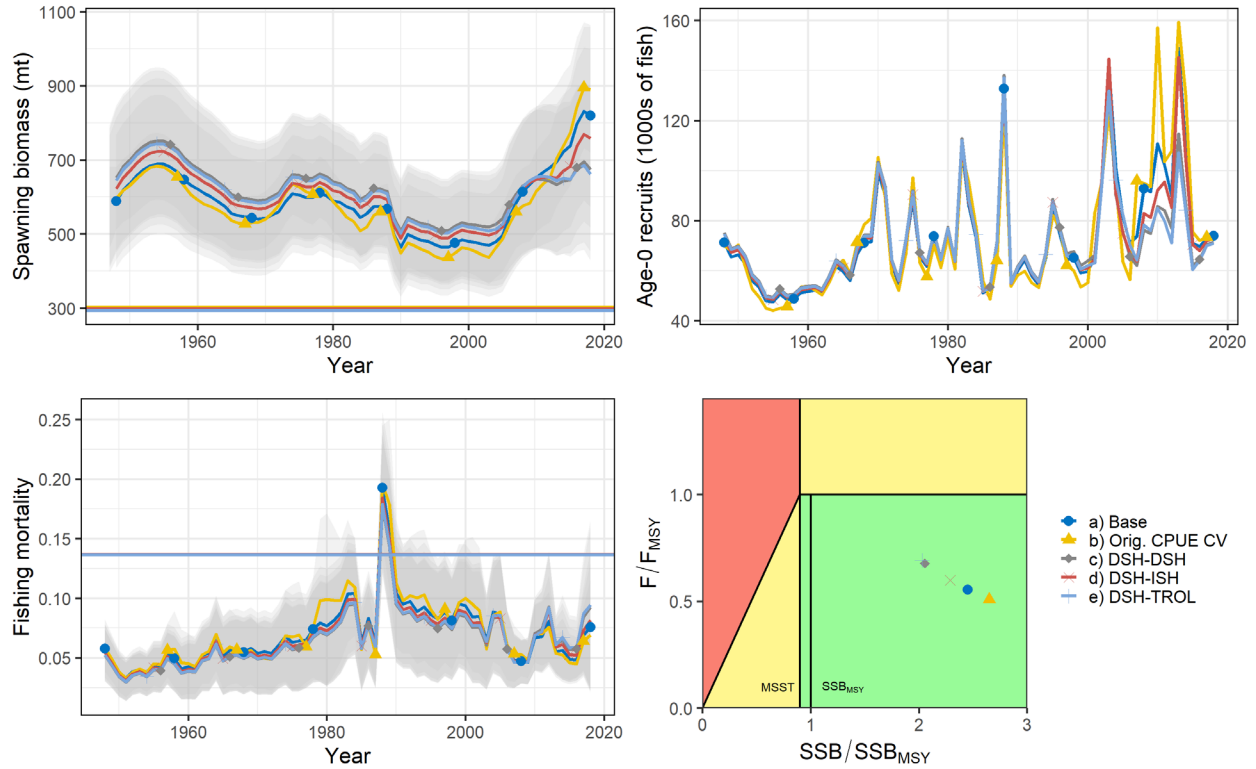
Figure 49. Sensitivity analyses showing differences in spawning biomass, fishing mortality, recruitment, and final year stock status (Kobe plot) under different length at 50% maturity values (L_{mat50}).
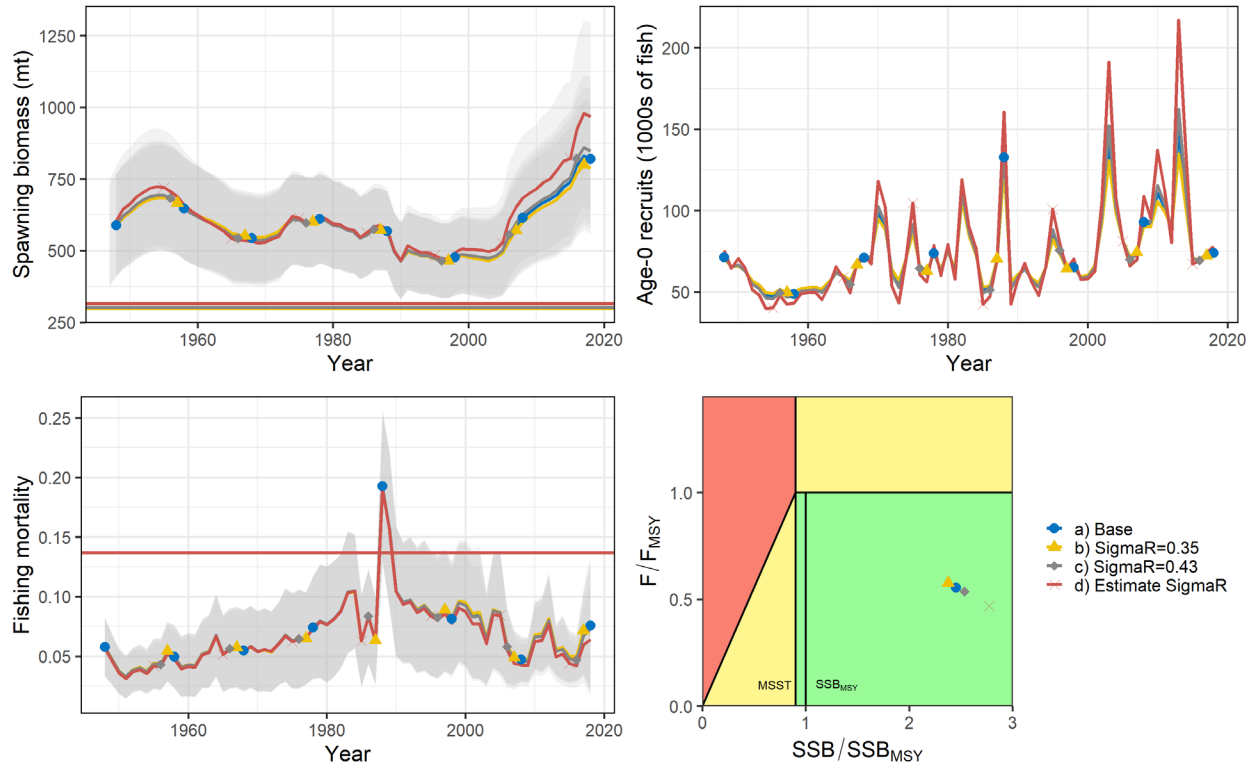
Figure 50. Sensitivity analyses showing differences in spawning biomass, fishing mortality, recruitment, and final year stock status (Kobe plot) under different recruitment variability (σ_R) values.
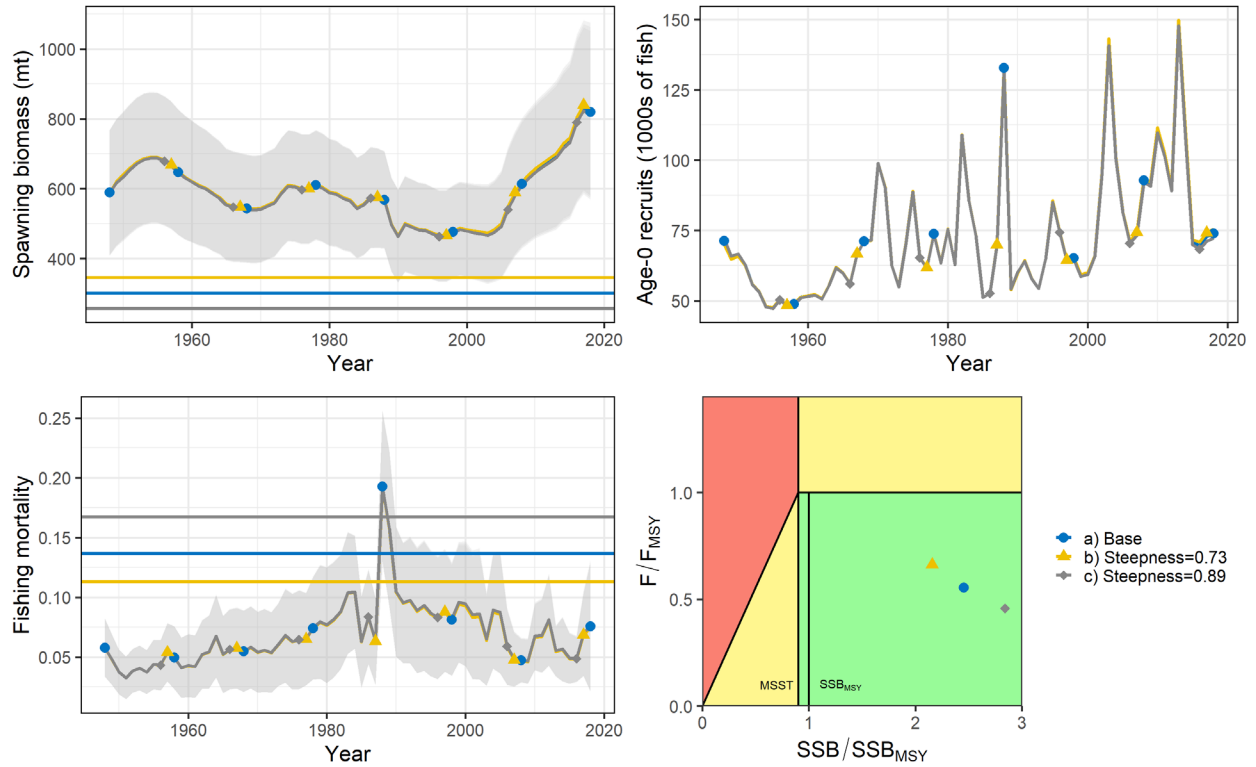
Figure 51. Sensitivity analyses showing differences in spawning biomass, fishing mortality, recruitment, and final year stock status (Kobe plot) under different stock-recruitment steepness (*h*) values.
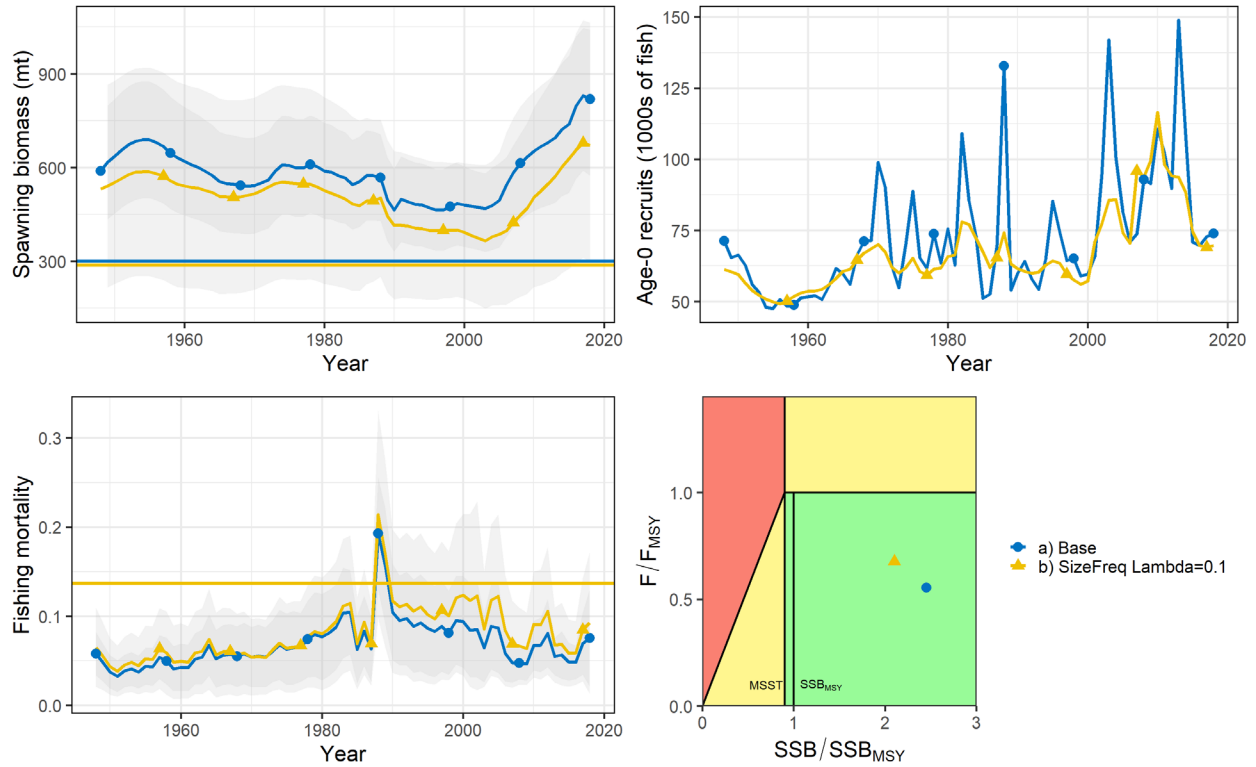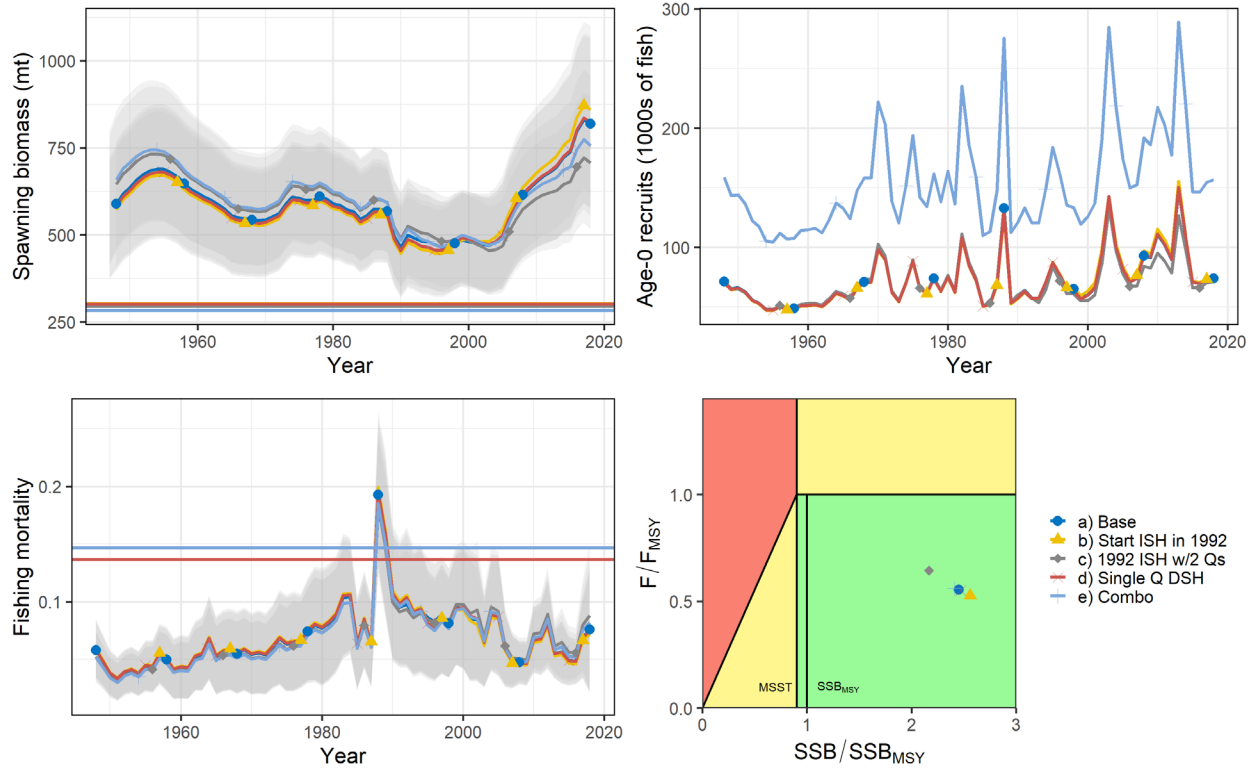
Figure 52. Sensitivity analyses showing differences in spawning biomass, fishing mortality, recruitment, and final year stock status (Kobe plot) under different recreational catch reconstruction scenarios. Corrected: 2003–2016 recreational catch with a linear adjustment for landline bias, Minus/Plus 30%: 1948–2002 recreational catch adjusted by plus or minus 30%, and Ratios: 2003–2018 mean commercial to recreational catch ratios applied to 1948–2002 commercial catch to re-create the 1948–2002 recreational catch.

Figure 53. Sensitivity analyses showing differences in spawning biomass, fishing mortality, recruitment, and final year stock status (Kobe plot) under different abundance (CPUE) index combinations, including a scenario where the original index CVs are used.
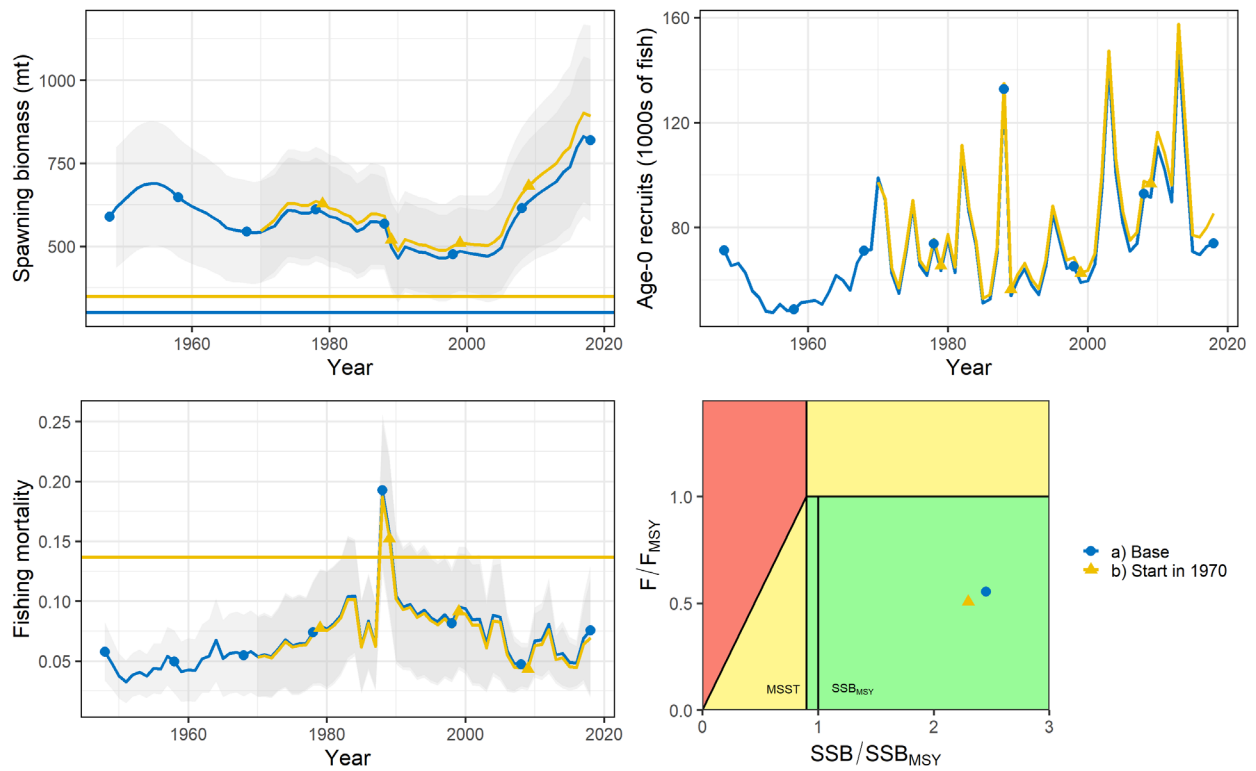
Figure 54. Sensitivity analyses showing differences in spawning biomass, fishing mortality, recruitment, and final year stock status (Kobe plot) when setting the likelihood weight (i.e., lambda) of the size-frequency data to 0.1.

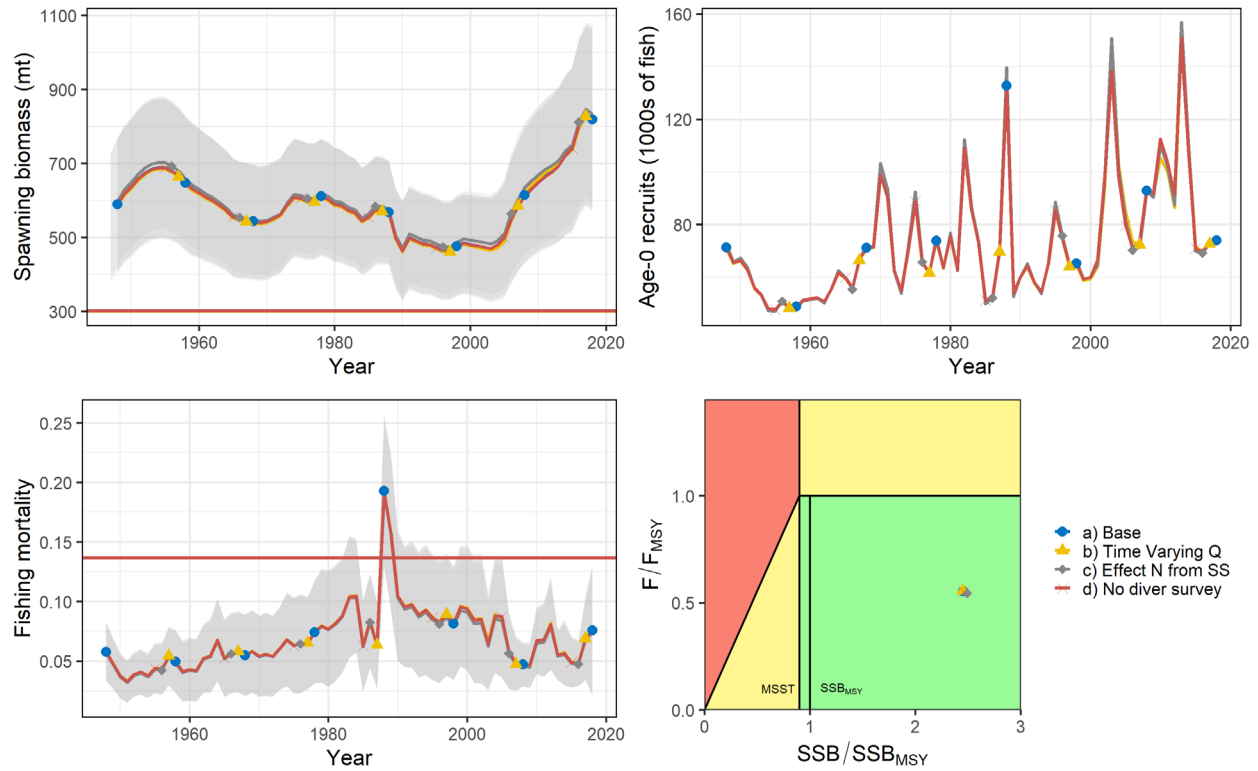Figure 55. Sensitivity analyses showing differences in spawning biomass, fishing mortality, recruitment, and final year stock status (Kobe plot) when extending the inshore handline CPUE index to 1992 as either a single or two time series, using the deep-sea handline index as a single time series from 1948 to 2018, and combining both extended CPUE time series and using the Lorenzen M age-specific estimates (Combo).

Figure 56. Sensitivity analyses showing differences in spawning biomass, fishing mortality, recruitment, and final year stock status (Kobe plot), when starting the model in 1970 instead of 1948.

Figure 57. Sensitivity analyses showing differences in spawning biomass, fishing mortality, recruitment, and final year stock status (Kobe plot) using time-varying catchability, effective sample size from SS for size frequency data, or excluding diver surveys from the model.
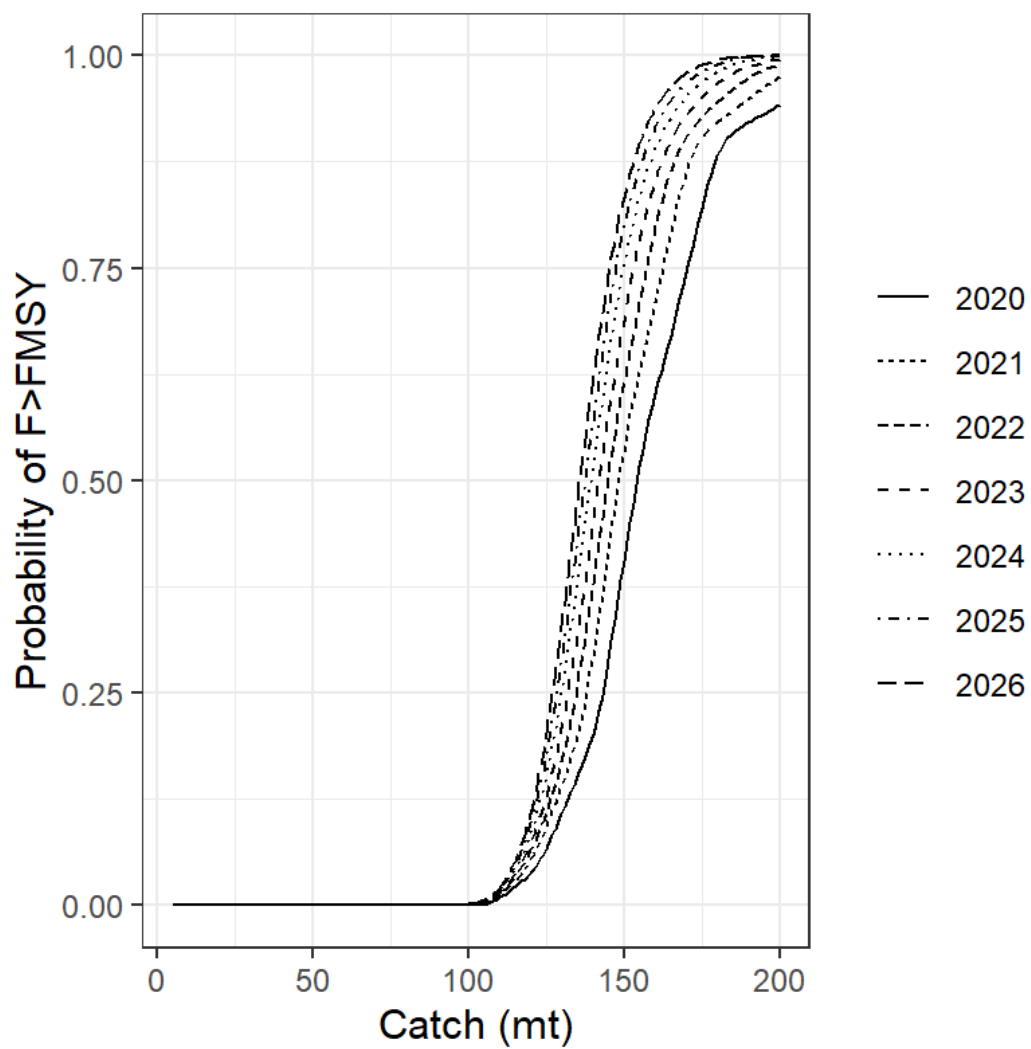
Figure 58. Probability of overfishing (i.e., $F/F_{MSY}>1$) uku in the main Hawaiian Islands in fishing years 2020 through 2026 as a function of projected catch varying from 0 to 200 metric tons.
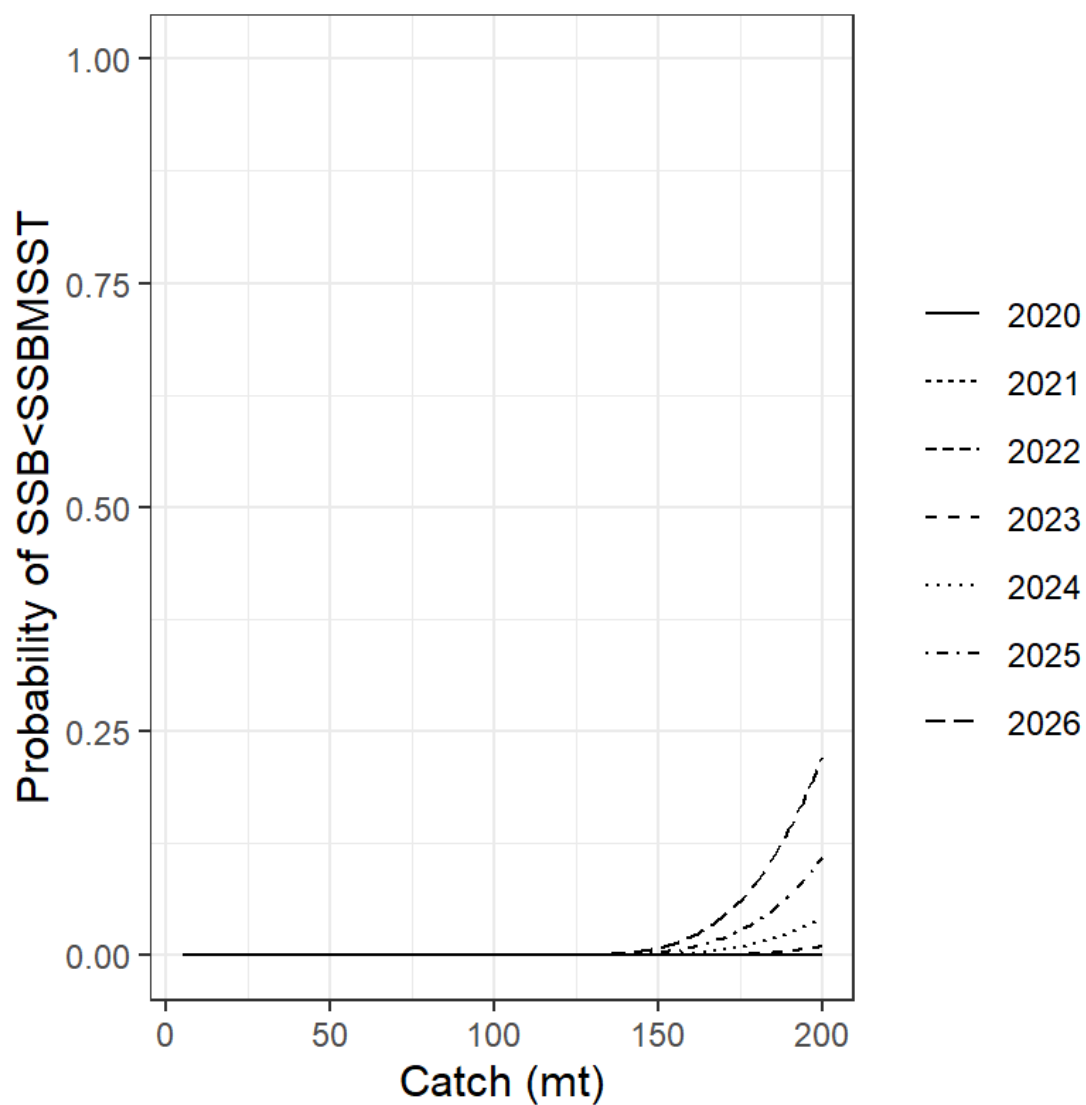
Figure 59. Probability of the stock being overfished (i.e., *SSB*/*SSB*$_{MSST}$<1) for uku in the main Hawaiian Islands in fishing years 2020 through 2026 as a function of projected catch varying from 0 to 200 metric tons.
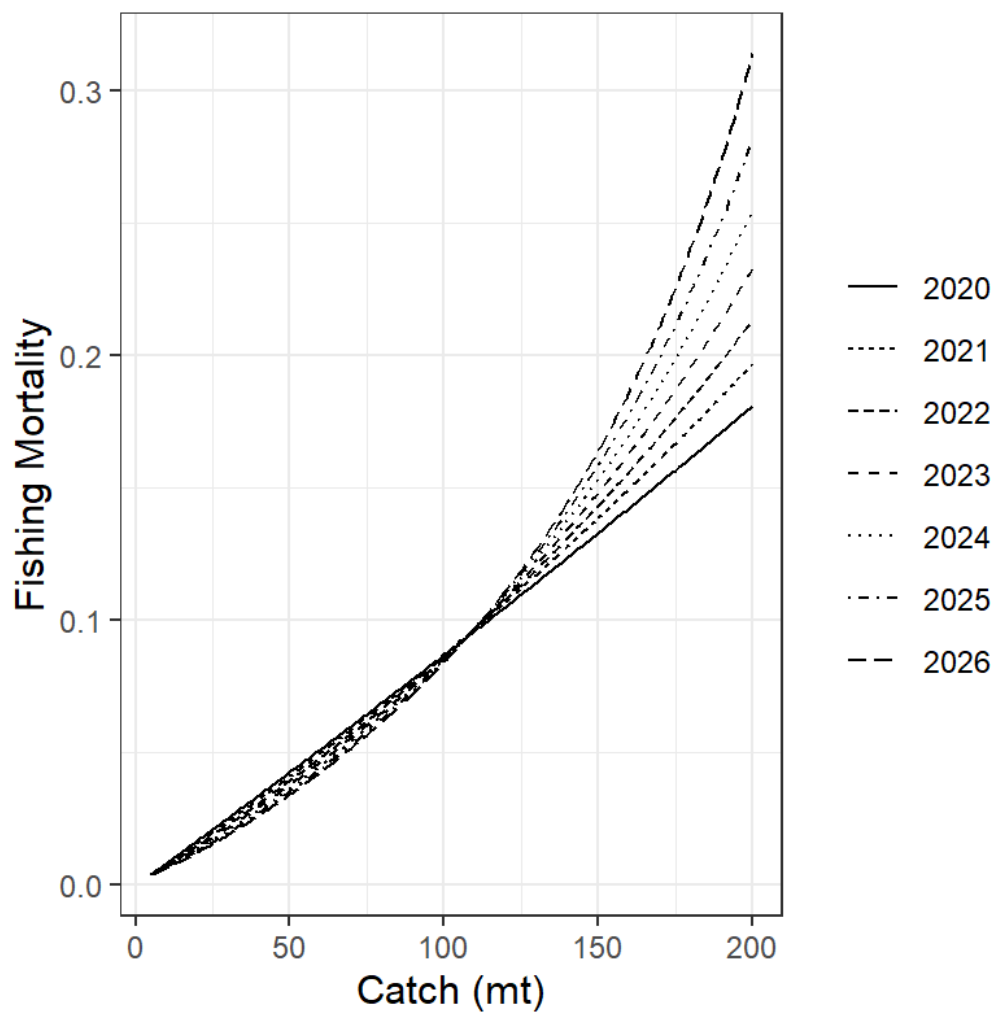
Figure 60. Mean fishing mortality for uku in the main Hawaiian Islands in fishing years 2020 through 2026 as a function of projected catch varying from 0 to 200 metric tons.
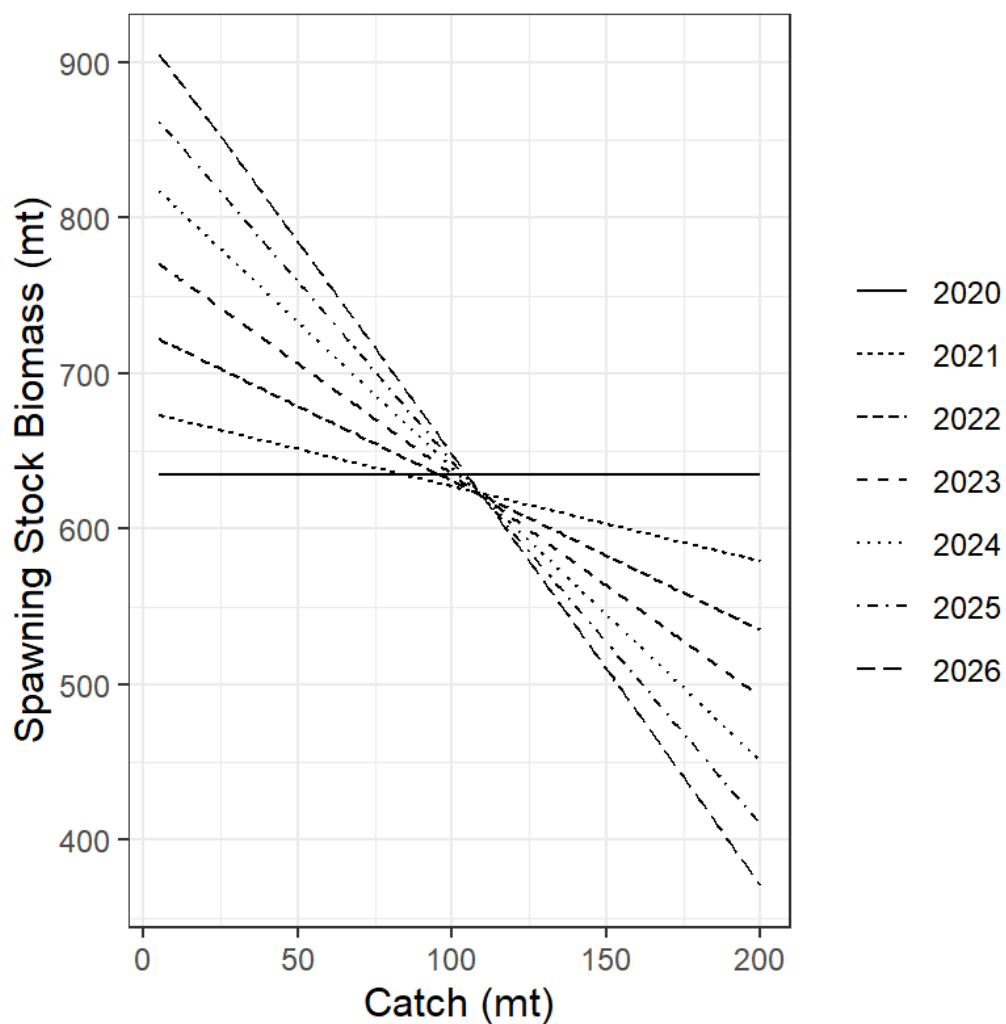
Figure 61. Mean spawning stock biomass for uku in the main Hawaiian Islands in fishing years 2020 through 2026 as a function of projected catch varying from 0 to 200 metric tons.